The Magnetization Process of Antiferromagnetic Quantum Spin Systems and Macroscopic Quantum Effects

Der Gemeinsamen Naturwissenschaftlichen Fakultät
der Technischen Universität Carolo-Wilhelmina
zu Braunschweig

von Dipl. Phys. Dr. rer. nat. Andreas Honecker
aus Tübingen

vorgelegte Habilitationsschrift
Kumulative Arbeit
zur Erlangung der Venia legendi
für das Lehrgebiet
Theoretische Physik

Braunschweig

(2003)

Contents

Part I

Overview and summary

1 Introduction

Strong electronic correlations have been an active field of research in solid-state physics during the past decades due to their relevance e.g. for heavy-fermion compounds [59] and high-temperature (high-T_c) superconductors [11, 16]. Recently, magnetism in low-dimensional strongly correlated electron systems has received a lot of attention. This interest was also triggered by the synthesis of new materials (see e.g. [105] for a recent review), in particular spin chains and ladders [39, 40, 156, 157].

Geometrically frustrated magnets constitute a class of systems exhibiting interesting quantum phenomena like different (unusual) quantum phases (see e.g. [106] for a review of two-dimensional models). New quantum phenomena are not only interesting in their own right, but also important for applications. One example is an enhanced magnetocaloric effect in frustrated spin systems [226] which may be useful for efficient magnetic refrigeration [17, 196]. The exact degeneracy which we will discuss in section 5.4 gives reason to believe that this will also work in a quantum-spin system although a quantitative theory is beyond the scope of this thesis.

In the following we will focus on the zero-temperature magnetization process of strongly correlated electron systems. The magnetization curve of these systems can exhibit the unusual phenomena which are sketched in Fig. 1:

(a) Plateaux have a fixed magnetization $\langle M \rangle$ in a region of the applied magnetic field h. They will be one of the main topics of the present thesis. Note that a plateau with magnetization $\langle M \rangle = 0$ corresponds to a spin gap at zero magnetic field $h = 0$.
On a plateau, the magnetization $\langle M \rangle$ typically assumes a (simple) rational fraction of its saturation value. Magnetization plateaux are thus reminiscent of the (fractional) quantum Hall effect [93, 94, 205].

(b) Also some examples of jumps (which can be regarded as field-induced first-order quantum phase transitions) will be discussed in this thesis.

(c) Cusp singularities can be observed in the middle of magnetization curves [52, 55, 88, 141, 142, 147, 221]. However, we will not discuss this phenomenon further.

One of the first theoretical investigations of plateaux in the $S = 1/2$ Heisenberg model is a study of the magnetization curve on the triangular lattice [134]. Almost a decade later, some first investigations of plateaux in one dimension were performed by Hida [74] and Okamoto [136] in an attempt to explain magnetization experiments on $3CuCl_2{\cdot}2$dioxane [5]. After a few other isolated cases were studied [199, 202], Oshikawa and collaborators have undertaken the first systematic study [146] of this problem and, by extending the Lieb-Schultz-Mattis theorem to systems in a magnetic field (compare section 2.3), they provided a necessary condition for the appearance of magnetization plateaux in one-dimensional spin systems. When the magnetization $\langle M \rangle$ is normalized to saturation values ± 1, this condition for the appearance of a plateau with magnetization $\langle M \rangle$ can be cast in the form

$$SV\,(1 - \langle M \rangle) \in \mathbb{Z}\,. \tag{1.1}$$

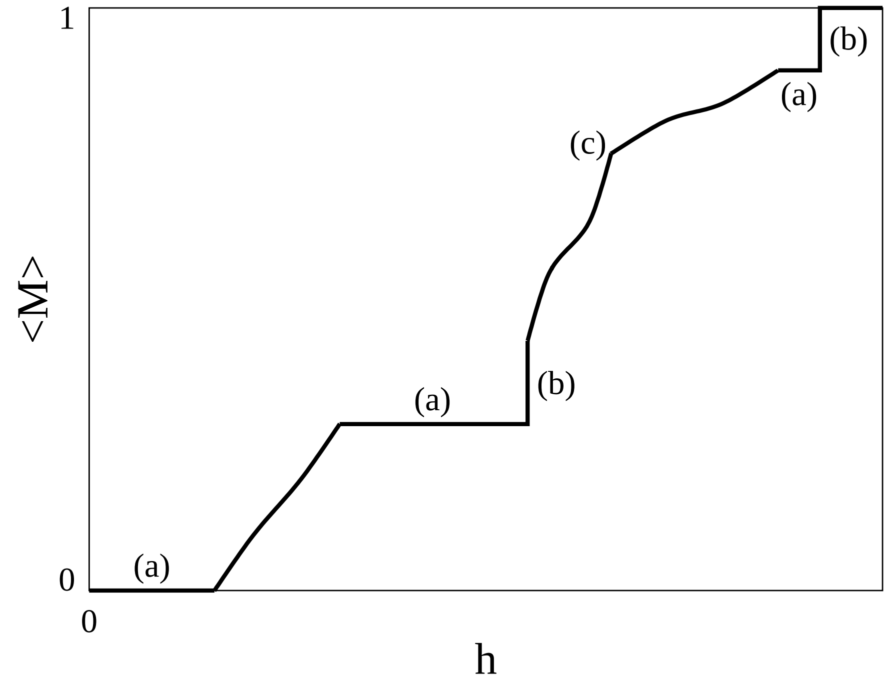

Figure 1: Schematic magnetization curve illustrating some unusual features: (a) plateaux, (b) jumps and (c) a cusp singularity.

Here S is the size of the local spin and V the number of spins in a translational unit cell of the magnetization $\langle M \rangle$ groundstate[1]. It should be noted that translational invariance can be spontaneously broken in the groundstate and then V can be larger than (namely an integer multiple of) the unit cell of the Hamiltonian. Nevertheless, the quantization condition (1.1) implies that the magnetization $\langle M \rangle$ always has a rational value on a plateau.

A famous result for spin chains is Haldane's conjecture [72] which states that such chains with integer S are gapful while those with half-integer S remain gapless, corresponding to the condition (1.1) with $\langle M \rangle = 0$ and $V = 1$ since a spin gap is equivalent to an $\langle M \rangle = 0$ plateau. This feature is indeed confirmed in seminal numerical studies of Heisenberg chains [15, 148], but no other plateaux are found for these systems. Other non-trivial plateaux, which for $S > 1$ would be permitted by (1.1), arise only when the model is modified, e.g. by adding a single-ion anisotropy [92, 146, 168] (see section 3.1 for more details).

The condition (1.1) probably also applies to two (and higher) dimensions with V remaining the volume of the unit cell of the groundstate under the group of translations. However, in dimensions higher than one also rotational symmetries can be spontaneously broken, giving rise to anisotropic unit cells whose volume is not easy to guess a priori. Starting with two dimensions, one can have another interesting phenomenon, namely long-range order at zero temperature in a quantum system. In higher dimensions, a magnetic field can therefore induce transitions between different (dis)ordered states (see chapter 4 for more details).

[1] In cases where the sites carry different spins [vi, 103, 104, 116, 169, 170, 222], the combination SV should be replaced by the maximal spin in the unit cell.

In the absence of translational symmetry, V is strictly infinite allowing one to reconcile plateaux at irrational $\langle M \rangle$ with the condition (1.1). Examples that have been studied include quasiperiodic [7, 197] and disordered [18, 76, 155] one-dimensional models. An old and amusing example is the self-similar magnetization curve Fig. 2 of [197] of a quasiperiodic chain with hierarchical interactions.

However, plateaux at irrational $\langle M \rangle$ also arise in systems with charge carriers that preserve translational symmetry. For example, in modulated Hubbard chains plateaux can be observed at values of $\langle M \rangle$ that depend on the doping n if the density of carriers is fixed (see section 3.7 for more details). In such a case, the condition (1.1) is replaced by commensurability conditions for the different magnetic species.

The transitions at the boundaries of plateaux are field-induced quantum phase transitions. At least the transition to saturation can be mapped to the problem of Bose condensation of magnons and, as we will discuss in chapter 5, universal properties of this transition can be studied.

Finally, in chapter 6 we review some experimental realizations relevant to the models discussed in the first chapters.

We conclude these introductory remarks with a word of caution. The first overview part of this thesis obviously has some review character. However, it should be noted that the main purpose is to put the author's own work into context. When taken as review, the following chapters are therefore not only selective (*i.e.* topics which would be relevant to the field in general are omitted[2]), but the focus is also biased by the author's perspective.

[2] One important topic that is mentioned only in passing are the plateaux observed in $SrCu_2(BO_3)_2$ at $\langle M \rangle = 1/8$, $1/4$ and $1/3$ [85, 95, 143] and the related theoretical analysis [50, 57, 58, 123–126, 128–130] of the magnetization process of the two-dimensional Shastry-Sutherland model [182].

2 Methods

2.1 Jordan-Wigner transformation

The Jordan-Wigner transformation can be used to treat $S = 1/2$ XX chains in a transverse field whose Hamiltonian reads for a chain of length L

$$\begin{aligned} H_{XX} &= \sum_{x=1}^{L} J_x \left(S_x^x S_{x+1}^x + S_x^y S_{x+1}^y \right) - \sum_x h_x S_x^z \\ &= \frac{1}{2} \sum_{x=1}^{L} J_x \left(S_x^+ S_{x+1}^- + S_{x+1}^+ S_x^- \right) - \sum_x h_x S_x^z \,. \end{aligned} \tag{2.1}$$

Here, the spin operators S_x^α ($\alpha \in \{x, y, z\}$) not only satisfy the usual $SU(2)$-commutation relations, but are representend in terms of the Pauli matrices at site x as $S_x^\alpha = \sigma_x^\alpha/2$.

The following identification maps this Hamiltonian onto one of free lattice fermions (see e.g. section 1.4 of [115])

$$d_x = \mathrm{e}^{i\phi_x} S_x^- \,, \qquad d_x^\dagger = \mathrm{e}^{-i\phi_x} S_x^+ \,, \tag{2.2}$$

where the phase factor

$$\phi_x = \pi \sum_{y=1}^{x-1} d_y^\dagger d_y \tag{2.3}$$

is needed to ensure fermionic anticommutation relations $[d_x, d_y]_+ = 0 = \left[d_x^\dagger, d_y^\dagger\right]_+$, $\left[d_x, d_y^\dagger\right]_+ = \delta_{x,y}$.

Observing that S_x^z is represented by the fermion density at site x as $S_x^z = d_x^\dagger d_x - \frac{1}{2}\mathbb{1}$, one can rewrite the Hamiltonian (2.1) in terms of the fermions $d_x^{(\dagger)}$ as

$$H_{XX} = \frac{1}{2} \sum_x J_x \left(d_x^\dagger d_{x+1} + d_{x+1}^\dagger d_x \right) - \sum_x h_x \left(d_x^\dagger d_x - \frac{1}{2} \right) \,. \tag{2.4}$$

Since this Hamiltonian is quadratic in fermions, it can be diagonalized completely by a Fourier transformation in a translationally invariant situation, *i.e.* $J_x = J$, $h_x = h$ and periodic boundary conditions $S_{x+L}^\alpha = S_x^\alpha$.

In a situation where one has a periodicity of p sites $J_x = J_{x+p}$, $h_x = h_{x+p}$, one can still apply a Fourier transformation to (2.4) and reduce the problem to the diagonalization of a $p \times p$ matrix. In this manner, one can obtain an analytic solution of XX chains in a transverse field where coupling constants and magnetic field have a modulation with period p (see e.g. [41]).

Even if there is no translational symmetry at all (like in quasiperiodic or random systems) the representation (2.4) is still useful. The computation of fermionic single-particle levels requires just the diagonalization of an $L \times L$ tridiagonal matrix (with two additional entries in the top right and bottom left corner for periodic boundary conditions). Once such a diagonalization is performed, the groundstate in the sector with a given total S^z (*i.e.* particle

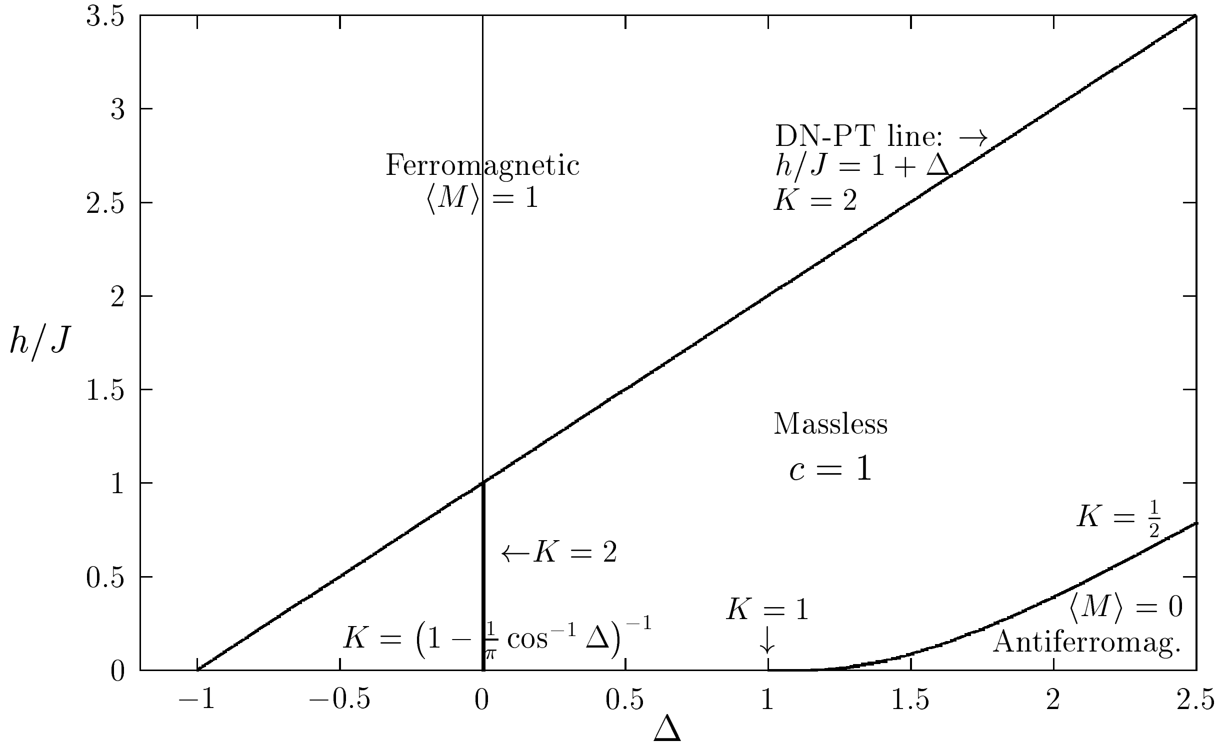

Figure 2: Magnetic phase diagram of the XXZ chain (2.5), reproduced after [ii]. The region for $\Delta > 1$ denoted by 'Antiferromag.' is of Ising-type and gapful. The region $h > J(1+\Delta)$ is also gapped and the groundstate is ferromagnetic. The low-energy physics in the intermediate region is described by a $c = 1$ Gaussian theory, *i.e.* a free boson which is characterized by the Luttinger parameter K.

number) is found by occupying the lowest $S^z + L/2$ single-particle states. In this manner, long XX chains in a uniform transverse field $h_x = h$ can be treated numerically up to $L \approx 10^5$ sites even in the presence of disorder [18, 155] or a quasiperiodic modulation [7].

By applying the Jordan-Wigner method as outlined above to magnetization curves of XX chains with discrete disorder, a rather nontrivial phenomenon was observed [18], namely magnetization plateaux whose magnetization values depend on the strength of disorder and thus are in general irrational (see also [76]).

2.2 Bosonization

The field-theory description e.g. of spin chains is a useful technique for one-dimensional models subject to weak perturbations directly in the thermodynamic limit (see e.g. [65]).

2.2.1 Spin-1/2 XXZ chain

For the spin-1/2 XXZ chain in an external magnetic field h

$$H_{XXZ} = J\sum_{x=1}^{L}\left\{\Delta S_x^z S_{x+1}^z + \frac{1}{2}\left(S_x^+ S_{x+1}^- + S_x^- S_{x+1}^+\right)\right\} - h\sum_{x=1}^{L} S_x^z \tag{2.5}$$

the Abelian bosonization technique has proven to be very efficient (see e.g. [1, 65, 181] for reviews). A standard way to obtain a low-energy large-scale effective Hamiltonian is to express the Hamiltonian (2.5) in terms of interacting fermions using the Jordan-Wigner transformation (see section 2.1). The interacting fermions are then rewritten in terms of non-interacting bosons. Alternatively, one can appeal to the Bethe ansatz which shows [220] that the low-energy properties of (2.5) are described by a Gaussian $c = 1$ conformal field theory, *i.e.* a compactified free boson. Both approaches lead to the Tomonaga-Luttinger Hamiltonian[3]

$$H_{\text{bos.}} = \frac{1}{2}\int \mathrm{d}x \left(vK(\partial_x\tilde{\phi})^2 + \frac{v}{K}(\partial_x\phi)^2\right) . \tag{2.6}$$

The bosonic field ϕ and its dual $\tilde{\phi}$ satisfy the canonical commutation relations ($\partial_x\tilde{\phi}(x)$ is the canonical momentum, sometimes also denoted by $\Pi(x)$). The constant $K = K(\langle M\rangle, \Delta)$ governs the conformal dimensions of the bosonic vertex operators and can be obtained exactly from the Bethe ansatz solution of the XXZ chain (see e.g. [ii] for a detailed summary). One has $K = 1$ for the $SU(2)$-symmetric case $\Delta = 1$, $\langle M\rangle = 0$ and it is related to the radius R of [ii] by $K^{-1} = 2\pi R^2$ (these conventions for K were used in [iii], e.g. [65, 181] use a convention where K is by a factor two smaller). The low-energy representation (2.6) is valid in the region between the two lines in Fig. 2 indicating a transition to the ferromagnetically polarized state for large h (denoted by 'DN-PT line' – see section 5.1 for an explanation) and a gapped antiferromagnet for $\Delta > 1$ and small h. Further values of the Luttinger parameter K are also given in Fig. 2. The velocity v can be computed by the Bethe ansatz as well, but its numerical value is not important for our purposes.

In terms of the free boson, the spin operators can be represented as

$$S_x^z = \frac{1}{\sqrt{2\pi}}\partial_x\phi + a : \cos(2k_F x + \sqrt{2\pi}\phi) : + \frac{\langle M\rangle}{2} , \tag{2.7}$$

$$S_x^{\pm} = (-1)^x : \mathrm{e}^{\pm i\sqrt{2\pi}\tilde{\phi}}\left(b\cos(2k_F x + \sqrt{2\pi}\phi) + c\right) : , \tag{2.8}$$

where the colons denote normal ordering with respect to the groundstate with magnetization $\langle M\rangle$. The Fermi momentum k_F is related to the magnetization of the chain as $k_F = (1 - \langle M\rangle)\pi/2$. An XXZ anisotropy and/or the external magnetic field modify the scaling dimensions of the physical fields through K and the commensurability properties of the spin operators, as can be seen from the explicit x-dependence in (2.7), (2.8). The non-universal constants a, b and c can be computed numerically [44, 78] or in some cases even analytically [3, 112–114].

[3] Note that a factor $(4R)^{-2}$ is missing in front of the Π^2 term in eqs. (2.2) and (3.4) of [ii].

2.2.2 Hubbard chain

The Hubbard model represents interacting electrons with spin 1/2 on a lattice subject to a Coulomb repulsion U. The Hamiltonian including a chemical potential μ and a magnetic field h is given by

$$\begin{aligned} H &= -t \sum_{x=1}^{L} \sum_{\alpha=\uparrow,\downarrow} (c^\dagger_{x+1,\alpha} c_{x,\alpha} + \text{h.c.}) + U \sum_x c^\dagger_{x,\uparrow} c_{x,\uparrow} c^\dagger_{x,\downarrow} c_{x,\downarrow} \\ &\quad + \mu \sum_{x,\alpha} c^\dagger_{x,\alpha} c_{x,\alpha} - \frac{h}{2} \sum_x (c^\dagger_{x,\uparrow} c_{x,\uparrow} - c^\dagger_{x,\downarrow} c_{x,\downarrow}) . \end{aligned} \tag{2.9}$$

The $c_{x,\alpha}$ and $c^\dagger_{x,\alpha}$ are annihilation and creation operators of electrons with spin $\alpha = \uparrow, \downarrow$ and satisfy the anticommutation relations $[c_{x,\alpha}, c_{x',\alpha'}]_+ = 0 = [c^\dagger_{x,\alpha}, c^\dagger_{x',\alpha'}]_+$, $[c^\dagger_{x,\alpha}, c_{x',\alpha'}]_+ = \delta_{x,x'}\delta_{\alpha,\alpha'}$. The density of electrons with spin α is denoted by $n_\alpha = \frac{1}{L}\sum_x c^\dagger_{x,\alpha} c_{x,\alpha}$ and the total density by $n = n_\uparrow + n_\downarrow$.

Like the XXZ chain (2.5), the Hubbard chain is integrable and can be solved by the Bethe ansatz [108]. A detailed analysis shows that the low-energy excitations of the Hubbard chain even with a magnetic field can be described in terms of *two* bosonic fields [43,51,65,150, 180,209], *i.e.* the bosonized version of the Hamiltonian (2.9) becomes the following Gaussian one

$$H_{\text{bos.},2} = \frac{u_s}{2} \int \mathrm{d}x \left((\partial_x \tilde{\phi}_s)^2 + (\partial_x \phi_s)^2 \right) + \frac{u_c}{2} \int \mathrm{d}x \left((\partial_x \tilde{\phi}_c)^2 + (\partial_x \phi_c)^2 \right) . \tag{2.10}$$

The fields labeled by s and c are particular combinations of the bosonic fields dictated by the Bethe ansatz solution [51]. The Bethe ansatz also yields the velocities u_s and u_c as well as the Luttinger liquid parameters[4] K_s and K_c associated to the spin (ϕ_s) and charge fields (ϕ_c), respectively. For vanishing magnetic field $h = 0$, the spin sector is $SU(2)$-symmetric and hence one has $K_s = 1$ for all values of the chemical potential μ and the Coulomb repulsion U.

For non-zero magnetic field, the choice of basis and the scaling dimensions of the fields are dictated by a 2×2 matrix, called 'dressed charge matrix' [51]. Further details and instructions how to bosonize operators can be found in section II.A and appendix B of [ix].

2.3 Lieb-Schultz-Mattis theorem

A generalized version of the Lieb-Schultz-Mattis theorem is one of the few exact results that have been obtained for the magnetization process of general one-dimensional spin systems [2, 4, 107, 146, 159]. The statement of this theorem is: *Either the condition (1.1) is satisfied or the spectrum is gapless or the groundstate is degenerate.*

[4] These parameters have been absorbed in the definition of the fields and therefore do not appear explicitly in (2.10).

Most versions of this theorem concern the case of zero field ($h = 0$, $\langle M \rangle = 0$). The theorem was first derived for an $S = 1/2$ Heisenberg chain ($S = 1/2$, $V = 1$ – see Theorem 2 in appendix B of [107]) and then extended to general-S chains (but still $V = 1$ [4]). In the case $\langle M \rangle = 0$, $V = 1$, the Lieb-Schultz-Mattis theorem states that a spin-S Heisenberg chain can have a unique gapful groundstate only for $S \in \mathbb{Z}$. This corresponds to Haldane's conjecture[5] [72] that a spin-S Heisenberg is gapless if S is not an integer and gapped if S is an integer.

In the extension of this theorem to N-leg spin ladders [2, 159], one should substitute $V = N$ (also $\langle M \rangle = 0$ still) into (1.1) such that this condition becomes $SN \in \mathbb{Z}$. In particular, for $S = 1/2$, the theorem then corresponds to a generalized 'Haldane conjecture', namely that N-leg spin-1/2 ladders with N even are gapped and those with N odd are gapless (see e.g. [40])[6].

The case which is most relevant in the present context was discussed in [146] where the Lieb-Schultz-Mattis theorem for spin-S chains (still $V = 1$) was generalized to non-zero magnetization $\langle M \rangle$ (see also [48] for the case of ladders in a magnetic field).

The proof always consists of the same steps which we now sketch briefly. Let $|\,\psi_0\,\rangle$ be the groundstate. Since a degenerate groundstate is never ruled out by the theorem, we can assume without loss of generality that $|\,\psi_0\,\rangle$ is unique. For a Hamiltonian with L identical unit cells $\mathcal{U}_x$ each containing V spins $\vec{S}_{\vec{x}}$ one then constructs a so-called 'twist'-operator

$$U_k = \exp\left(-ik \sum_{x=1}^{L} x \sum_{\vec{x}\in\mathcal{U}_x} S^z_{\vec{x}}\right) . \tag{2.11}$$

First we note that $\exp\left(2\pi i \sum_{\vec{x}\in\mathcal{U}_x} S^z_{\vec{x}}\right) = (-1)^{2S_{\text{cell}}} = \exp\left(2\pi i S_{\text{cell}}\right)$ where $S_{\text{cell}} = SV$ is the total spin in the cell $\mathcal{U}_x$. Denoting the translation operator by one cell by T and the z-component of the total spin by S^z one then verifies by straightforward computation

$$T\,U_k\,T^{-1} = U_k\,\exp\left(ik\left(L\sum_{\vec{x}\in\mathcal{U}_L} S^z_{\vec{x}} - S^z\right)\right) = U_k\,\exp\left(ik\,LSV\left(1-\langle M\rangle\right)\right) . \tag{2.12}$$

Next one considers the excitation (in general not an eigenstate of the Hamiltonian)

$$|\,\psi_k\,\rangle := U_k|\,\psi_0\,\rangle . \tag{2.13}$$

Two properties of this state yield the proof the theorem.

[5]Indeed, the version of the Lieb-Schultz-Mattis theorem derived in [4] aimed at supporting the Haldane-conjecture.

[6]Note that this conjecture should be formulated a little more carefully. For example, we will mention in section 3.4 that spin-1/2 ladders with N odd but periodic (frustrating) boundary conditions along the rungs have a gap at least for large rung coupling [ii, 89]. Of course, the Lieb-Schultz-Mattis theorem remains valid since the opening of such a gap is accompanied by spontaneous breaking of translational symmetry, *i.e.* the groundstate becomes degenerate.

Translational invariance of the Hamiltonian and uniqueness of the groundstate imply $T|\,\psi_0\,\rangle = \mathrm{e}^{i\delta}|\,\psi_0\,\rangle$. This and (2.12) lead to

$$\langle\,\psi_0\,|\,\psi_k\,\rangle = \langle\,\psi_0\,|U_k|\,\psi_0\,\rangle = \langle\,\psi_0\,|T\,U_k\,T^{-1}|\,\psi_0\,\rangle = \exp\left(ik\,LSV\,(1-\langle M\rangle)\right)\,\langle\,\psi_0\,|\,\psi_k\,\rangle\,. \quad (2.14)$$

By comparison of the left and right side of this equation one concludes that $|\,\psi_k\,\rangle$ is orthogonal to $|\,\psi_0\,\rangle$ (since it corresponds to a different eigenvalue of T) for suitable k (e.g. $k = 2\pi/L$) unless $SV\,(1-\langle M\rangle)$ is an integer. Note that with the last condition one recovers precisely (1.1).

The second property (also to be checked by explicit computation) is that the expectation value of the Hamiltonian H in the state $|\,\psi_k\,\rangle$ for suitable k (e.g. again $k = 2\pi/L$) satisfies

$$\langle\,\psi_k\,|H|\,\psi_k\,\rangle - \langle\,\psi_0\,|H|\,\psi_0\,\rangle = \mathcal{O}\left(\frac{1}{L}\right)\,. \quad (2.15)$$

In this manner one obtains a low-lying excitation with a variational upper bound for the energy of the order $1/L$ provided that $|\,\psi_k\,\rangle$ is orthogonal to $|\,\psi_0\,\rangle$, *i.e.* (1.1) is *not* satisfied. This completes the proof of the theorem.

Although this theorem is very useful to gain some intuition, certain problems remain. First, the existence of a gap if (1.1) is satisfied was not shown and indeed examples show that a gap does not always open when it would be permitted by this condition. Conversely, the condition (1.1) allows a gap to open at any rational $\langle M\rangle$ provided that V becomes sufficiently large by suitable spontaneous breaking of translational symmetry.

Besides such issues an important observation in the context of magnetic properties is that the twist operator (2.11) preserves the total S^z, hence the excitation (2.13) can be non-magnetic. Consequently, one needs complementary arguments to link magnetic and non-magnetic excitations. A possible route (in fact the one taken in [146]) uses Abelian bosonization (see section 2.2.1). In this approach, the condition (1.1) then also appears as a commensurability condition for certain perturbing operators (examples will be presented in sections 3.3 and 3.4). A second possibility is to perform a variational computation for the total spin of the state $|\,\psi_k\,\rangle$ similarly to (2.15) [48]. In this approach, one needs certain properties of the transverse structure factor [48] which have to be derived by methods (e.g. exact diagonalization) which allow one to study the original problem directly without much additional effort.

A completely different approach to the condition (1.1) is to use perturbation theory (see e.g. [iv]). This approach is conceptually very simple and can be used to establish the opening of a magnetic gap (*i.e.* the existence of a plateau) whenever it can be applied. We will briefly discuss such a perturbative approach in the next section.

2.4 Perturbation theory

The magnetization process is easy to understand if the system decouples into clusters of V sites [i, ii, iv, viii, ix]. These 'strongly coupled' clusters magnetize independently such that at zero temperature the magnetization $\langle M\rangle$ can only take finitely many values. For

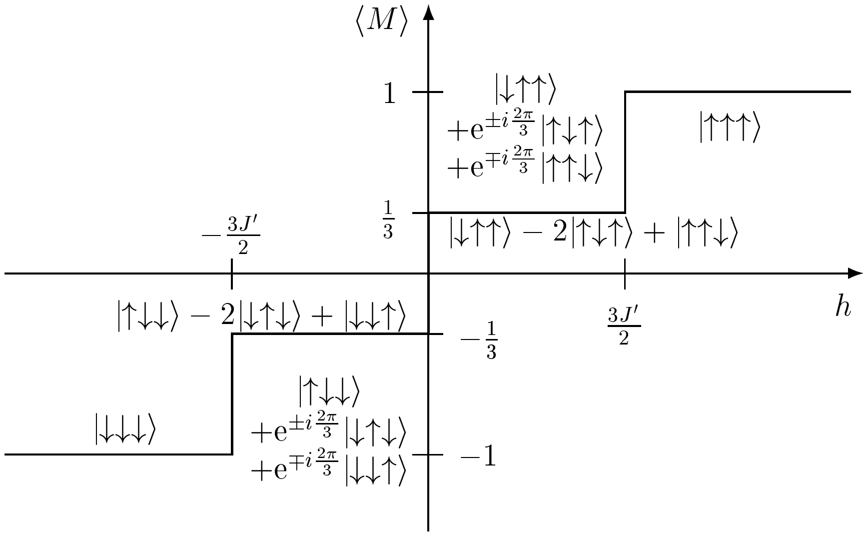

Figure 3: Magnetization curve of three spins-1/2 with coupling constant J'. The $|\langle M \rangle| = 1/3$ groundstates for the middle spin coupled only to the exterior left and right spins are shown close to the horizontal axis and the ones for equal coupling between all three spins are shown above the $\langle M \rangle = 1/3$ and below the $\langle M \rangle = -1/3$ plateaux, respectively.

a spin-system with spin S they are subject to the quantization condition (1.1) where V is directly the number of spins in one of the decoupled clusters. Fig. 3 illustrates this general observation for three $S = 1/2$ spins. This figure exhibits a step-like magnetization curve and clear plateaux with[7] $\langle M \rangle = \pm 1/3$. Note that for this case, the magnetization curve turns out to be identical for an open and periodic arrangement of the spins. However, the $\langle M \rangle = \pm 1/3$ groundstates (also shown in Fig. 3) depend on the boundary conditions. Using (higher order) series expansions around such a decoupling point [i, ii, iv, v], the quantization condition obtained in this simple manner can be argued to be valid also for more general parameters, *i.e.* the spin gap above the plateaux protects them against (small) perturbations.

In its simplest form, this argument explains magnetization plateaux which arise because the unit cell of the Hamiltonian contains several spins. However, the argument can be refined to account also for spontaneous breaking of translational symmetry e.g. by a period of two. The transitions between plateau states can be treated by degenerate perturbation theory, leading to effective Hamiltonians which in many one-dimensional cases turn out to be effectively an XXZ chain (2.5) if only the lowest order(s) are kept [iii, v, 28, 60, 120, 195, 203, 213]. If the effective XXZ anisotropy is sufficiently large ($\Delta > 1$, see Fig. 2), a gap opens and translational symmetry is spontaneously broken. In this manner one finds a further plateau precisely in the middle between the two values of $\langle M \rangle$ predicted by considering just the decoupling limit itself. This illustrates that V in (1.1) should be taken from the unit cell of the groundstate whose size is an integer multiple (in general larger than 1) of the unit cell

[7] Here we also show the region with $h < 0$. In general we omit it since due to the symmetry $h \to -h$, $\langle M \rangle \to -\langle M \rangle$, the complete information is contained in the region $h \geq 0$.

of the Hamiltonian.

Even if degenerate perturbation theory leads to an effective Hamiltonian that is not exactly solvable, it may still be a useful starting point for a further numerical or approximate treatment. For example, such an approach has been used [57, 58, 126, 128, 129] to study the magnetization process of the two-dimensional Shastry-Sutherland model [182].

2.5 Exact diagonalization (ED)

Coupling constants do not always lie in the weak- or strong-coupling regimes discussed before. In such cases, accurate results can be obtained only numerically e.g. by exact diagonalization (ED), as was already done in pioneering works [15, 148]. Since on the one hand, vector spaces are large already for moderate system sizes and on the other hand, only a few extreme eigenvalues of sparse matrices are needed to compute the zero-temperature magnetization curves, one frequently resorts to the Lanczos method (see e.g. [38]) as was done already in [148]. In the present situation the magnetic field couples to a conserved quantity S^z_{tot}. One therefore only needs the groundstate energy $E(S^z_{\text{tot}}, h = 0)$ at $h = 0$ in each of the magnetization subspaces with $S^z_{\text{tot}} \in \{0, 1, \ldots, S\mathcal{V}\}$ (here $\mathcal{V}$ is the total number of spins). Then one can readily obtain the energy in a finite field h through the relation

$$E(S^z_{\text{tot}}, h) = E(S^z_{\text{tot}}, 0) - hS^z_{\text{tot}} \tag{2.16}$$

and construct the groundstate magnetization curve.

We normalize the magnetization

$$\langle M \rangle = \frac{\langle S^z_{\text{tot}} \rangle}{S\mathcal{V}} \tag{2.17}$$

such that $|\langle M \rangle| \leq 1$. Note that the magnetization curve has steps on a finite system since the possible values of S^z_{tot} are quantized. However, it was observed in [15, 148] that the finite-size effects of the midpoints of the steps of the magnetization curves of spin chains are small. A conventional method (which will also be used in some of the following sections) is therefore to approximate the thermodynamic limit by connecting the midpoints of the finite-size steps at the largest available system sizes.

2.6 Density-matrix renormalization group (DMRG) method

An alternative method specific to one dimension is the density-matrix renormalization group (DMRG) method [151, 215] which permits to study larger systems. The number of applications of this method or variants thereof to the magnetization process is increasing steadily [vi, x, 24, 35, 46, 47, 77, 110, 111, 116, 131, 140, 142, 176, 195, 201, 217, 218]. The only technical complication is that the infinite system algorithm does not give good approximations to the incommensurate structures which generally arise at finite $\langle M \rangle$ and therefore the finite system algorithm should be used if one wants to compute the complete magnetization curve.

2.7 Quantum Monte Carlo (QMC) method

Finally, recent advances have also made it possible to use the quantum Monte Carlo (QMC) method for spin systems in a magnetic field (see e.g. [12, 87, 171, 191, 192, 214] and [45] for a recent review). However, geometric frustration still causes severe sign problems. Frustrated systems tend to give rise to more complicated and therefore interesting behavior. In fact, a large part of the models discussed in this work are frustrated and therefore even advanced QMC methods are currently not applicable to them.

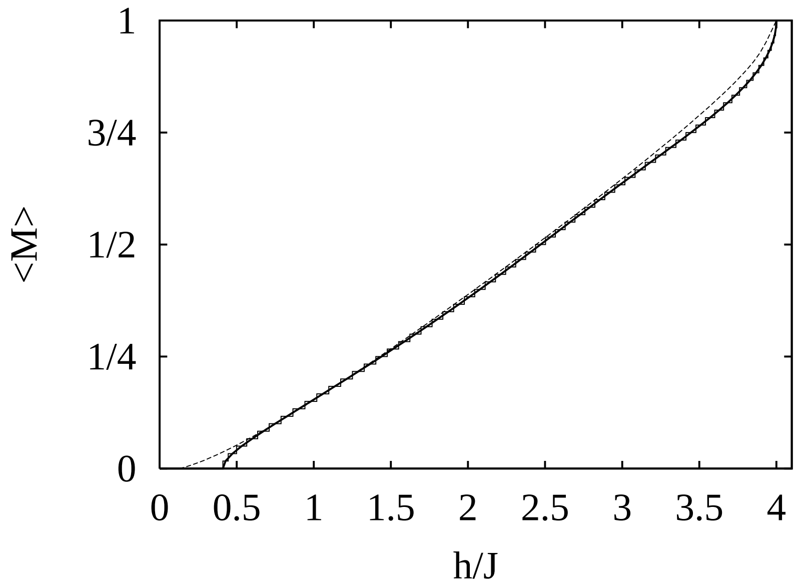

Figure 4: Magnetization curve of the $S = 1$ Heisenberg chain. The steps show the curve obtained for a periodic chain with $L = 60$ sites by DMRG [vi]. The bold smooth and dashed curves denote an extrapolation to the thermodynamic limit and a renormalized spinwave theory result [228], respectively.

3 One dimension

3.1 Homogeneous spin-S chains

The magnetization process of antiferromagnetic homogeneous spin-S chains has been studied in detail already a while ago. The smooth curve for $S = 1/2$ was computed by the Bethe ansatz in [68]. Comparison with numerical data for $L \leq 11$ sites has then established the midpoint-method mentioned in section 2.5, *i.e.* the extrapolation to the thermodynamic limit using the middles of the finite-size steps [15]. Magnetization curves for $S \leq 5/2$ were computed numerically in [148]. The numerical data was later extended to larger system sizes e.g. for $S = 1$ [167] and $S = 3/2$ [168] and more recently using QMC for $S \leq 2$ [191]. The overall picture which has emerged from these studies is a rather featureless magnetization curve for homogeneous isotropic antiferromagnetic Heisenberg chains: For integer S there is just an $\langle M \rangle = 0$ plateau corresponding to the Haldane gap [72], but no further plateaux are observed. In particular, for S half-integer, the magnetization curve varies smoothly between $\langle M \rangle = -1$ and 1. Other non-trivial plateaux, which are permitted by the quantization condition (1.1) for $S > 1$, arise only when e.g. a single-ion anisotropy is added [92,146,168][8].

Let us now discuss the case $S = 1$ in a little more detail. According to (2.16) one needs the energies $E(S^z_{\text{tot}}, 0)$ in order to compute the magnetization curves. These energies were

[8] In fact, anisotropic Heisenberg chains were the focus of the seminal paper [146].

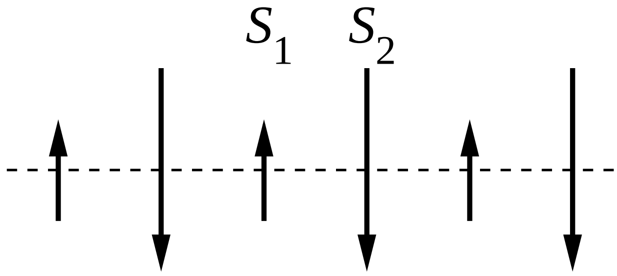

Figure 5: Schematic view of a ferrimagnetic Heisenberg chain, consisting of alternating small spins (S_1) and large spins (S_2).

tabulated for $S = 1$ chains with length up to $L = 14$ in [148] and for $L \leq 16$ in [167][9]. DMRG results for the magnetization curve of the $S = 1$ chain were obtained in [vi, 24, 110, 140]. QMC computations for $L = 100$ sites were also performed using the worm and directed loop algorithms [87, 191]. Fig. 4 shows the magnetization curve based on DMRG data for a periodic chain with $L = 60$ sites [vi]. One can see quite clearly that there is only an $\langle M \rangle = 0$ plateau, corresponding to the Haldane gap [72]. The asymptotic behavior of the magnetization curve both near the saturation field as well as above the Haldane gap is compatible with $\langle M \rangle \sim \sqrt{|h - h_c|}$ [66, 87, 110, 140] (see also section 5.1).

For comparison, Fig. 4 also shows a renormalized spinwave theory result (see eq. (13) of [228]) at $S = 1$. The overall agreement with the numerical curve is quite good; the largest deviations occur at low fields, *i.e.* in the vicinity of the Haldane gap.

3.2 Ferrimagnetic spin chains

Ferrimagnetic spin chains are illustrated in Fig. 5. They consist of antiferromagnetically coupled alternating small spins S_1 and large spins S_2. For $S_2 > S_1$, they cannot combine to form a singlet even if they align antiferromagnetically. This leads to a groundstate with a macroscopic spin $S_{\mathrm{g}} = \frac{L\,(S_2 - S_1)}{2}$ if the total length of the chain is L. Consequently, ferrimagnetic chains immediately develop a magnetization $\langle M_0 \rangle = \frac{S_2 - S_1}{S_2 + S_1}$ once a small magnetic field $h \neq 0$ is switched on.

The ferrimagnetic chain with the smallest spins is the $S = 1$-$1/2$ chain with alternating spins $S_1 = 1/2$ and $S_2 = 1$. The magnetization curve of this chain was computed by exact diagonalization in [103,165,169] and by DMRG in [116]. These studies observed the expected plateau at $\langle M_0 \rangle = 1/3$, but no further ones.

Fig. 6 illustrates the magnetization process of ferrimagnetic Heisenberg spin chains with that of the $S = 3/2$-$1/2$ alternating chain. Surprisingly, numerical data for this case seems to have been obtained first in [vi] where it was needed for other purposes (see section 3.6). Again, one observes only the expected plateau at $\langle M_0 \rangle = 1/2$.

More generally, homogeneous ferrimagnetic chains are similar to completely homogeneous Heisenberg chains in so far as they do not seem to give rise to any plateau other than the

[9]The data of [148] is partially reproduced in [167], however with typographic errors at $L = 14$.

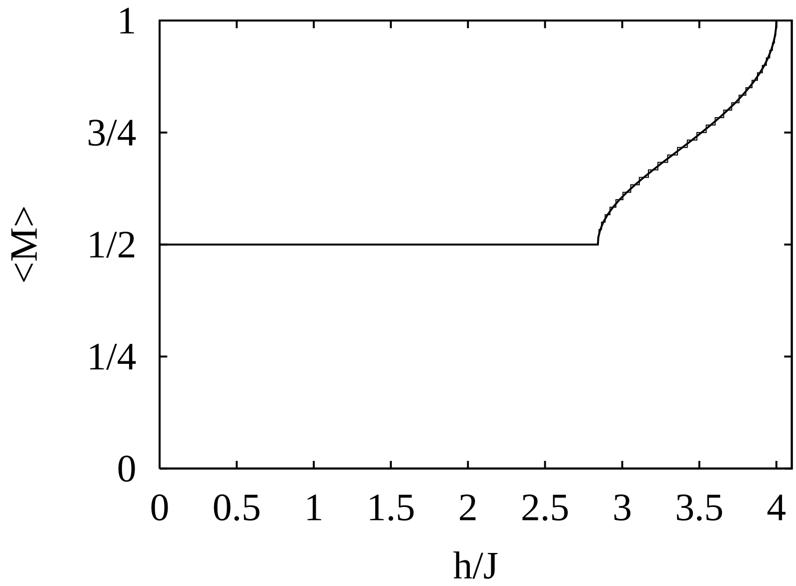

Figure 6: Magnetization curve of the $S = 3/2$-$1/2$ ferrimagnetic Heisenberg chain. The steps show the curve obtained for a periodic chain with $L = 60$ sites by DMRG [vi] while the smooth curve denotes an extrapolation to the thermodynamic limit.

groundstate plateau at $\langle M_0 \rangle = \frac{S_2 - S_1}{S_2 + S_1}$. Interestingly however, an easy-plane XXZ anisotropy leads to the appearance of $2S_1$ plateaux (not counting saturation $\langle M \rangle = 1$) [170, 222] which are allowed by the quantization condition (1.1) with $VS = S_1 + S_2$, *i.e.* for

$$(S_1 + S_2)\ (1 - \langle M \rangle) \in \mathbb{Z} \tag{3.1}$$

and $\langle M \rangle \geq \langle M_0 \rangle$.

3.3 Modulated spin-1/2 Heisenberg chains

Modulated Heisenberg chains are some of the simplest examples that give rise to non-trivial plateaux in their magnetization curves. Several authors have investigated the magnetization process of trimerized [74, 136, 137], frustrated trimerized [v, 201], quadrumerized [31] and more generally periodically modulated $S = 1/2$ Heisenberg spin chains with period p [iv, 20, 32, 41, 218]. Modulated spin-S chains have been studied by Totsuka using bosonization in a remarkable series of papers [202, 203]. For reasons of simplicity, here we review just the bosonization analysis of modulated $S = 1/2$ chains following [20].

To be specific, let us introduce periodically modulated couplings for an $S = 1/2$ Heisenberg chain such that $J_x = J$ if $x \neq np$ and $J_x = J'$ if $x = np$, *i.e.* the strength of every pth coupling constant is changed from J to J'. In the continuum limit one finds [20] the following perturbation for the original Hamiltonian (2.6)

$$H_{\text{pert.}} = \lambda \int\ \mathrm{d}x\ \ \cos(2\, p\, k_F\, x + \sqrt{2\pi}\, \phi)\ , \tag{3.2}$$

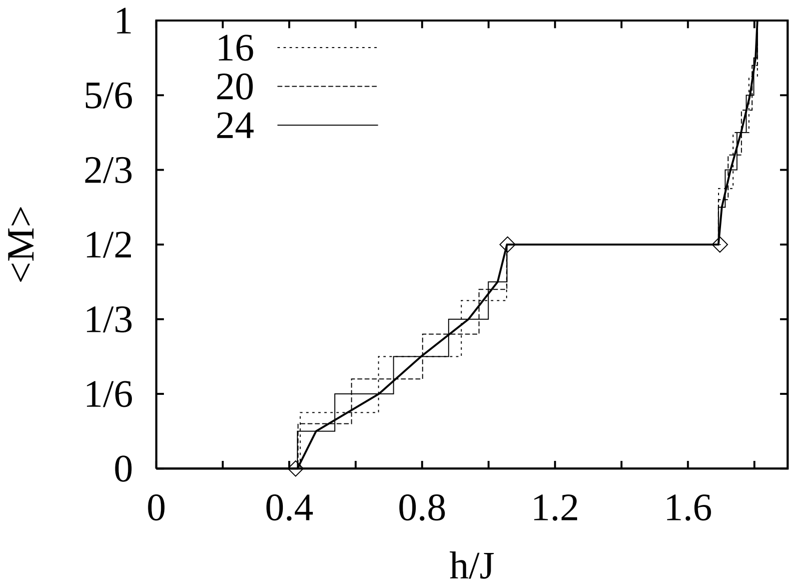

Figure 7: Magnetization curve of the quadrumerized chain with $J' = J/2$. Thin lines show results for finite chains with $L = 16$, 20 and 24 sites, see [20] for equivalent ED data. The diamonds show results of second-order strong-coupling expansions for the plateau boundaries [iv]. The bold line is an extrapolation to the thermodynamic limit.

where $\lambda \sim J' - J$.

Now one has to identify the values of the magnetization $\langle M \rangle$ for which the operator (3.2) is commensurate. Inspecting the explicit dependence on x in (3.2) one concludes that this operator is commensurate if $2\,p\,k_F = p\,(1 - \langle M \rangle)\,\pi$ is a multiple of 2π, *i.e.* at values of the magnetization given by (1.1) with $S = 1/2$ and $V = p$. Furthermore, the scaling dimension of the operator is

$$\dim\left(\cos\left(\sqrt{2\pi}\,\phi\right)\right) = \frac{K}{2}\,. \tag{3.3}$$

Since for XXZ anisotropies $\Delta \geq 0$ this dimension is at most one (in particular less than two), the operator (3.2) is always relevant in the renormalization-group sense. Therefore, modulated $S = 1/2$ Heisenberg chains open a gap for arbitrarily small $J' \neq J$, implying a plateau in the magnetization curve [20].

For stronger deviations $J' \neq J$, ED has been used to check that the condition (1.1) with $V = p$ is necessary *and* sufficient for the opening of a plateau in a modulated $S = 1/2$ Heisenberg chain at least for modulations with periodicity $p \leq 6$ [20]. Further evidence for this picture can be obtained by applying the strong-coupling arguments mentioned in section 2.4 to the limits $J' \to 0$ or $J \to 0$ [iv].

As an example, Fig. 7 shows ED results [20] for the magnetization curve of a quadrumerized $S = 1/2$ Heisenberg at $J' = J/2$. One observes two clear plateaux at $\langle M \rangle = 0$ and $1/2$, as expected. The diamonds in Fig. 7 show second-order series for the boundaries of these plateaux [iv]. In spite their low order, these series are in good agreement with the ED data.

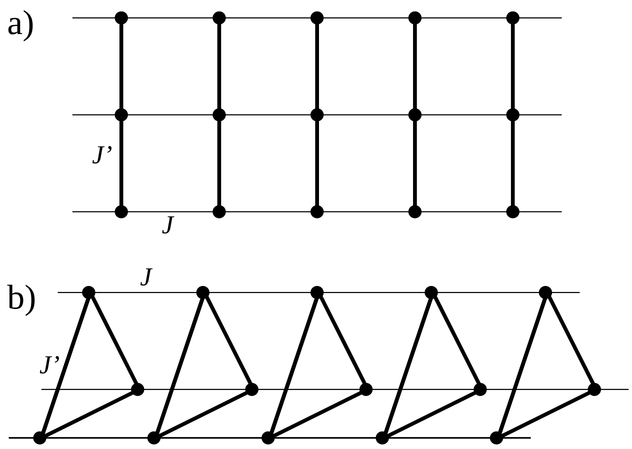

Figure 8: Illustration of three-leg ladders with coupling J along the legs (thin lines) and coupling J' along the rungs (bold lines). Panels a) and b) show open (OBC) and periodic boundary conditions (PBC) along the rungs, respectively. Points denote the positions of $S = 1/2$ spins.

3.4 $S = 1/2$ spin ladders

Spin ladders consist of N identical chains (called 'legs') coupled along so-called 'rungs' with a transverse coupling J'

$$H = \sum_{a=1}^{N} H^a_{XXZ} + J' \sum_a \sum_{x=1}^{L} \vec{S}^a_x \cdot \vec{S}^{a+1}_x \,. \tag{3.4}$$

For $N > 2$, two types of boundary conditions along the rungs have been considered in [i, ii]: Open boundary conditions (OBC) yield a planar arrangement and periodic boundary conditions (PBC) give rise to a cylindrical geometry. These two types of boundary conditions are illustrated in Fig. 8 for $N = 3$.

In the strong-coupling limit along the rungs $J' \gg J$ one can use the arguments of section 2.4 to predict plateaux for those values of $\langle M \rangle$ satisfying (1.1) with $V = N$. Complementary results can be obtained in the limit of weakly coupled chains $J \gg J'$ using the bosonization approach of section 2.2.1.

In the continuum limit one obtains N identical copies of the Hamiltonian (2.6) with perturbation terms coupling the fields of the different chains. There are always relevant perturbations involving the differences $\phi_a - \phi_b$ (or their duals $\tilde{\phi}_a - \tilde{\phi}_b$) of the fields for two coupled chains a, b. Therefore at most one degree of freedom, namely the 'diagonal' combination of fields $\phi_D \sim \sum_a \phi_a$, remains massless. The large-scale effective action for the spin ladder is then given again by a Hamiltonian of the form (2.6) for ϕ_D. The following interaction term can be generated radiatively in the Nrth order of perturbation theory

$$H_{\text{pert.}} \sim (J')^{Nr} \int \mathrm{d}x \;\; \cos(2Nrk_F x + r\sqrt{4\pi N}\phi_D) \,, \tag{3.5}$$

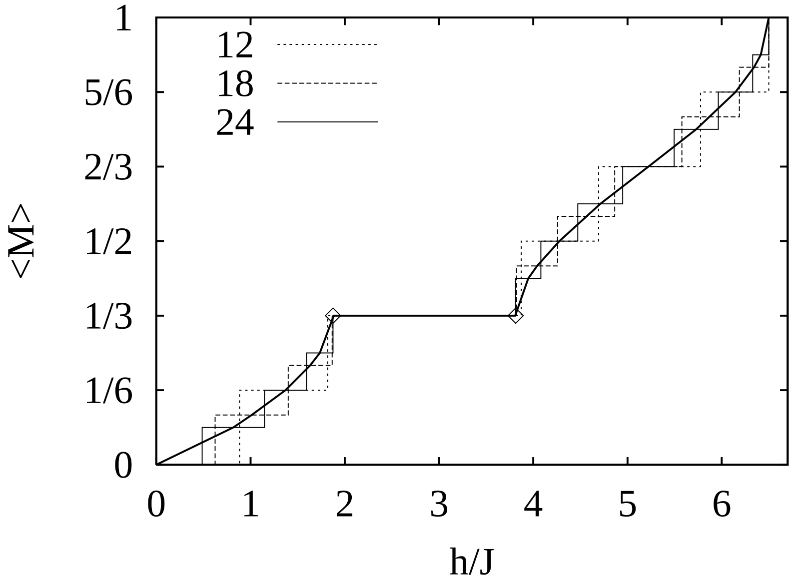

Figure 9: Magnetization curve of the $S = 1/2$ OBC three-leg ladder (Fig. 8a)) at $J' = 3J$. The thin lines denote ED results for finite systems with a total of 12, 18 and 24 spins [i], the bold line is an extrapolation to the thermodynamic limit. The diamonds show results of fourth-order strong-coupling expansions [ii] for the boundaries of the $\langle M \rangle = 1/3$ plateau.

where $k_F = (1 - \langle M \rangle)\pi/2$ is related to the total magnetization $\langle M \rangle$.

Two further steps complete the analysis [i,ii]. First, one has to determine the values of the magnetization for which the perturbation operator (3.5) is commensurate, *i.e.* the coefficient of the explicit x-dependence becomes a multiple of 2π. This operator is commensurate for the values of $\langle M \rangle$ satisfying (1.1) with $S = 1/2$ and $V = Nr$. Second, the zero-loop scaling dimension of this operator

$$\dim\left(\cos\left(r\sqrt{4\pi N}\phi_D\right)\right) = \frac{Nr^2}{\frac{2}{K} + \frac{4(N-1)J'}{\pi J}} \tag{3.6}$$

has to be less than two in order for it to be relevant in the renormalization-group sense. This dimension increases with the number of legs N, the magnetic field h (since K increases with increasing h for $\Delta > 0$) and with r, whereas a finite rung coupling $J' > 0$ lowers the dimension. The perturbation (3.5) is therefore most relevant for $r = 1$ where plateaux were predicted also by the simple strong-coupling argument mentioned above. The integer r can be identified as the periodicity of the groundstate and consequently $r \geq 2$ implies spontaneous breaking of translational symmetry. However, since the dimension (3.6) increases quadratically with r, it is very hard to imagine this perturbation becoming relevant for $r > 2$ and even for $r = 2$ one needs very favorable conditions, *i.e.* small N, small field h and strong inter-chain coupling J' in order to permit the opening of a plateau by the perturbing operator (3.5).

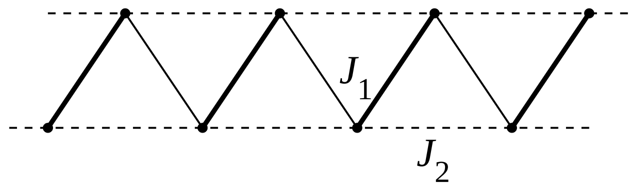

Figure 10: Heisenberg chain with nearest and next-nearest neighbor coupling J_1 and J_2, respectively, also called a two-leg zig-zag ladder. Points denote the locations of $S = 1/2$ spins.

Most plateaux open in fact at non-zero $J'_c > 0$. The bosonization analysis shows [ii] that the transition associated to a critical point $J'_c \neq 0$ is of the Kosterlitz-Thouless type [100]. Accordingly, the width of the plateau is exponentially suppressed [99] as J' approaches J'_c from above.

Complementary checks can be performed by an explicit ED computation of the magnetization curves in particular for intermediate J'/J. This is illustrated by Fig. 9 which shows the magnetization curve of the $S = 1/2$ three-leg ladder with open boundary conditions along the rungs at $J' = 3J$ [i]. As expected, there is a clear plateau with $\langle M \rangle = 1/3$ and the fourth-order strong coupling series for the boundaries of the plateau [ii] are in good agreement with the ED results.

For ladders with an odd number of legs, OBC and PBC are rather different since the latter boundary conditions are frustrating whereas the former are not. Based mainly on a strong-coupling effective Hamiltonian[10], an $\langle M \rangle = 0$ plateau (*i.e.* a spin gap at $h = 0$) was found not only in the PBC three-leg ladder [181] (see also [8]), but also more generally in ladders with odd N and PBC [ii, 89]. In view of the quantization condition (1.1), the opening of this $\langle M \rangle = 0$ plateau implies spontaneous breaking of translational symmetry by a period two. Such spontaneous symmetry breaking would also permit the opening of a plateau at $\langle M \rangle = 2/3$ in the PBC three-leg ladder. However, no evidence for the presence of such a plateau was obtained in [ii]. In addition, the corresponding operator at weak rung coupling J' is highly irrelevant (see (3.6) with $r = 2$ and $N = 3$) at $\langle M \rangle = 2/3$ whereas marginal perturbations are present for $\langle M \rangle = 0$ (see also [iii]). Further investigations [35, 195] indeed confirmed the absence of an $\langle M \rangle = 2/3$ plateau in the PBC three-leg ladder.

The results obtained for $2 \leq N \leq 4$ by combination of the methods are summarized in the magnetic phase diagrams, Fig. 6 of [ii]. Further plateaux and even richer phase diagrams are found when the coupling constants are modulated along the legs [21].

3.5 $S = 1/2$ zig-zag ladders

One possible generalization of spin ladders is a zig-zag coupling between the chains. The two-leg zig-zag ladder is shown schematically in Fig. 10. As can be observed from this figure, the two-leg zig-zag ladder is equivalent to a frustrated Heisenberg chain with nearest-neighbor

[10] In fact, this effective Hamiltonian was already derived and studied in [187] although this work appears to have had no impact on later developments.

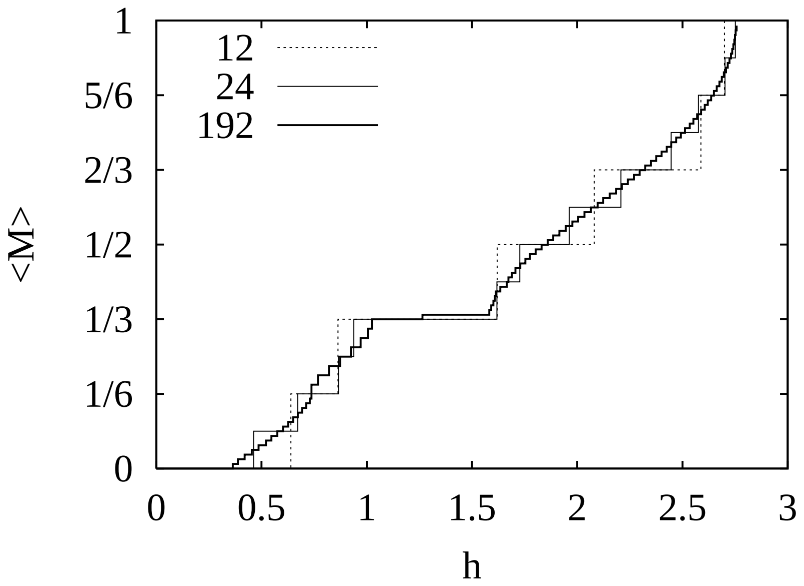

Figure 11: Magnetization curve of the $S = 1/2$ two-leg zig-zag ladder with $J_1 = 1$, $J_2 = 0.8$. The thin dashed and solid curves were obtained by ED of rings (periodic boundary conditions) with $L = 12$ and 24 sites, respectively [iii] and the bold solid curve was obtained by DMRG for $L = 192$ sites with open boundary conditions [142].

coupling $J_1 = J'$ and next-nearest-neighbor coupling $J_2 = J$. The thin and bold solid lines in Fig. 10 indicate a possible dimerization along the zig-zag chain. In the limit where one of these alternating inter-chain couplings vanishes one recovers the two-leg ladder of section 3.4.

The $S = 1/2$ frustrated Heisenberg chain has been studied extensively since sufficiently strong frustration gives rise e.g. to incommensurability and a spin gap (see for example [216] and references therein). In the presence of a magnetic field, the spin gap leads to an $\langle M \rangle = 0$ plateau. The $S = 1/2$ frustrated Heisenberg (or two-leg zig-zag ladder) is among the models where the study of the magnetization process by the Lanczos method has a particularly long tradition [53, 62, 63, 174, 198, 200, 207]. Nevertheless, in such studies plateaux with $\langle M \rangle \neq 0$ were observed only for modulated coupling constants [22, 176, 200, 203] or for more than two legs [iii, 218].

In particular for a certain three-leg zig-zag ladder indications for an $\langle M \rangle = 1/3$ plateau were obtained [iii] which implies spontaneous breaking of translational symmetry by a periodicity three since this particular three-leg zig-zag ladder can be identified with a Heisenberg chain with frustrating couplings up to distance four. Remarkably, a recent DMRG study of the two-leg zig-zag ladder exhibited a plateau at $\langle M \rangle = 1/3$ in the region of strong frustration $J_1 \approx J_2$ [142]. This $\langle M \rangle = 1/3$ plateau in the two-leg zig-zag ladder is also accompanied by spontaneous breaking of translational symmetry by a period three.

Fig. 11 shows the magnetization curve of the two-leg zig-zag ladder for $J_2 = 0.8\,J_1$ as obtained by DMRG for $L = 192$ sites and open boundary conditions [142] in comparison to ED results for $L = 12$ and 24 sites with periodic boundary conditions [iii]. In this figure, one observes a clear $\langle M \rangle = 1/3$ plateau[11] in addition to the spin gap mentioned above. The analysis of results on small clusters is subject to several problems. First, the groundstates of zig-zag ladders in a magnetic field have in general incommensurate momenta [iii] which leads to oscillating finite-size effects. Second, one should concentrate on system sizes that can accommodate the known antiferromagnetic groundstates in the limiting cases $J_1 \to 0$ and $J_2 \to 0$. For the case of two legs, this implies that L should be a multiple of 4. In addition, only those values of the magnetization can be studied which are realized for a given system size. In particular, $\langle M \rangle = 1/3$ is realized only if L is a multiple of 3. These considerations restrict the system sizes that should be used for the discussion of an $\langle M \rangle = 1/3$ plateau in the two-leg zig-zag ladder to multiples of 12. The first two cases are $L = 12$ and $L = 24$. These are used in Fig. 11 and are in good agreement with the DMRG results of [142].

The two-leg zig-zag ladder is also interesting for ferromagnetic inter-chain coupling [iii]: For weak ferromagnetic $J_1 < 0$, spins flip in pairs. The number of spins flipping simultaneously increases for stronger ferromagnetic coupling until one reaches the uniformly distributed RVB state at $J_1 = -4\,J_2$ [73]. Beyond this point, the behavior becomes completely ferromagnetic.

The field-theory analysis of zig-zag ladders is particularly interesting in the absence of a magnetic field: Contributions to the low-energy action from the staggered magnetization in the legs cancel for zig-zag coupling. Therefore, the leading perturbations include a new left-right asymmetric term [132]. However, at finite magnetization $\langle M \rangle \neq 0$, the bosonization analysis becomes similar to that of the 'normal' spin ladders discussed in section 3.4 [iii].

Finally, we mention in passing that the magnetization process of XXZ zig-zag ladders is also relevant to the physical problem of adsorption of noble gases on the surface of carbon nanotubes [67].

3.6 Models with local conservation laws

For certain systems with local conservation laws first-order strong-coupling results for the magnetization process (see section 2.4) remain exact over a finite range of parameters [vi, 30, 96, 120, 177, 178]. These models have the property that one can define conserved cell spins for cells x

$$\vec{T}_x = \sum_{\vec{x} \in \text{cell } x} \vec{S}_{\vec{x}} \,. \tag{3.7}$$

Then the original Hamiltonian with fixed spins $\vec{S}_{\vec{x}}$ at sites $\vec{x}$ can be mapped to a family of Hamiltonians

$$H(\{T_x\}) = \sum_{\langle x,y \rangle} J_{x,y}\, \vec{T}_x \cdot \vec{T}_y + \frac{1}{2} \sum_x J'_x\, \vec{T}_x^2 - h \sum_x T_x^z \tag{3.8}$$

[11] The step on the $\langle M \rangle = 1/3$ plateau in the DMRG curve is due to the open boundaries.

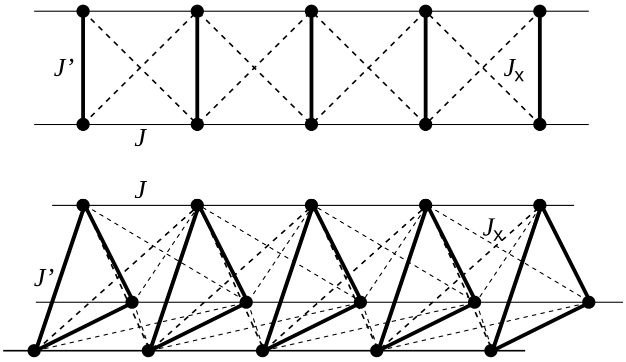

Figure 12: Frustrated ladders with leg coupling J, rung coupling J' and diagonal coupling $J_\times$. The top panel shows a two-leg ladder, the bottom one a three-leg ladder with periodic boundary conditions along the rungs. Points denote the locations of the spins.

with the cell spin $\vec{T}_x^2 = T_x(T_x + 1)$ taking all possible values of the total spin in this cell. Note that in passing from the original spin Hamiltonian to the family (3.8) we have dropped an irrelevant additive constant.

The family of Hamiltonians (3.8) has several advantages as compared to the original Hamiltonian. First, some of the coupling constants (J'_x) appear only linearly in front of a constant. The behavior as a function of these coupling constants can therefore be investigated analytically. Second, examples show that only a very small number of combinations of the quantum numbers $\{T_x\}$ give rise to groundstates in a magnetic field, implying that only few of the Hamiltonians (3.8) need to be studied. Finally, in those cases where $T_x = 0$, the coupling with cell x vanishes. This can lead to a decoupling of different parts of the chain and then only 'fragments' with a finite length have to be investigated – again a considerable simplification.

The Hamiltonian of the frustrated ladders shown in Fig. 12 can be cast in the form (3.8) provided that the diagonal coupling $J_\times$ and the leg coupling J are equal $J = J_\times$. In this case, each spin on one rung has equal couplings with every spin on a neighboring rung. The Hamiltonian is therefore invariant under local permutations of the spins on a rung which leads to the local conservation laws in this case.

The frustrated $S = 1/2$ two-leg ladder can be mapped to the $S = 1$ chain for sufficiently weak J', as was already noticed in [61]. For large J', one finds a plateau with $\langle M \rangle = 1/2$ in the two-leg ladder [120] in addition to a spin gap at $\langle M \rangle = 0$. The groundstate of this $\langle M \rangle = 1/2$ plateau manifestly breaks translational symmetry since on it singlets $T_x = 0$ and triplets $T_x = 1$ alternate. The competition of different groundstates for intermediate J' was analyzed in detail in [vi] yielding the family of magnetization curves Fig. 3 of [vi] and the groundstate phase diagram Fig. 4 of [vi]. The three-leg ladder shown in the lower panel of Fig. 12 was first discussed in [vi] and plateaux with $\langle M \rangle = 1/3$ and $2/3$ were found – see the family of magnetization curves Fig. 6 of [vi] and the groundstate phase diagram Fig. 7 of [vi]. The states of both plateaux in this three-leg ladder are macroscopically degenerate, *i.e.* give rise to a finite zero-temperature entropy. Furthermore, the state of the $\langle M \rangle = 2/3$

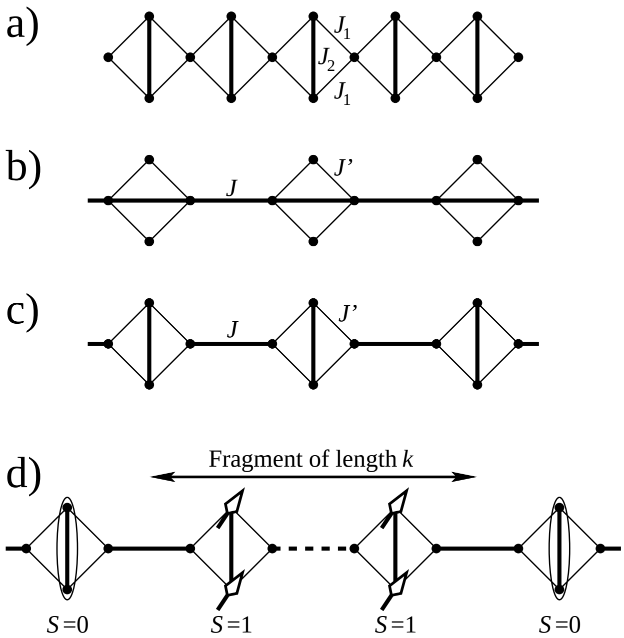

Figure 13: Several models with local conservation laws associated to the vertical dimers: a) diamond chain, b) quadrumer chain, c) orthogonal dimer chain. Panel d) illustrates a 'fragment' of length k in the orthogonal dimer chain: k consecutive vertical dimers form triplets ($S = 1$) terminated by vertical dimer singlets ($S = 0$ – denoted by ellipses). Points denote again the locations of the spins.

plateau again manifestly breaks translational symmetry by a period two [vi].

In the frustrated ladders studied in [vi], spontaneous breaking of translational symmetry was observed with periodicity at most two. However, it should be noted that the finite accuracy of the underlying numerical data never allows one to rigorously rule out the appearance of higher-periodicity symmetry breaking in small parameter regions. Of course, further plateaux can be found if translational symmetry is broken *explicitly*, e.g. in the two-leg ladder with a suitable modulation of the coupling constants [30].

Further models with local conservation laws are indicated in Fig. 13a)-c). In these models, the local conservation laws are associated to local reflections of a pair of spins above and below the center of the chains. Fig. 13a) shows the diamond chain. A zero-field gap opens in the $S = 1/2$ diamond chain model for sufficiently large J_2, with a spontaneously dimerized groundstate for intermediate J_2 [193]. A plateau with $\langle M \rangle = 1/3$ is present in this model for all $J_1, J_2 > 0$ and even for $J_1 < 0$, $J_2 > -J_1$ [v].

The $S = 1/2$ quadrumer chain of Fig. 13b) was studied in the context of the low-temperature charge-ordered state of $\alpha'{-}\mathrm{NaV_2O_5}$ [vii, 69, 204]. Note that in this model, the coupling across the quadrumers prevents a decoupling of chain segments by formation of a singlet $T_x = 0$ on a pair of vertical dimer spins, leading to the absence of simple fragmented eigenstates. The magnetization process of this model was studied in the appendix of [vii] by ED of the effective Hamiltonians (3.8) (see in particular Fig. 11 loc. cit.) and clear

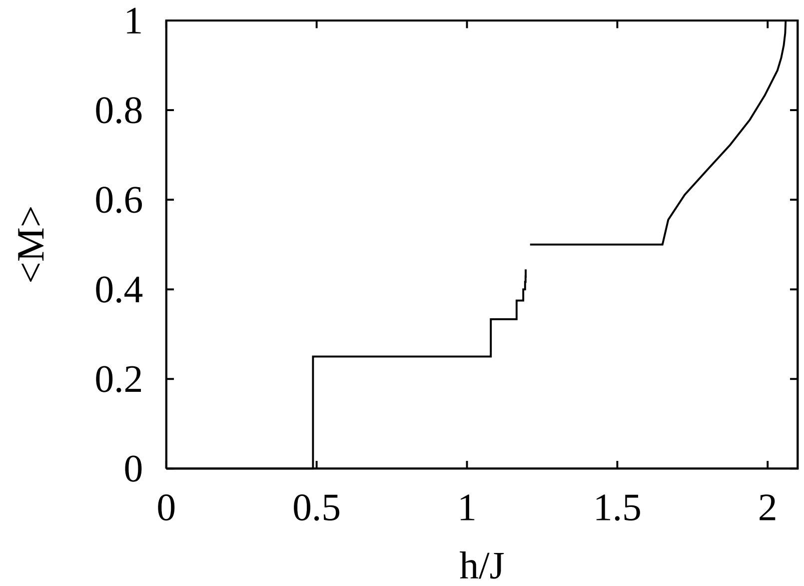

Figure 14: Magnetization curve the $S = 1/2$ orthogonal dimer chain of Fig. 13c) with $J' = 0.7J$, see [177]. Note the long (probably infinite) sequence of plateaux for $\langle M \rangle < 1/2$.

plateaux were found at precisely those values permitted by the quantization condition (1.1) with $V = 4$ given by the volume of the unit cell of the Hamiltonian, namely $\langle M \rangle = 0$ and $1/2$.

The $S = 1/2$ orthogonal dimer chain shown in Fig. 13c) was originally introduced as a one-dimensional toy model for CaV_4O_9 [82, 86, 158]. It attracted renewed attention recently since it can also be regarded as a one-dimensional version of the two-dimensional Shastry-Sutherland model [182] which was found to be realized in $SrCu_2(BO_3)_2$ [85], a material which exhibits several plateaux (at $\langle M \rangle = 1/8$, $1/4$ and $1/3$) in its magnetization curve [85, 143].

A first study [96] of the magnetization process of the $S = 1/2$ orthogonal dimer chain found plateaux with $\langle M \rangle = 1/4$ and $1/2$. However, this study missed further plateaux and thus the remarkable property of the orthogonal dimer chain that it gives rise to a magnetization curve with many plateaux, possibly even an infinite sequence for some values of the parameters [177, 178]. The mechanism underlying this sequence of plateaux [177] is sketched in Fig. 13d): k consecutive vertical dimers form triplets ($S = 1$), separated by singlets ($S = 0$). Covering the chain periodically with such 'fragments' of length k each in the sector $S^z = k$ yields

$$\langle M \rangle = \frac{k}{2k+2}\,. \tag{3.9}$$

At $J' = 0.7J > 0$ it was found in [177] that for $\langle M \rangle < 1/2$ only precisely these states consisting of fragments of length k with $S^z = k$ appear as groundstates in a magnetic field, whereas for $\langle M \rangle \geq 1/2$ the groundstate is in a sector where all vertical dimers form triplets $S = 1$. In this case, fragments of increasing length become groundstates with increasing field, leading to a magnetization curve with infinitely many plateaux at the magnetization values given by (3.9) and jumps in between, compare Fig. 14. This infinite series accumulates at $\langle M \rangle = 1/2$, where one finds a further pronounced plateau before a smooth transition to saturation follows.

The infinite sequence of plateaux arises in the orthogonal dimer chain because the groundstates manifestly break translational symmetry with arbitrarily long periodicity $k+1$, *i.e.* there is no upper bound on the spontaneous breaking of translational symmetry. The present author believes this to be a very important observation, but he is not aware of a rigorous proof that the groundstates are indeed the aforementioned ones. He has therefore performed some checks[12] for $k \le 8$. Thus, at least the presence of the plateaux associated to fragments of length $k \lesssim 5$ is on rather safe grounds. Even a spontaneous breaking of translational symmetry by a period 5 is remarkable, as the author is not aware of any other case where such a large period was observed.

Due to the local conservation laws, transitions in all the models discussed in this section can occur via crossings of levels with different quantum numbers T_x and may thus be of first order. This also leads to jumps in the magnetization curves which are associated to linear parts in the energy $E(\langle M \rangle)$ as a function of magnetization $\langle M \rangle$ (see Fig. 2 of [vi] for an illustration). In particular the latter property is intimately linked to the presence of the local conservation laws and thus unstable against perturbations of the parameters (such as $J \neq J_\times$ for the models in Fig. 12) which destroy these conservation laws. On the other hand, the plateau states have a spin gap and are therefore stable under perturbations (see [v, 139, 166, 201] for examples).

3.7 Charge carriers: Modulated Hubbard chains

In the preceding sections we have discussed models with localized spins. One may now wonder what happens if mobile charge carriers are introduced. It turns out that plateaux can appear at values of the magnetization that are not subject to the quantization condition (1.1) if a fixed incommensurate density of carriers is doped into the system. One example is the one-dimensional Kondo-lattice model where unpaired spins are polarized spontaneously and thus give rise to a doping-dependent magnetization plateau at small magnetic fields (see e.g. [206, 211]). Also an integrable spin-S generalization of the $t-J$ chain doped with mobile $(S-1/2)$ carriers exhibits a plateau at a value of the magnetization controlled by doping [54]. In this section we will summarize results for modulated Hubbard chains [viii, ix] (see [19] for a discussion of Hubbard ladders).

Consider a Hubbard chain (2.9) where the hopping amplitude t and the chemical potential μ are modulated

$$H = -\sum_{x,\alpha} t(x)\ (c^\dagger_{x+1,\alpha} c_{x,\alpha} + \text{h.c.}) + U \sum_x c^\dagger_{x,\uparrow} c_{x,\uparrow} c^\dagger_{x,\downarrow} c_{x,\downarrow}$$

[12]Fig. 14 shows a version of the magnetization curve which is based on data of the present author. A careful reader might indeed observe small differences of this figure as compared to the original one, Fig. 3 of [177].

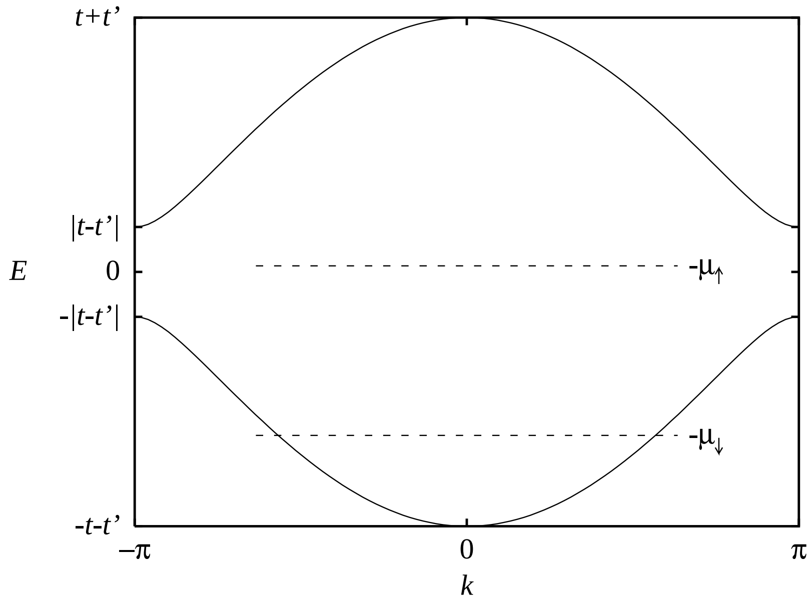

Figure 15: The two bands arising in a dimerized Hubbard chain with $U = 0$. The horizontal axis shows momentum k and the vertical axis the one-particle energy E. Dashed lines indicate the chemical potentials for up- and down-electrons.

$$+\sum_{x,\alpha} \mu(x)\ c^{\dagger}_{x,\alpha} c_{x,\alpha} - \frac{h}{2} \sum_{x} (c^{\dagger}_{x,\uparrow} c_{x,\uparrow} - c^{\dagger}_{x,\downarrow} c_{x,\downarrow})\,. \tag{3.10}$$

$t(x)$ and $\mu(x)$ are assumed to be periodic in the variable x with period p. For most explicit discussions, $t(x) = t$ if $x \neq m\,p$, $t(m\,p) = t'$ for an integer m and a uniform chemical potential $\mu(x) = \mu$ were assumed in [viii, ix]. Note that for $U \gg t$, the Hamiltonian (3.10) maps to the $t - J$ model with a modulated coupling constant $J_x = 4t(x)^2/U$. In this large-U limit and at half filling $n = 1$ one therefore recovers exactly the modulated $S = 1/2$ Heisenberg chains discussed in section 3.3.

Several approaches can be used to study the groundstate phase diagram of the model (3.10) [viii, ix]. First, in the spirit of section 2.4, one can consider the limit $t' \to 0$ of strongly coupled clusters of p Hubbard sites. One then finds fully gapped states (*i.e.* a spin and a charge gap) if both conditions

$$p\,n_{\uparrow} = \frac{p}{2}\,(n + \langle M \rangle) \in \mathbb{Z}\,, \qquad p\,n_{\downarrow} = \frac{p}{2}\,(n - \langle M \rangle) \in \mathbb{Z} \tag{3.11}$$

are satisfied. Here we use the generalization $\langle M \rangle = n_{\uparrow} - n_{\downarrow}$ of the previous definition (2.17) at half filling $n = 1$.

A more interesting situation arises if only one of the conditions (3.11) is satisfied. This case is most easily understood in the limit of weak U. At $U = 0$, the Hamiltonian (3.10) can be diagonalized analytically and one finds p bands, as is illustrated for $p = 2$ in Fig. 15. For $h \neq 0$, up- and down-electrons experience different chemical potentials $\mu_{\uparrow} = \mu - h/2$,

$\mu_\downarrow = \mu + h/2$. Now consider the case $n_\uparrow = 1/2$, *i.e.* $\langle M \rangle = 1 - n$. In this case, the lower band is completely filled with up-electrons and the corresponding chemical potential $-\mu_\uparrow$ lies in the band gap. Assume further that $n < 1$. In this situation $-\mu_\downarrow$ is not in the band gap, but somewhere in the lower band, as indicated in Fig. 15. If h is now changed a little, also $\mu_\uparrow$ changes slightly, but remains in the band gap if the change is not too large. If one imposes a fixed filling n, the chemical potential μ must then be readjusted to keep $\mu_\downarrow$ and thus $n_\downarrow$ fixed. This implies a magnetic gap and thus a plateau whose magnetization value depends linearly on n if $h/2 - \mu$ is tuned through the band gap at fixed filling. Corrections to this non-interacting picture can be computed to first order in U by standard quantum-mechanical perturbation theory [ix].

An alternative approach which treats the Coulomb repulsion U exactly, but uses perturbation theory in $t' - t$, is bosonization, see section 2.2.2. For simplicity, we will concentrate on zero magnetic field here and refer the reader to [viii, ix] for a complete discussion. In the continuum limit of (3.10) one obtains the Gaussian part (2.10) and several perturbation terms among which the most relevant one is given by

$$O_{\text{pert.}} = \lambda_1 \sin[\pi n/2 + pn\pi x - \sqrt{\pi}\xi\phi_c] \cos[\sqrt{2\pi}\phi_s] + \lambda_2 \sin[\pi n + 2pn\pi x - \sqrt{4\pi}\xi\phi_c] \ . \quad (3.12)$$

The operator with coefficient λ_2 involves only the charge field ϕ_c and is commensurate for $pn \in \mathbb{Z}$. Since it is also relevant, it leads to the opening of a charge gap for $pn \in \mathbb{Z}$. Note that this conclusion remains valid at non-zero field (although this is not strictly covered by the conditions (3.11)), *i.e.* there is always a charge gap for $pn \in \mathbb{Z}$. This generalizes the well-known charge gap in the half-filled Hubbard chain ($n = 1$) and the charge gap in the quarter-filled dimerized Hubbard chain ($p = 2$, $n = 1/2$) [149]. If one further restricts to densities satisfying $pn \in 2\mathbb{Z}$, the operator with coefficient λ_1 in (3.12) which couples to the spin field ϕ_s also becomes commensurate. This leads to an additional spin gap at zero magnetic field, *i.e.* a plateau with $\langle M \rangle = 0$.

The case of non-zero magnetic field is more complicated. However, each of the conditions (3.11) is recovered as a commensurability condition for a perturbing operator [viii, ix]. Consequently, a gap opens in the spectrum. If one imposes a fixed doping n, a detailed analysis [ix] of this constraint shows that the system has a magnetization plateau. Note, however, that if only one of the conditions (3.11) is satisfied, some massless modes remain which lead e.g. to a continuous dependence of the magnetization value on doping, a specific heat vanishing linearly as temperature goes to zero and metallic charge transport. Furthermore, certain superconducting correlations exhibit power-law behavior on such a doping-dependent plateau [ix].

Finally, the aforementioned conclusions can also be checked by ED. This is illustrated in Fig. 16 for a dimerized Hubbard chain ($p = 2$) at intermediate Coulomb repulsion $U = 3t$ and intermediate modulation strength of the hopping amplitude $t' = 0.7t$, *i.e.* a region which is not particularly well controlled by the aforementioned perturbative approaches. The polygons in this figure indicate regions in the μ-h plane where the groundstate has a certain number of up- and down-electrons. For those states that correspond to a completely gapped state in the thermodynamic limit, the equivalent quantum numbers n and $\langle M \rangle$ are

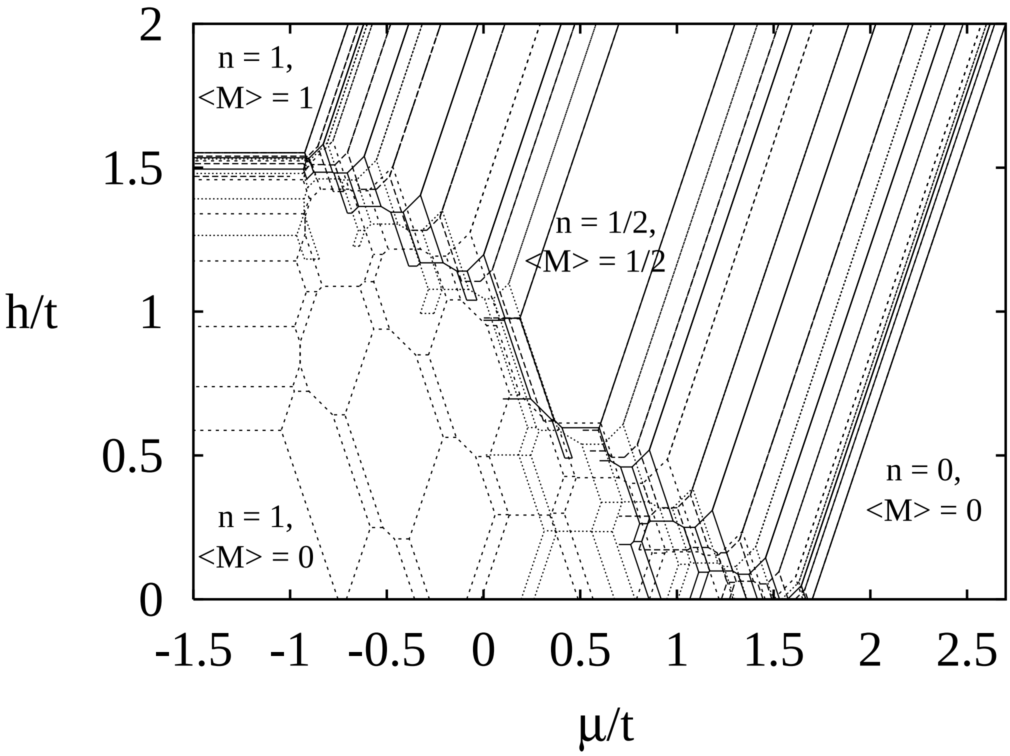

Figure 16: Groundstate phase diagram of the dimerized Hubbard chain ($p = 2$) with $U = 3t$, $t' = 0.7t$ as a function of chemical potential μ and magnetic field h. The lines are for $L = 16$ (long dashes), $L = 18$ (dotted), $L = 20$ (short dashes) and $L = 24$ (full). Note that only the data for $L = 16$ [ix] is complete.

indicated in Fig. 16. The data for $L = 16$ sites was already presented in [ix] while the data for larger system sizes is new, although for these cases it was not possible to study all sectors[13]. The fermionic nature of the Hubbard model is reflected in large finite-size effects, even close to the fully polarized state $\langle M \rangle = n$[14]. Nevertheless, one can also recognize the charge gap at half filling ($n = 1$) as well as the doping-dependent plateau with $\langle M \rangle = 1 - n$ (the reader may use the schematic groundstate phase diagram Fig. 1a) of [viii] as a guide). Further data for this dimerized Hubbard chain at smaller system sizes is shown in Fig. 2 of [ix] and similar results for a trimerized chain are presented in Fig. 3 of [ix]. All conclusions can be summarized in the schematic groundstate phase diagrams, shown in Fig. 1 of [viii], which are based on the ED results.

[13]The largest sector that was studied occurs for $L = 24$ sites with 12 up- and 2 down-electrons. After exploiting symmetries, in particular translational invariance, this required a computation of the smallest eigenvalue in dimension 62 196 512.

[14]Since in the polarized state one has $n_{\downarrow} = 0$ for $n \leq 1$, the Coulomb repulsion in (3.10) is absent and accordingly the eigenvalues can be computed analytically. However, this is no longer possible even if only one down-electron is present and therefore there is no analytic expression for the saturation field.

To summarize, magnetic systems doped with charge carriers are systems with different magnetic species whose individual densities of particles can vary. If a magnetic field is applied to such a system while keeping the total density of particles fixed, plateaux can appear in the magnetization curve at irrational values of the magnetization $\langle M \rangle$, violating the quantization condition (1.1). However, a gap opens only if one of the species is commensurate, leading to the conditions (3.11) for modulated Hubbard chains.

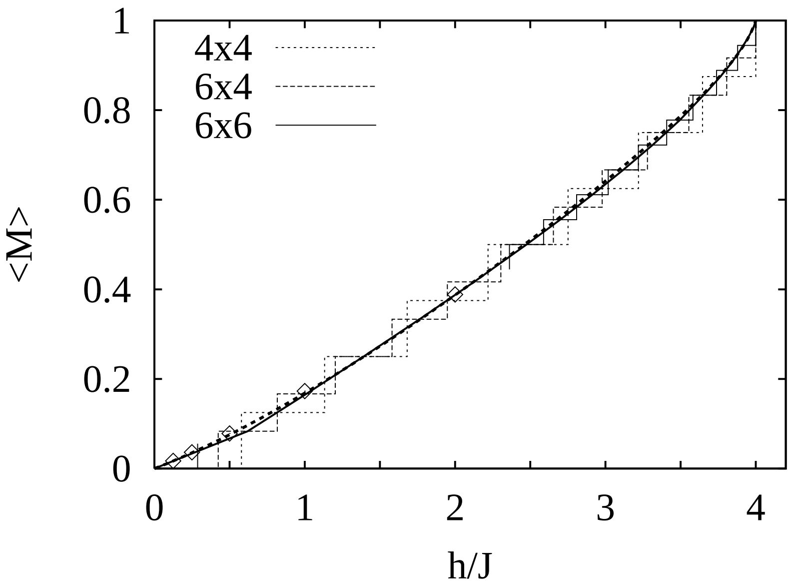

Figure 17: Magnetization curve of the $S = 1/2$ Heisenberg antiferromagnet on the square lattice, based on data of [xi] with extensions at larger system sizes (the value of the finite-size spin gap on the 6×6 cluster is taken from [208]). The full bold line is an extrapolation to the thermodynamic limit, the dashed bold line the second-order spinwave result of [227]; diamonds show QMC results [171].

4 Two dimensions

4.1 Square lattice

Given its relevance to the high-T_c cuprates [117], the magnetization process of the $S = 1/2$ square lattice antiferromagnet has received surprisingly little attention until recently. ED for the magnetization process of the isotropic Heisenberg model was first performed on a 4×4 cluster in [109] and extended for the complete curve up to $5 \times 5 + 1 = 26$ sites in [223]. The magnetization curve of the isotropic Heisenberg model on the square lattice was also computed by second-order spinwave theory based on a Néel-ordered state [227]. ED results for the XXZ model with $\Delta \neq 1$ were reported in [xi]. QMC computations were first performed only for Ising-like anisotropies $\Delta > 1$ on clusters with up to 100 sites [98]. More recently, high-quality QMC results are becoming available e.g. also for $\Delta = 1$ [171,192] and the XX model ($\Delta = 0$) [12].

Fig. 17 shows the magnetization curve of the $S = 1/2$ square-lattice Heisenberg model ($\Delta = 1$), based mainly on the ED data of [xi] with some extensions at larger system sizes[15]. The full bold line denotes an extrapolation to the thermodynamic limit which is obtained by connecting the midpoints of the finite-size steps at the largest available system size. One

[15]The value of the finite-size spin gap on the 6×6 cluster is taken from [208].

observes a smooth magnetization curve with no peculiar features (in particular no plateaux) for $|\langle M\rangle| < 1$.

Note that close to saturation the extrapolated curve includes data at large system sizes, which is not shown explicitly in Fig. 17 (see, however, section 5.2). More precisely, for $\langle M\rangle \geq 0.84375$, the curve is based exclusively on clusters with at least 8×8 sites. The high-field part of the magnetization curve is therefore particularly well controlled by ED.

The second-order spinwave result [227] is shown by the bold dashed line in Fig. 17 and available stochastic-series-expansion QMC results [171] by diamonds. These data compare well with each other. Also the curves based on the extrapolation of finite-system ED and spinwave theory [227] generally show good agreement with small deviations around $h \approx 3J$. For example, at $h = 3.7J$ the data on the 8×8 cluster interpolates to a value of $\langle M\rangle$ which is approximately 0.003 lower than the second-order spinwave result [227]. Comparison of the finite-size data with the extrapolated curve in Fig. 17 indeed shows that the mid-point method tends to underestimate the magnetization $\langle M\rangle$ close to saturation. Nevertheless, as long as no accurate QMC results are available in this high-field range, it remains an open issue which of the other two methods yields the more accurate approximation (both of them are certainly quite good) to the thermodynamic limit of the $S = 1/2$ Heisenberg model on the square lattice.

Finally, we note that Néel order prevails in the transverse components for $|\langle M\rangle| < 1$ (see e.g. [223]).

4.2 Triangular lattice

In contrast to the square lattice, the $S = 1/2$ XXZ model on the triangular lattice is among the first models whose magnetization process was studied by ED [134]. These early studies already found a plateau with $\langle M\rangle = 1/3$, at least for Ising-like anisotropies $\Delta > 1$. Due to the restriction to at most 21 sites, it was not completely clear at that time whether the plateau persists in the isotropic regime $\Delta \approx 1$. The magnetization process of the isotropic model was analyzed further using spinwave theory [34]. This study provided evidence that the $\langle M\rangle = 1/3$ plateau exists also at $\Delta = 1$ and estimates for its boundaries were obtained. The state of the $\langle M\rangle = 1/3$ plateau corresponds to all spins on two of the three sublattices of the triangular lattice pointing up and all spins on the third sublattice pointing down, as is also easily understood in the Ising limit $\Delta \gg 1$ [xi, 127].

The magnetization process of the XX model in longitudinal and transverse fields was studied in [188] on clusters with up to 24 sites using a transfer QMC method and it was found that no plateau is present for a longitudinal field (*i.e.* a field along the anisotropy axis). Nevertheless, a plateau-like feature emerges at $\langle M\rangle = 1/3$ for a transverse field [188].

The magnetization process of the XXZ model on the triangular lattice was again investigated by ED in [xi] using also larger clusters and for general anisotropies Δ. Fig. 18 shows the magnetization curve obtained by ED for $\Delta = 1$ (this figure is essentially taken from [xi] with minor extensions at larger system sizes). One observes a clear plateau at $\langle M\rangle = 1/3$ in an otherwise smooth magnetization curve. The first-order spinwave results for the magnetic fields both at the lower and the upper boundaries of the $\langle M\rangle = 1/3$ plateau [34] are about

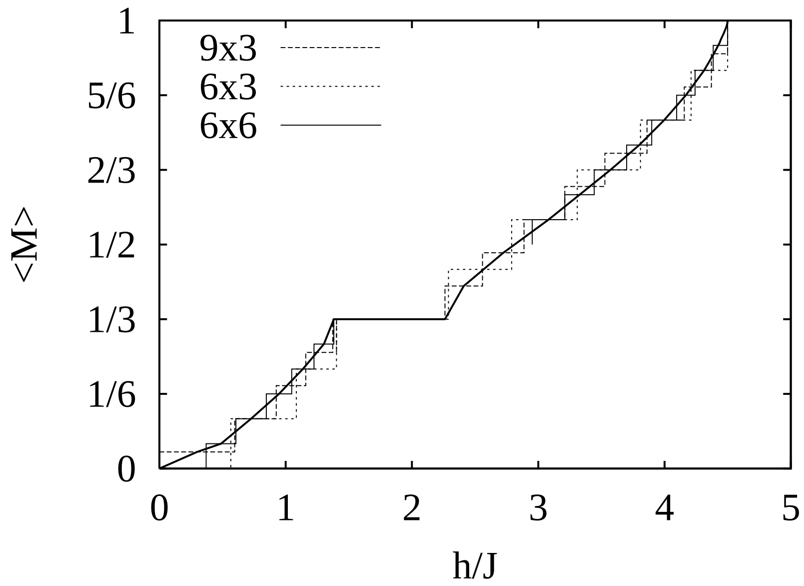

Figure 18: Magnetization curve of the $S = 1/2$ Heisenberg antiferromagnet on the triangular lattice, reproduced after [xi] with small extensions at larger system sizes. For $\langle M \rangle \leq 1/3$, the curves with 27 and 36 spins are based on data of [13]. The bold line is an extrapolation to the thermodynamic limit.

$0.13J$ smaller than the ED results for $S = 1/2$.

Other approaches are still less successful. E.g. a Chern-Simons theory [123] predicts a spurious plateau at $\langle M \rangle = 0$.

4.3 Frustrated square lattice

The frustrated square lattice differs from the ordinary square lattice by the presence of frustrating diagonal couplings J', see Fig. 19. The $S = 1/2$ model has received a lot of attention at zero magnetic field since strong frustration leads to a melting of magnetic long-range order at zero temperature (*i.e.* opening of a spin gap – see [102] for a recent review). Also the magnetization process of the $S = 1/2$ model has been studied by several authors [xii, xiii, xiv, 29, 49, 109, 223]. Candidates for plateaux in this model were observed already quite early [109]. However, the first numerical works [109, 223] used rather peculiar boundary conditions and investigated only a limited region of parameters (e.g. $J' \leq J/2$ in [223]). It was therefore important to perform checks on bigger rectangular clusters and in a wider range of parameters [xii, xiii, xiv].

It may be instructive to consider some limiting cases first. For $J' = 0$, one recovers the square lattice which is Néel-ordered even in the presence of a magnetic field (see section 4.1 – for $h \neq 0$ Néel order is observed only in the transverse spin components). On the other hand, for $J = 0$, the system decouples into two interpenetrating square lattices which are again Néel-ordered up to the saturation field. For weak $J > 0$, the Néel vectors of the two

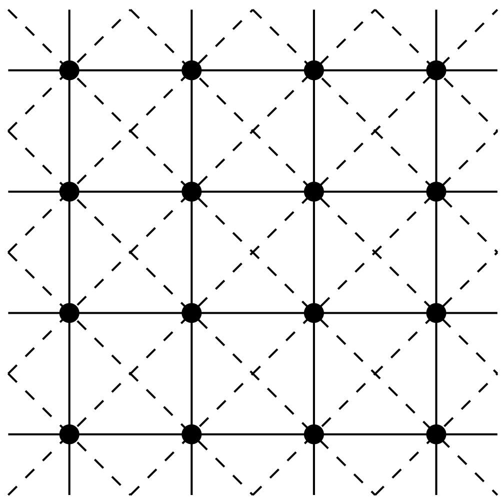

Figure 19: Frustrated square lattice. Points denote positions of spins, full lines coupling constants of strength J and dashed lines coupling constants of strength J'.

sublattices are coupled, leading to a 'striped' state. The stability region of these two ordered states can be analyzed by linear spinwave theory, leading to the groundstate phase diagram shown in Fig. 1 of [xii] for $S = 1/2$. The most interesting region is the intermediate region where neither of the two ordered states is stable. In the classical limit $S \to \infty$, it arises due to a high degeneracy of the groundstate at $J' = J/2$.

Just for $\langle M \rangle = 1/2$, there is a special ordered 'collinear' state with three spins pointing up and one down around each plaquette, see Fig. 2 of [xii]. We will call this state the 'uuud-state'. Now one can argue that this ordered uuud-state is stabilized by fluctuations (called 'order by disorder') [xii]. Indeed, Monte Carlo simulations [xii, xiv] show stabilization of the uuud-state by thermal fluctuations at low temperatures in the classical model for $J' \approx J/2$.

For $S = 1/2$ one can study the static structure factors by ED and finds that the uuud-state is also stabilized at zero temperature by quantum fluctuations for $0.5 \lesssim J'/J \lesssim 0.66$ [xii, xiii, xiv]. Furthermore, for $S = 1/2$ there is a magnetic gap above the uuud-state, giving rise to a plateau at $\langle M \rangle = 1/2$ in the magnetization curve. This is illustrated in Fig. 20: For $J' = 0.5J$ (a) one observes no plateau whereas for $J' = 0.6J$ (b) there is a clear plateau at $\langle M \rangle = 1/2$ (a spin gap is believed to be present in both cases [101]). Most of this data was presented in [xii, xiii]. Fig. 20 contains extensions mainly for bigger systems sizes or smaller values of $\langle M \rangle$ where the dimensions of the vector spaces are largest.

Due to limitations of computational resources, some selections had to be made a priori in [xii, xiii, xiv] regarding the spatial symmetry of the states considered for the largest vector space dimensions. In the meantime, the symmetry of the groundstates was reconsidered more systematically and it turned out that the correct ones were in fact missed for a few parameters in the $S^z = 9$ sector on the 6×6 cluster and in the $S^z = 17$ sector on the 8×6 cluster. Nevertheless, the energy differences are so small that the corrections to the

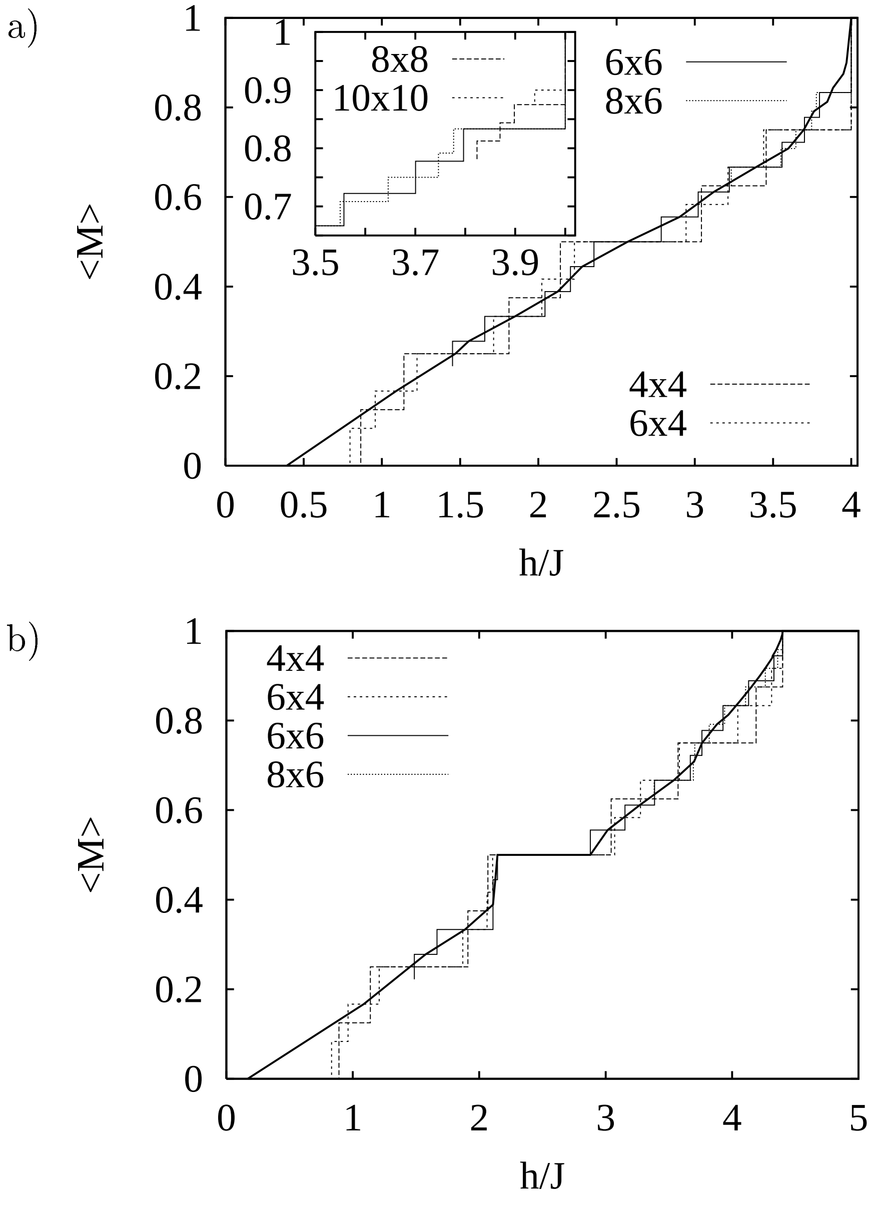

Figure 20: Magnetization curves of the $S = 1/2$ Heisenberg antiferromagnet on the frustrated square lattice at $J' = 0.5J$ (a) and $J' = 0.6J$ (b). The magnetization curves, in particular the one at $J' = 0.6J$ (b), are based on data presented in [xii,xiii] with some extensions at the larger system sizes. Thin lines denote finite-size data; the full bold line is an extrapolation to the thermodynamic limit which at $\langle M \rangle = 0$ uses values of the spin gap given in [101].

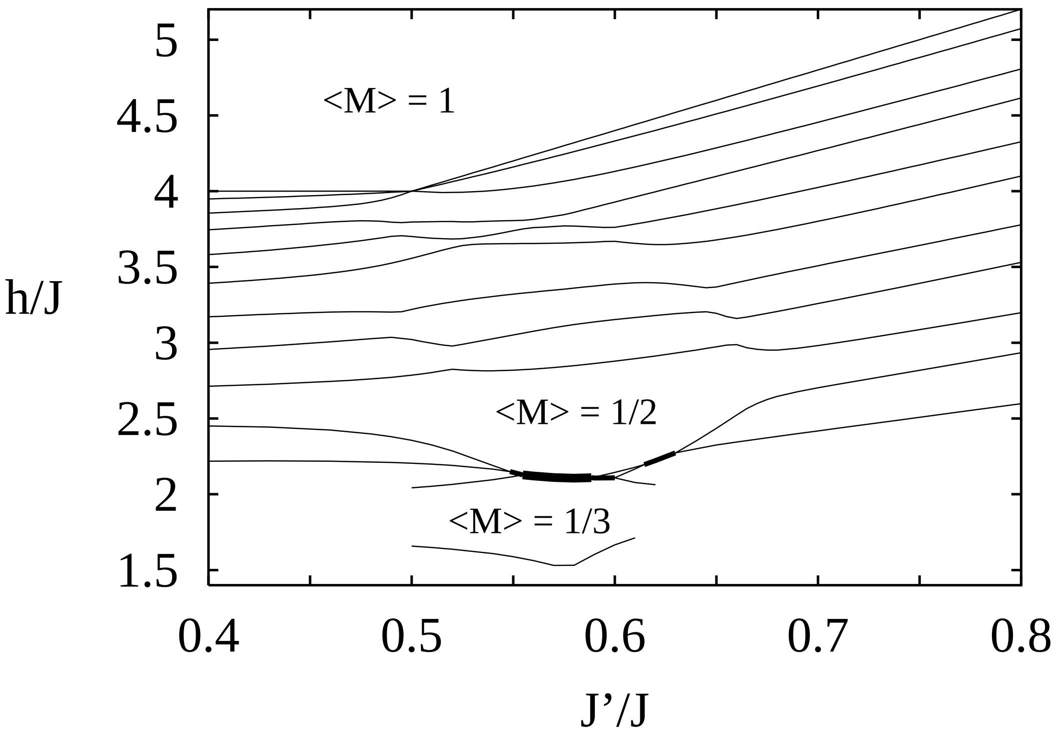

Figure 21: Groundstate phase diagram of the $S = 1/2$ frustrated square lattice on a 6×6 cluster, reproduced after [xiii] with some extensions at smaller $\langle M \rangle$. Lines separate regions of stability of different values of $\langle M \rangle$. Thin full lines indicate flips of single spins whereas the thicker lines at the lower boundary of the $\langle M \rangle = 1/2$ plateau indicate simultaneous flips of two and three spins (in order of increasing thickness).

upper panel of Fig. 4 in [xii] and Figs. 1 and 2 of [xiii] can be neglected[16]. This also implies corrections to the static structure factors shown in Fig. 2 of [xiv] at one point at $\langle M \rangle = 4/9$ for the 6×6 cluster as well as at $\langle M \rangle = 17/24$ for the 8×6 cluster. Nevertheless, adding further data points will probably lead to bigger changes than these corrections.

The dependence of the magnetization curves on J'/J for a 6×6 cluster can be extracted from Fig. 21 which shows the projection of the step positions onto the axis of the magnetic field, *i.e.* the transition lines separate regions where different values of $\langle M \rangle$ are realized in the groundstate. The $\langle M \rangle = 1/2$ plateau can be identified clearly for $0.5 \lesssim J'/J \lesssim 0.66$ [xii,xiii]. However, the new results[17] for smaller $\langle M \rangle$ reveal that on this cluster up to three spins flip simultaneously at the lower boundary of the $\langle M \rangle = 1/2$ plateau, which may be an indication that this transition becomes first order in the thermodynamic limit. Below this jump one observes a further broad step at $\langle M \rangle = 1/3$ in Fig. 21. In fact, an $\langle M \rangle = 1/3$ plateau was

[16]Unfortunately, the statement about the groundstate quantum numbers at $\langle M \rangle = 4/9$ for the 6×6 cluster in Fig. 5 of [xiii] is invalidated by these corrections.

[17]This data is presently restricted to $0.5 \le J'/J \lesssim 0.61$.

predicted by a Chern-Simons theory in [29]. However, one can see in in Fig. 20b) and Fig. 2 of [xiii] that the step at $\langle M \rangle = 1/3$ becomes very narrow on the 6×4 cluster in favor of a broad step at $\langle M \rangle = 1/4$ (which is not realized with 36 spins). It is therefore presently difficult to decide whether this $\langle M \rangle = 1/3$ plateau is just a finite-size effect specific to the 6×6 cluster or survives in the thermodynamic limit.

The $S = 1/2$ frustrated square lattice is realized in Li_2VOSiO_4 and Li_2VOGeO_4 [118,119]. However, according to recent investigations the diagonal coupling is rather strong $J' \approx 5 - 10J$ [122, 160, 161], *i.e.* these materials are rather far from the region $J' \approx J/2$ which is the most interesting one from our point of view.

5 Transition to saturation

At very high magnetic fields, the groundstate is the fully polarized (ferromagnetic) state. The transition to saturation is controlled by single-magnon excitations relative to this fully polarized state. Since magnons are bosonic excitations, it is useful to consider a mapping to a Bose gas [10]. We concentrate on the case of $S = 1/2$ (the discussion of general S follows the same lines with slight generalizations) and the following $SU(2)$-symmetric Hamiltonian (inclusion of an XXZ anisotropy is again possible with small generalizations)

$$H = \sum_{\langle x,x'\rangle} J_{x,x'} \vec{S}_x \cdot \vec{S}_{x'} - h \sum_x S_x^z = \frac{1}{2} \sum_{x \neq x'} J_{x,x'} \vec{S}_x \cdot \vec{S}_{x'} - h \sum_x S_x^z \,. \tag{5.1}$$

We then introduce Pauli operators to represent the flipping of single spins

$$S_x^- = \beta_x^\dagger \,, \qquad S_x^+ = \beta_x \,, \qquad S_x^z = \frac{1}{2}\,\mathbb{1} - \beta_x^\dagger \beta_x \,. \tag{5.2}$$

A spin at site x can only be in one of two states (up or down) for $S = 1/2$. Consequently, we have the hard-core constraints

$$\beta_x^2 = \left(\beta_x^\dagger\right)^2 = 0 \,, \qquad \beta_x^\dagger \beta_x + \beta_x \beta_x^\dagger = \mathbb{1}. \tag{5.3}$$

Insertion of the representation (5.2) into (5.1) leads to

$$H = E_0(h) + H_0 + H_1 \tag{5.4}$$

with

$$\begin{aligned} E_0(h) &= \frac{1}{8} \sum_{x \neq x'} J_{x,x'} - \frac{1}{2} h \mathcal{V} \,, & (5.5)\\ H_0 &= \frac{1}{2} \sum_{x \neq x'} J_{x,x'} \beta_x^\dagger \beta_{x'} + \sum_x \left(h - \frac{1}{2} \sum_{x'} J_{x,x'} \right) \beta_x^\dagger \beta_x \,, & (5.6)\\ H_1 &= \frac{1}{2} \sum_{x \neq x'} J_{x,x'} \beta_x^\dagger \beta_{x'}^\dagger \beta_{x'} \beta_x \,. & (5.7) \end{aligned}$$

The three terms in the decomposition (5.4) have the following meaning:

- $E_0(h)$ is the energy of the polarized state $|\uparrow\uparrow \ldots \uparrow\rangle$ ($\mathcal{V}$ is the volume of the system).
- H_0 is the part of the Hamiltonian which is quadratic in the Pauli operators β_x. A Fourier transformation diagonalizes this part and yields the one-magnon dispersion $\omega(\vec{k})$ (if there are several magnon bands, only the lowest one is relevant to the present discussion).
- H_1 encodes the magnon-magnon interactions.

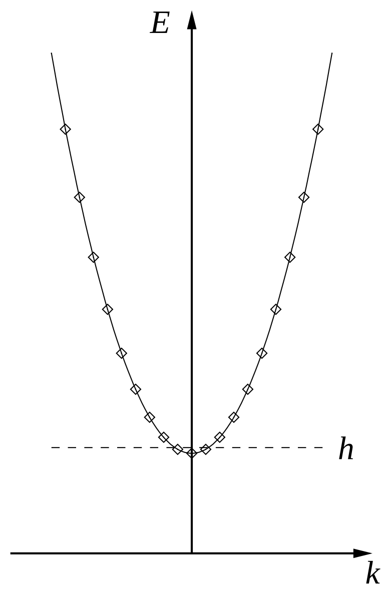

Figure 22: Schematic view of the one-magnon dispersion close to a minimum. Available one-magnon states on a finite one-dimensional system are indicated by diamonds. The magnetic field h acts as a chemical potential, shown by the dashed line.

So far, this is just a rewriting and therefore exact. Now we replace the Pauli operators β_x by Bose operators, *i.e.* we relax the constraints (5.3). However, in order to exclude double spin-flips at one site, an additional interaction $H' = U \sum_x \beta_x^\dagger \beta_x^\dagger \beta_x \beta_x$ should be added with $U \to \infty$. Putting everything together, the original spin Hamiltonian (5.1) is replaced by a bosonic Hamiltonian of the form

$$H_B = \sum_{\vec{k}} \left(\omega(\vec{k}) - \omega_0 + h - h_{\rm uc} \right) \beta_{\vec{k}}^\dagger \beta_{\vec{k}} + \frac{1}{\mathcal{V}} \sum_{\vec{k}_l} \left(U + \omega\left(\vec{k}_3 - \vec{k}_2\right)\right) \beta_{\vec{k}_1}^\dagger \beta_{\vec{k}_2}^\dagger \beta_{\vec{k}_3} \beta_{\vec{k}_4} \, . \quad (5.8)$$

Here ω_0 is the minimum value of the one-magnon dispersion and $h_{\rm uc}$ the saturation field.

A crucial observation is that a perturbative treatment of the four-boson interaction term in (5.8) is a good, controlled approximation in the low-density limit of excited magnons although U is implicitly assumed to be large. Qualitatively, this can be understood as follows. The four-boson interaction term does not affect the one-magnon problem. If there is only a small number of magnons in the system, they meet only at a few sites and therefore interact weakly although the on-site interaction is of a strong hard-core nature.

Finally, we observe that the dispersion $\omega(\vec{k})$ is usually quadratic close to its minimum ω_0, as illustrated in Fig. 22, and that in the bosonic picture the magnetic field plays the rôle of a chemical potential leading to a condensation of magnons just below the saturation field $h_{\rm uc}$. The further procedure is standard, but depends on the dimension.

5.1 One dimension

Below, we will see that in one dimension one obtains a universal behavior characterized by the 'DN-PT' universality class which was first derived by Dzhaparidze and Nersesyan in the context of magnetism [42] and by Pokrovsky and Talapov in the context of the equivalent problem of commensurate-incommensurate phase transitions [152] (see also [179]).

In one dimension, the number of states available below a given energy $E \sim k^2$ is proportional to k (see the diamonds in Fig. 22). Furthermore, the detailed nature of the excitations does not matter in one dimension. Therefore, the one-magnon states are filled uniformly as long as one has an exclusion principle. Since the particle density is directly proportional to the magnetization (see (5.2)), the horizontal axis in Fig. 22 can be identified with the deviation of the magnetization from the critical value M_c at saturation (or at a boundary of a plateau)

$$k \equiv M_c - \langle M \rangle \,. \tag{5.9}$$

On the other hand, the energy axis can be identified with the magnetic field h. A quadratic dispersion $E \sim k^2$ therefore directly leads to the universal result [42, 152]

$$M_c - \langle M \rangle \sim \sqrt{|h_c - h|} \,, \tag{5.10}$$

where h_c is either the saturation field h_{uc} or a critical magnetic field at a boundary of a plateau.

In a fermionic language, this result can be cast into the statement that interactions renormalize to zero in the low-density limit for one dimension. This can be verified in the the exactly solvable $S = 1/2$ XXZ chain [71]: As is shown in Fig. 2, the value of the Luttinger liquid parameter K approaches the free fermionic value $K = 2$ as one comes closer to saturation. At the boundary of the $\langle M \rangle = 0$ plateau (present for $\Delta > 1$) one instead finds the dual value $K = 1/2$, *i.e.* again a free fermionic theory. This identification with free fermions has important consequences for other physical properties besides the asymptotic behavior of the magnetization curve (5.10). In particular, correlation functions have a universal algebraic decay at a DN-PT transition [33], although the rôle of longitudinal and transverse components may be interchanged, depending on whether a free fermionic description ($K = 2$) or its dual ($K = 1/2$) applies. Using e.g. the strong-coupling effective Hamiltonian of section 2.4, these universal properties of the $S = 1/2$ XXZ chain can be argued to be valid for more general one-dimensional models [iv].

The DN-PT asymptotic behavior (5.10) is very general close to plateau boundaries (not just saturation) in one dimension and has been verified in many one-dimensional models (see e.g. [ii, iii, iv, 66, 77, 79, 87, 110, 140]). One of the few possibilities to find a behavior different from (5.10) at a continuous transition in one dimension is a fine-tuning of the parameters such that the leading quadratic term of the dispersion close to the minimum cancels and one has $E \sim k^4$. Using the same arguments as above, one expects an asymptotic behavior $M_c - \langle M \rangle \sim \sqrt[4]{|h_c - h|}$ in this case. Indeed, such a fourth root was observed in the two-leg zig-zag ladder [174] and the biquadratic spin-1 chain [140] at a special point in parameter space where the single-particle dispersion close to a minimum becomes fourth

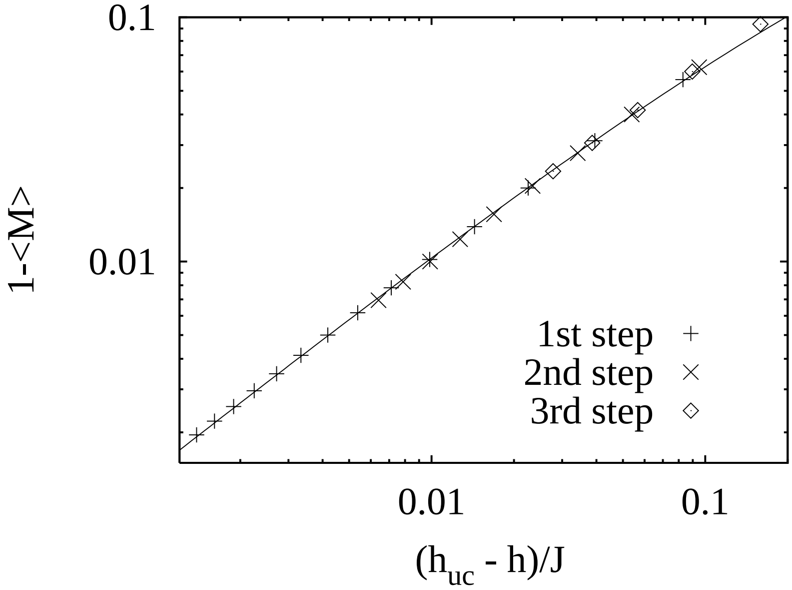

Figure 23: Doubly logarithmic plot of the final steps close to saturation of the magnetization curve of the $S = 1/2$ Heisenberg antiferromagnet on the square lattice (see [xi] for data concerning the 1st step). The line shows the formula (5.11) with $a = 0.1776$ and $b = 3.49$.

order in k [iii, 66] (see also [52] for a corresponding observation in an integrable version of the zig-zag ladder).

5.2 Two dimensions

In two dimensions, interactions lead to a logarithmic correction to the density of hard-core bosons [153] (see also chapter 6 of [154]). Accordingly, using the mapping to a hard-core Bose gas sketched at the beginning of this chapter, the asymptotic behavior of the magnetization curve of a two-dimensional system close to a plateau-boundary was predicted [64, 163] to be linear with a logarithmic correction. In particular, close to the saturation field h_{uc}, the magnetization curve can be approximated by

$$1 - \langle M \rangle = a \left(\frac{h_{\text{uc}} - h}{J} \right) \ln \left(\frac{bJ}{h_{\text{uc}} - h} \right) . \tag{5.11}$$

This result was also found for the square lattice antiferromagnet [227] within a first-order spinwave approximation, yielding at $S = 1/2$ the constants $a = 1/(2\pi)$, $b = \pi^2$.

A numerical check of the asymptotic behavior (5.11) was performed in [xi] for the $S = 1/2$ Heisenberg model on the square, triangular and hexagonal lattice using the midpoint of the last step. Since the magnetization of the last step is $\langle M \rangle = 1 - 2/\mathcal{V}$ for a volume of $\mathcal{V}$ spins and its boundaries are determined by the one- and two-particle excitation energies, this amounts to a test of (5.11) on the two-particle level via their finite-size effects.

Let us now discuss the results for the square lattice [xi] in more detail, including an extension to higher steps. The comparison of different steps is complicated by the fact that the midpoint $h_{n,\mathrm{mid.}}$ of the last few steps (in particular the last one) is not a good approximation to the thermodynamic limit, as can be clearly seen in Fig. 17. Therefore, we allow for a scaling factor α_n in the field h_n for the nth step below saturation

$$h_n = h_{\mathrm{uc}} - \alpha_n \left(h_{\mathrm{uc}} - h_{n,\mathrm{mid.}}\right) , \tag{5.12}$$

where the saturation field for the $S = 1/2$ square lattice Heisenberg model is given by $h_{\mathrm{uc}} = 4J$. The scaling factors α_1, α_2 and α_3 are then determined as follows:

1. The midpoint of the first step h_1 on the 6×6 cluster ($\langle M \rangle = \frac{17}{18}$) is scaled to the midpoint of the fourth step on the 12×12 cluster using $\alpha_1 = 1.37282$. The data point for the 12×12 cluster is not used further in the analysis.

2. Similarly, the midpoint of the second step h_2 on the 8×8 cluster ($\langle M \rangle = \frac{15}{16}$) is scaled to the midpoint of the fourth step on the 16×8 cluster using $\alpha_2 = 1.05359$. The data point for the 16×8 cluster is not used further in the analysis.

3. The third step is used directly as computed from the midpoint method, *i.e.* $\alpha_3 = 1$.

The step positions h_1, h_2 and h_3 determined by this procedure are shown in Fig. 23 on a doubly logarithmic scale. One observes that the data points for different steps collapse well onto a single line, as desired. A small but visible curvature of the data points in this plot shows that the asymptotic behavior of the magnetization curve is not dictated by a power-law, but rather supports a logarithmic correction as in (5.11). A simultaneous fit of (5.11) to all data points (excluding only a few at the smaller system sizes) yields $a = 0.1766 \pm 0.0026$ and $b = 3.49 \pm 0.28$. Fig. 23 shows that the resulting curve agrees well with the ED data. Note that while the preceding extends the test of the linear behavior with a logarithmic correction up to the four-particle level (which enter through h_3), the values of a and b mainly agree with those determined in [xi] when rescaled appropriately with α_1; deviations from the values of the constants found in first-order spinwave approximation [227] are more significant although not surprising.

5.3 Three and higher dimensions

Starting from three dimensions, one has true Bose condensation. In three dimensions this leads to a $1/k$ singularity in the density of states close to the minimum (known as Bogoliubov's $1/k$ law) which when combined with the general arguments of the beginning of this chapter leads to a linear $T = 0$ magnetization curve close to the saturation field h_{uc} [10]

$$1 - \langle M \rangle \sim h_{\mathrm{uc}} - h \, . \tag{5.13}$$

In fact, also a classical spin system ($S \to \infty$) has a linear magnetization curve close to critical fields. Since the classical (mean-field) picture should yield the correct exponents starting with

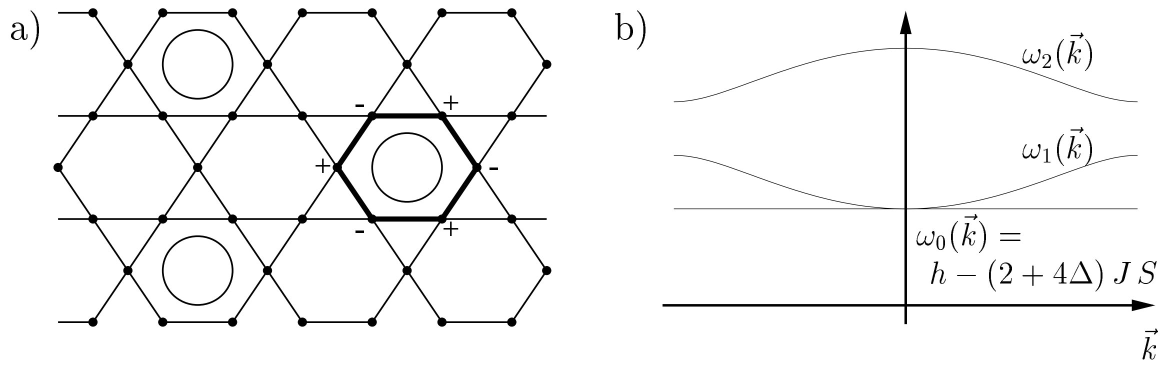

Figure 24: a) Part of the Kagomé lattice. Points denote the positions of spins with length S. b) Schematic view of the three branches $\omega_i(\vec{k})$ of one-magnon excitations for the Kagomé lattice. Note that $\omega_0(\vec{k})$ is completely independent of $\vec{k}$.

the upper critical dimension, one expects (5.13) to be true for all sufficiently high dimensions. Indeed, the relation (5.13) was verified for the $S = 1/2$ Heisenberg antiferromagnet on the (hyper)cubic lattice in three and four dimensions using the last step of the magnetization curve [xi].

One should expect the linear behavior (5.13) in three and higher dimensions (or the one with a logarithmic correction (5.11) in two dimensions) to be true not only for the saturation field, but more generally for continuous transitions – at least as long as the fundamental excitations are bosons. However, the asymptotic form of the magnetization curve becomes more difficult to check numerically for values of $\langle M \rangle$ that are not close to saturation.

5.4 Independent magnons and macroscopic magnetization jumps

In highly frustrated spin models, one finds surprisingly often not just a cancellation of the leading terms in the dispersion close to the minimum, but that the lowest magnon branch $\omega_0(\vec{k})$ is completely flat (*i.e.* independent of $\vec{k}$) or has some flat directions (*i.e.* does not depend on some of the components k_i). In this case, the condensation problem changes dramatically as compared to the preceding sections and one finds a special type of jump just below the saturation field [xv].

In the following, we will outline the construction of [xv], using the Kagomé lattice shown in Fig. 24a) as example. Since the Kagomé lattice has a basis containing three sites, the spectrum of one-magnon excitations above the ferromagnetically polarized state is solved by diagonalization of a 3×3 matrix. For the spin-S XXZ model one then finds three magnon branches $\omega_i(\vec{k})$ ($i = 0, 1, 2$) which are shown schematically in Fig. 24b). Remarkably, the lowest branch $\omega_0(\vec{k}) = h - (2 + 4\Delta)\, J\, S$ is completely flat, *i.e.* independent of $\vec{k}$. This property is a fingerprint of the strong frustration caused by the triangles in the Kagomé lattice. In fact, the lowest magnon branch relative to the ferromagnetically polarized state is also completely flat for some other popular highly frustrated lattices including the pyrochlore lattice [xv].

Using an inverse Fourier transformation, the one-magnon excitations can be localized in the real-space directions corresponding to a flat direction in k-space. If the dispersion is completely flat, one can construct a magnon excitation that is localized in a finite volume. The structure of such a local magnon excitation is indicated by the bold hexagon in Fig. 24a). Up to normalization, it is given by

$$|1\rangle \sim \sum_x (-1)^x S_x^- \left|\uparrow \ldots \uparrow\right\rangle , \tag{5.14}$$

where the sum runs over the 6 corners of the hexagon. Localization can be verified since each spin next to the hexagon is coupled to two spins in the hexagon such that contributions of flipped spins propagating onto the exterior site are added with different signs and thus cancel. Therefore, a localized magnon is an exact eigenstate of the XXZ Hamiltonian on the Kagomé lattice. Similar constructions can be given for other lattices [xv] and finite clusters [175].

Now one can create further localized magnon excitations. As long as the local magnons are sufficiently well separated in space, they do not interact and consequently the many-magnon state is still an exact eigenstate. The non-trivial step is to verify that these non-interacting localized magnon excitations are not only eigenstates but in fact groundstates in their respective magnetization subspaces. This result is probably true for general S, $J_{i,j} \geq 0$ and XXZ anisotropy $\Delta \geq 0$. In [xv] the groundstate property was verified numerically for some cases and it has been shown rigorously for certain subsets of the parameters, namely for $S = 1/2$, $\Delta \geq 0$ and all coupling constants $J_{i,j}$ equal [175] or for general S and $J_{i,j} \geq 0$, but isotropic interaction $\Delta = 1$ [173].

If the localization region is finite, a macroscopic fraction of the spins in the system can be flipped using local magnon excitations. The energies of the individual excitations add without interaction terms. This leads to a finite interval of the magnetization $\langle M \rangle$ where the groundstate energy $E(\langle M \rangle)$ becomes a linear function. Since the magnetic field is related to $E(\langle M \rangle)$ through $h \sim \frac{\partial E(\langle M \rangle)}{\partial \langle M \rangle}$, this linear behavior leads to a finite jump in the magnetization curve $\langle M \rangle(h)$. At first sight, this mechanism is very similar to the one giving rise to jumps in the magnetization curves of models with local conservation laws (see section 3.6). Note, however, that the present construction does not rely on the existence of local conservation laws. In fact, it is remarkable that the construction of [xv, 175] works for higher-dimensional models which do not have any local conservation laws. Conversely, the present construction is restricted to the transition to saturation since it relies on the knowledge of a reference state, namely the fully polarized state which is a trivial eigenstate of the Hamiltonian.

One can see in Fig. 24a) that a local magnon excitation for the Kagomé lattice involves 9 spins. Therefore, a jump of height $\delta\langle M \rangle = 1/(9S)$ is predicted for the Kagomé lattice. For the $S = 1/2$ Heisenberg model on the Kagomé lattice one indeed observes numerically a jump of height $\delta\langle M \rangle = 2/9$ which is independent of the system size for suitable clusters (see Fig. 2 of [xv]). Note that the height of the jump is in general proportional to $1/S$ and vanishes in the classical limit $S \to \infty$. Therefore, this macroscopic jump caused by independent local magnons is a true macroscopic quantum effect.

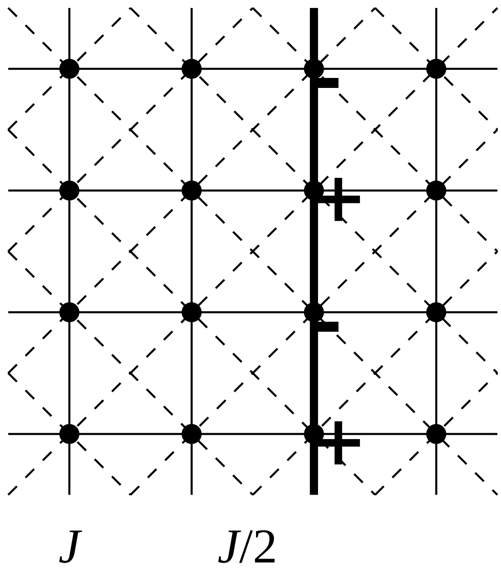

Figure 25: A magnon localized along one of the vertical lines of the frustrated square lattice with diagonal coupling $J' = J/2$.

The closest possible packing of local magnon excitations for the Kagomé lattice is indicated by the circles in Fig. 24a). This state with the maximal number of magnon excitations is clearly an ordered (crystalline) state. According to general arguments [128, 145], one expects a gap above such a crystalline state and consequently a plateau in the magnetization curve at the foot of the jump. This conclusion is supported by the numerical magnetization curve of the $S = 1/2$ Heisenberg model on the Kagomé lattice, Fig. 2 of [xv], which exhibits a clear plateau at $\langle M \rangle = 7/9$.

The magnetization curve of the $S = 1/2$ Heisenberg model on the Kagomé lattice probably gives rise to several further plateaux [xv, 210] including one at $\langle M \rangle = 1/3$ [23, 75]. The $\langle M \rangle = 1/3$ plateau has a classical counterpart whose origin can be attributed to the order-by-disorder mechanism [xii, xiv], although the structure of the groundstate remains highly non-trivial at the classical level [225].

In dimensions larger than one it is also possible that the minima of the one-magnon excitations form a manifold of a dimension smaller than the total one. One example is the frustrated square lattice at $J' = J/2$, shown in Fig. 25, where one finds lines of minima at $k_x = \pi$ or $k_y = \pi$ [xiii]. In this case, magnon excitations can be constructed [xv] that are localized in some directions, but not all. For the frustrated square lattice, this is indicated by the bold line in Fig. 25 where a magnon of the form

$$|1\rangle \sim \sum_{y=1}^{L} (-1)^y S^-_{x_0,y} \, |\uparrow \ldots \uparrow\rangle \tag{5.15}$$

is localized along the vertical line at position x_0. Here, the y-direction is assumed to have periodic boundary conditions and even linear size L.

The frustrated square lattice can accommodate $L/2$ local magnon excitations (5.15), leading to a finite-size jump $\delta\langle M\rangle = L/(2\,\mathcal{V}\,S) = 1/(2\,L'\,S)$, where L and L' are the lengths of the longer and shorter edges, respectively if the cluster is rectangular. A finite-size jump of height $\delta\langle M\rangle = 1/L'$ is indeed observed in ED of the $S = 1/2$ frustrated square lattice [xiii], compare also Fig. 20a) (in particular the inset) and Fig. 21. However, due to the incomplete localization, the height of the jump vanishes in the thermodynamic limit, *i.e.* the transition to saturation remains continuous in such a case. Nevertheless, the magnetization curve should be exceptionally steep. A first guess [223] was that the typically one-dimensional square-root behavior (5.10) would be valid for this particular two-dimensional system. However, a non-analytic form of $h(\langle M\rangle)$ such as $h(\langle M\rangle) \sim \exp(-1/(1-\langle M\rangle))$ (corresponding to $1-\langle M\rangle \sim 1/\log(h_{\rm uc}-h)$) seems more plausible [xv].

6 Experimental realizations

Plateaux and jumps in magnetization curves have been known e.g. in rare earth compounds for a long time (see for instance [37] and references therein) and can be understood in terms of classical anisotropic spin models. In comparison, plateaux and jumps that are induced by quantum fluctuations (in particular in isotropic situations) are a new research field. An early example in this category is the step-like magnetization curve of $FeSiF_6{\cdot}6H_2O$ [9,224]. In this compound, two plateaux are observed at $\langle M \rangle = 0$ and $1/2$ which can be understood [84] in a manner very similar to the strong-coupling picture of section 2.4, namely in terms of the levels of a single anisotropic spin $S = 2$ carried by Fe^{2+} ions.

In the following sections we will discuss some experimental realizations of quantum spin systems that are relevant to the preceding chapters. In most of the substances, a localized spin $S = 1/2$ is carried by Cu^{2+} ions. The strong Coulomb repulsion in the Cu-d_{xy} orbitals renders these substances insulating. The magnetic coupling is mediated in many cases by the p-orbitals of O^-, Cl^- or Br^- ions. According to the Goodenough-Kanamori rules (see e.g. [6]), one expects superexchange across a Cu-X-Cu bond (X = O, Cl or Br) to be strong and antiferromagnetic if the bond angle is close to 180°. The magnetic exchange becomes weaker and finally ferromagnetic as the bond angle approaches 90°. The latter case is of interest for high-field magnetization experiments since the presently available (pulsed) magnets can achieve a notable polarization of a sample only if the magnetic exchange is not too strong.

6.1 Ferromagnetically stacked triangular antiferromagnet $CsCuCl_3$

The interest of the author in the subject was stimulated by an old magnetization experiment on $CsCuCl_3$ [135]. The magnetization curve is reproduced in Fig. 26. In the vicinity of one third of the saturation magnetization one observes a small jump for a magnetic field parallel to the crystal (c-) axis and a plateau-like feature for an in-plane magnetic field (perpendicular to the c-axis). The magnetic model for $CsCuCl_3$ is that of $S = 1/2$ spins interacting antiferromagnetically on a triangular lattice with ferromagnetic stacking along the c-axis (see Fig. 1 of [x]). The anisotropic behavior for different field directions can be attributed to a weak Dzhalozhinski-Moriya interaction pointing along the c-axis.

Based on a semiclassical analysis, Nikuni, Shiba and Jacobs [83,133] proposed that the features shown in Fig. 26 arise due to a competition between the anisotropy associated with the Dzhalozhinski-Moriya interaction and quantum fluctuations. Several variants of the full $S = 1/2$ model were then investigated in [x] by ED, DMRG and perturbation theory. Particular attention was paid to three periodically coupled chains which lend themselves as a minimal model since the ferromagnetic exchange along the c-axis is about three times stronger than the antiferromagnetic coupling in the triangular planes [x]. The results of [x] are consistent with the weak easy-plane anisotropy caused by the Dzhalozhinski-Moriya interaction stabilizing a plateau-like feature around $\langle M \rangle = 1/3$ for an in-plane magnetic field. However, no indications for a jump close to $\langle M \rangle = 1/3$ were found in [x] for a magnetic field along the c-axis. This is puzzling since for a magnetic field along the anisotropy axis, the

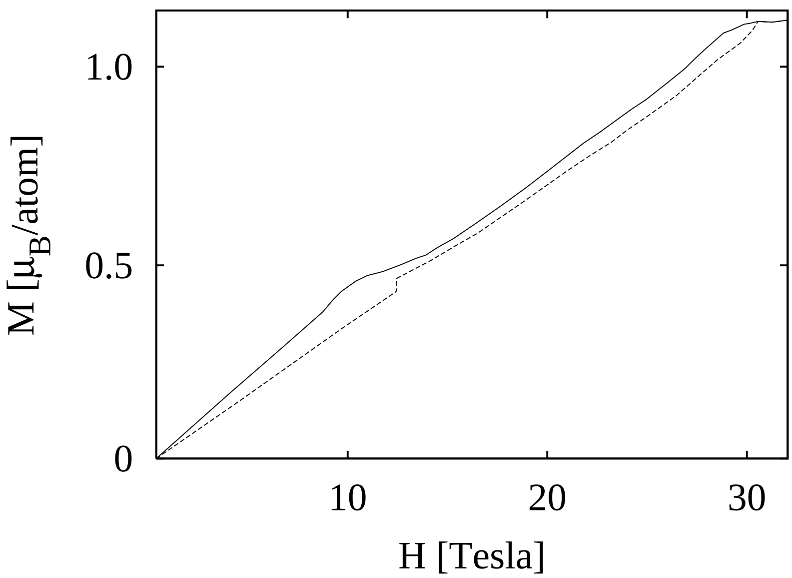

Figure 26: High-field magnetization curve of a $CsCuCl_3$ single crystal at $T = 1.1$K, reproduced from [135]. The full line is for a magnetic field perpendicular to the c-axis, the dashed line for a magnetic field parallel to the c-axis.

corresponding projection of the total spin is conserved and therefore the theoretical analysis of the magnetic model should be under better control in the latter case. Nevertheless, it should be noted that $CsCuCl_3$ is really a three-dimensional compound and that reliable computations for a frustrated three-dimensional quantum spin system are still a challenge.

$CsCuCl_3$ is a member of a big family of triangular antiferromagnets [36]. Further substances that yield good two-dimensional triangular antiferromagnets include $RbFe(MoO_4)_2$ and $CsFe(SO_4)_2$ whose high-field magnetization process exhibits a plateau-like feature in the vicinity of $\langle M \rangle = 1/3$ [80]. In $RbFe(MoO_4)_2$ and $CsFe(SO_4)_2$, a localized spin $S = 5/2$ is carried by Fe^{3+} ions. The plateau-like feature at $\langle M \rangle = 1/3$ can be attributed to a small Ising-like anisotropy [80]. One may nevertheless speculate that it is further supported by the quantum effects discussed in section 4.2 even if $S = 5/2$ is already quite large and accordingly a semiclassical description should work well.

6.2 Modulated spin chains

In this section we mention a few selected examples of (modulated) spin chains exhibiting plateaux in their magnetization curves.

The magnetization curve of the bond-alternating $S = 1$ chain compound $[Ni_2(Medpt)_2(\mu\text{-}ox)(\mu\text{-}N_3)]ClO_4{\cdot}0.5H_2O$ has plateaux at $\langle M \rangle = 1/2$ and 0 [131]. These observations agree with theoretical predictions [199, 202].

The ferrimagnetic $S = 1$-$1/2$ chain is probably realized in $NiCu(pba)(D_2O)_3 \cdot 2D_2O$ and a plateau with $\langle M \rangle \approx 1/3$ is indeed observed in this material [70], as expected (see section

3.2).

In a trimer system, one expects theoretically a plateau with $\langle M \rangle = 1/3$ (see section 3.3). A good candidate for an experimental realization of a (frustrated) trimer system was $Cu_3Cl_6(H_2O)_2{\cdot}2H_8C_4SO_2$ [81, 190] (see [5, 14, 189] for further materials with trimer constituents). The experiments in [81] stimulated investigations of the associated frustrated trimer chain model [v, 138, 172, 201]. A careful analysis [v] of the magnetic susceptibility [81] showed that earlier proposals of coupling constants [172, 201] were unable to describe the thermodynamic properties adequately. Nevertheless, a completely satisfactory description of all physical properties observed in [81] was not achieved within the frustrated trimer chain model [v]. In the meantime, the crystal structure of the material was checked by X-ray diffraction and it turned out that a different material was in fact studied in [81], namely $Cu_2Cl_4{\cdot}H_8C_4SO_2$ which is believed to be a weakly alternating Heisenberg double chain [56]. More recently, a frustrated trimer system (or the distorted diamond chain) has actually been found to be realized in $Cu_3(CO_3)_2(OH)_2$ (azurite) where one obtains indeed a good fit to the susceptibility of [v] and observes a clear plateau with $\langle M \rangle = 1/3$ [90, 91].

6.3 Spin ladders

The plateau-like feature observed at $\langle M \rangle = 1/3$ in $CsCuCl_3$ [135] can be understood in the approximation of a weakly anisotropic PBC 3-leg ladder with ferromagnetic legs [x] (compare also section 6.1). In fact, this was one of the motivations for the study of completely antiferromagnetic frustrated PBC spin ladders [i, ii].

Antiferromagnetic N-leg spin ladders with OBC are realized in modifications of high-T_c materials [39, 40, 156, 157]. In these compounds, 180° Cu-O-Cu bonds lead to strong antiferromagnetic coupling in the ladder structures with a rather weak coupling to the neighboring ladders through 90° bonds. Unfortunately, magnetization plateaux are predicted for these systems at fields of (several) thousand Tesla which is clearly outside the presently accessible experimental range. One alternative is provided by organic compounds. In this category, $Cu_2(C_5H_{12}N_2)_2Cl_4$ (CuHpCl) was considered to be a two-leg ladder material in the limit of strong rung coupling (see e.g. [28]). In this compound, a clear $\langle M \rangle = 0$ plateau followed by a smooth transition to saturation was observed in high-field magnetization experiments [27, 28], consistent with theoretical expectations for a two-leg ladder. Just the absence of sufficient curvature in the magnetization curves at the lowest temperatures [27, 28] as compared to a one-dimensional model (see section 5.1) might have been considered as evidence for relevant higher-dimensional coupling. Indeed, inelastic neutron scattering measurements finally turned out to be inconsistent with the interpretation of CuHpCl as a two-leg spin ladder [186]. Fortunately, other two-leg ladder materials have been found in the meantime. For example, a magnetization experiment on $(C_5H_{12}N)_2CuBr_4$ [212] not only exhibits an $\langle M \rangle = 0$ plateau followed by a smooth transition to saturation, but also good quantitative agreement of the magnetization curve with the one-dimensional model down to the lowest temperatures.

Vanadium oxides may in general provide another alternative and e.g. some PBC 3-leg ladder is suspected in the compound $Na_2V_3O_7$ [121].

6.4 Plateau substance NH_4CuCl_3

One of the substances exhibiting the most beautiful plateaux is NH_4CuCl_3 where clear plateaux with $\langle M \rangle = 1/4$ and $3/4$ have been observed [184]. However, attempts at a theoretical explanation in terms of $S = 1/2$ models [iii, 22, 97] have not been really successful so far, as we will indicate in the following.

NH_4CuCl_3 belongs to a family of isostructural compounds which include also $KCuCl_3$ and $TlCuCl_3$. Based on their crystal structure, these compounds were originally considered to be quasi-one-dimensional (dimerized) zig-zag chains – compare Fig. 10. Accordingly, one expects a spin gap (see section 3.5) and the high-field magnetization curve of $KCuCl_3$ and $TlCuCl_3$ indeed exhibits an $\langle M \rangle = 0$ plateau corresponding to a spin gap [185]. However, the absence of curvature in the magnetization curve just above the magnetic field needed to close the spin gap [185] might have been taken as an indication that in particular $KCuCl_3$ is not one-dimensional (see chapter 5). Indeed, inelastic neutron scattering showed first for $KCuCl_3$ [25] and later for $TlCuCl_3$ [26] that these two compounds are three-dimensional networks of weakly coupled dimers[18] (with somewhat stronger inter-dimer coupling for $TlCuCl_3$).

Since the size of the ions separating the double-chain structures increases from K^+ and Tl^+ to NH_4^+, NH_4CuCl_3 might still be suspected to be quasi-one-dimensional even if the other two compounds are not. Although one can indeed obtain plateaux with $\langle M \rangle = 1/4$ and $3/4$ in a zig-zag ladder with dimerized legs [iii, 22], neither this point of view nor other proposals [97] have so far resulted in a really satisfactory theoretical description of the experimental observations. More generally, a one-dimensional model has the problem that the quantization condition (1.1) with $S = 1/2$ implies a groundstate periodicity $V = 8$ (four dimers) in order to allow plateaux with $\langle M \rangle = 1/4$ and $3/4$. Indeed, recent ^{15}N-NMR investigations of the $\langle M \rangle = 1/4$ plateau state indicate a superstructure with a periodicity of four dimers along the a-axis [183], *i.e.* the direction of the zig-zag chain structures. However, $V = 8$ would permit also plateaux with $\langle M \rangle = 0$ and $1/2$ which are *not* observed experimentally [184], but are very pronounced e.g. in the dimerized zig-zag ladder [22]. Note further that an additional dimerization was used e.g. in [22] in order to obtain plateaux with $\langle M \rangle = 1/4$ and $3/4$. However, a new determination of the low-temperature structure of ND_4CuCl_3 (which exhibits the same physical properties as NH_4CuCl_3 but is better suited for neutron scattering) using elastic neutron scattering [162] did not give any hints at a dimerization as compared to the room-temperature structure of NH_4CuCl_3. Consequently, a one-dimensional model remains questionable. Indeed, a recent inelastic neutron scattering study of ND_4CuCl_3 observed only two weakly dispersive modes at 1.5meV$\approx$17.5K and 3meV$\approx$35K [144], *i.e.* no preferred direction. However, this energy scale corresponds to the one of the magnetization plateaux and one may expect to find a spinwave excitation at lower energies [144] which would encode the information about the exchange constants and thus the true dimensionality of the system.

A first hint to a solution of the puzzle why these three isostructural compounds have completely different magnetic properties may be obtained by consideration of the Cu-Cl-Cu bond angles in the dimer units. These are $95.9°$ in $KCuCl_3$ [219] and $95.6°$ in $TlCuCl_3$ [194] (see

[18] Note that a strongly dimerized system exhibits a spin gap independent of dimensionality.

also [164]), but noticeably smaller in NH_4CuCl_3, namely 93.8° at 1.5K [162]. Accordingly, the intra-dimer couplings J of the former two compounds are weak and similar: $J \approx 49$K for $KCuCl_3$ [25] and $J \approx 63$K for $TlCuCl_3$ [26]. The value of the intra-dimer coupling for ND_4CuCl_3 is not known, but the approximately 2° smaller bond angle strongly suggests that it is weaker or even ferromagnetic. A weaker intra-dimer coupling J is consistent with the fact that NH_4CuCl_3 becomes fully polarized for a magnetic field of approximately 29T [184] whereas $KCuCl_3$ and $TlCuCl_3$ remain partially polarized up to a higher magnetic field of 39T [185]. The absence of a spin gap in NH_4CuCl_3 also shows that this material is not strongly dimerized which is again consistent with the intra-dimer coupling J not being the dominant exchange. One may therefore expect inter-dimer coupling to be even *more* important in NH_4CuCl_3 than in $KCuCl_3$ and $TlCuCl_3$, although the contribution of the NH_4^+ groups to magnetic exchange remains to be clarified.

In general, it is intriguing that doping can push magnetization plateaux into the low-field region at least for modulated Hubbard chains [viii,ix] and ladders [19] (see section 3.7). This points towards the possibility of observing magnetization plateaux in doped systems whose parent compounds would exhibit plateaux only at inaccessibly high fields.

7 Conclusions and outlook

In the first part of this thesis we have reviewed the macroscopic quantum effects associated to plateaux and jumps in the magnetization curves of correlated quantum systems.

In one dimension the opening of plateaux is controlled by the group of translations and the allowed values of the magnetization $\langle M \rangle$ on a plateau are quantized by (1.1). The main complication is to determine V since translational symmetry can be spontaneously broken in the groundstate. In chapter 3 we have encountered many examples of symmetry breaking by a period two, but also a period of three is realized in some cases (see e.g. [iii, 142]) and even arbitrarily large periodicities have been observed in one model [177]. This is remarkable in so far as it shows that there is no upper bound for the periodicity of the groundstate and hence any rational value of $\langle M \rangle$ is allowed in principle by a sufficiently large periodicity of spontaneous breaking of translational symmetry.

An exception to the quantization condition (1.1) is found in systems doped with a fixed amount of charge carriers, in particular the modulated Hubbard chains discussed in section 3.7. Although plateaux now arise at doping-dependent irrational values of the magnetization $\langle M \rangle$, commensurability of one of the magnetic species remains fundamental, as is reflected by the generalized quantization conditions (3.11).

The condition (1.1) is probably also valid in higher dimensions although it becomes more difficult to verify the presence of certain plateaux in a given quantum spin model. At least a plateau with $\langle M \rangle = 1/3$ is well established in the triangular lattice (see section 4.2), one with $\langle M \rangle = 1/2$ is found in the frustrated square lattice (see section 4.3) and some with $\langle M \rangle = 1/3$ and $\langle M \rangle = 7/9$ are found in the $S = 1/2$ Kagomé lattice (see section 5.4). Note that most examples are associated with spontaneously broken translational symmetry. This is particularly interesting in the case of the frustrated square lattice where an ordered uuud-state is stabilized by the order-by-disorder mechanism at $\langle M \rangle = 1/2$.

The transitions at the boundaries of the plateaux can be regarded as field-induced quantum phase transition. If such a transition is continuous one can associate certain universal properties to it that depend only on the dimension of the system, as we have reviewed in chapter 5 with particular emphasis on the transition to saturation.

Jumps in the magnetization curve can be associated to true first-order transitions (the frustrated square lattice is probably one example for such a first-order transition, see Fig. 21). Another possibility giving rise to a jump is a linear part in the groundstate energy $E(\langle M \rangle)$ as a function of magnetization $\langle M \rangle$, yielding an exact degeneracy for a particular value of the magnetic field h. The latter possibility is realized in (one-dimensional) models with local conservation laws, see section 3.6, and in certain frustrated higher-dimensional models via independent local magnon excitations, see section 5.4.

In chapter 6 we have reviewed some related experimental realizations. Many cases are well understood, other cases such as NH_4CuCl_3 remain a challenge for theory, although the new experimental results mentioned in section 6.4 should aid a theoretical understanding of the remarkable magnetization curve with plateaux at $\langle M \rangle = 1/4$ and $3/4$.

Acknowledgements

Thanks go to my collaborators in the projects submitted with this thesis: Wolfram Brenig, Daniel Cabra, Alessandro De Martino, Matthias Kaulke, Andreas Läuchli, Frederic Mila, Oleg Petrenko, Pierre Pujol, Johannes Richter, Klaus-Dieter Schotte, Hans-Jürgen Schmidt, Jürgen Schnack, Jörg Schulenburg, Pascal Simon, Matthias Troyer and Mike Zhitomirsky. I have benefited from discussions with many further people during this research among whom I am particularly indebted to Marcelo Grynberg, Maurice Rice and Ursula Schotte. I am also grateful to Nordal Cavadini, Reinhard Kremer, Peter Lemmens, Bruno Lüthi, Christian Rüegg and Hidekazu Tanaka for enlightening discussions of experimental issues. Some of the new ED results presented in the first part of this thesis have been made possible only by the compute-server `cfgauss` at the Rechenzentrum of the Technische Universität Braunschweig and the technical support of Josef Schüle. Finally, I am grateful to Wolfram Brenig, Daniel Cabra, Fabian Heidrich-Meisner and Mike Zhitomirsky for useful comments on this thesis.

Publications submitted with this thesis

[i] D.C. Cabra, A. Honecker, P. Pujol, *Magnetization Curves of Antiferromagnetic Heisenberg Spin-$\frac{1}{2}$ Ladders*, Phys. Rev. Lett. **79** (1997) 5126-5129.

[ii] D.C. Cabra, A. Honecker, P. Pujol, *Magnetization Plateaux in N-Leg Spin Ladders*, Phys. Rev. **B58** (1998) 6241-6257.

[iii] D.C. Cabra, A. Honecker, P. Pujol, *Magnetic Properties of Zig-Zag Ladders*, Eur. Phys. J. **B13** (2000) 55-73.

[iv] A. Honecker, *Strong-Coupling Approach to the Magnetization Process of Polymerized Quantum Spin Chains*, Phys. Rev. **B59** (1999) 6790-6794.

[v] A. Honecker, A. Läuchli, *Frustrated Trimer Chain Model and $Cu_3Cl_6(H_2O)_2{\cdot}2H_8C_4SO_2$ in a Magnetic Field*, Phys. Rev. **B63** (2001) 174407.

[vi] A. Honecker, F. Mila, M. Troyer, *Magnetization Plateaux and Jumps in a Class of Frustrated Ladders: A Simple Route to a Complex Behaviour*, Eur. Phys. J. **B15** (2000) 227-233.

[vii] A. Honecker, W. Brenig, *Magnetic Properties of a Spin-$\frac{1}{2}$ Quadrumer Chain*, Phys. Rev. **B63** (2001) 144416.

[viii] D.C. Cabra, A. De Martino, A. Honecker, P. Pujol, P. Simon, *Doping-Dependent Magnetization Plateaux in p-merized Hubbard Chains*, Phys. Lett. **A268** (2000) 418-423.

[ix] D.C. Cabra, A. De Martino, A. Honecker, P. Pujol, P. Simon, *Emergence of Irrationality: Magnetization Plateaux in Modulated Hubbard Chains*, Phys. Rev. **B63** (2001) 094406.

[x] A. Honecker, M. Kaulke, K.D. Schotte, *A Spin-$\frac{1}{2}$ Model for $CsCuCl_3$ in an External Magnetic Field*, Eur. Phys. J. **B15** (2000) 423-434.

[xi] A. Honecker, *A Comparative Study of the Magnetization Process of Two-Dimensional Antiferromagnets*, J. Phys.: Condensed Matter **11** (1999) 4697-4713.

[xii] M.E. Zhitomirsky, A. Honecker, O.A. Petrenko, *Field Induced Ordering in Highly Frustrated Antiferromagnets*, Phys. Rev. Lett. **85** (2000) 3269-3273.

[xiii] A. Honecker, *Lanczos Study of the $S = 1/2$ Frustrated Square-Lattice Anti-Ferromagnet in a Magnetic Field*, Can. J. Phys. **79** (2001) 1557-1563.

[xiv] A. Honecker, O.A. Petrenko, M.E. Zhitomirsky, *Field-Induced Order and Magnetization Plateaux in Frustrated Antiferromagnets*, Physica **B312-313** (2002) 609-611.

[xv] J. Schulenburg, A. Honecker, J. Schnack, J. Richter, H.-J. Schmidt, *Macroscopic Magnetization Jumps Due to Independent Magnons in Frustrated Quantum Spin Lattices*, Phys. Rev. Lett. **88** (2002) 167207.

General references

[1] I. Affleck, in *Fields, Strings and Critical Phenomena, Les Houches, Session XLIX*, edited by E. Brézin, J. Zinn-Justin, North-Holland (Amsterdam, 1988).

[2] I. Affleck, *Spin-Gap and Symmetry Breaking in CuO_2 Layers and Other Antiferromagnets*, Phys. Rev. **B37** (1988) 5186-5192.

[3] I. Affleck, *Exact Correlation Amplitude for the $S = \frac{1}{2}$ Heisenberg Antiferromagnetic Chain*, J. Phys. A: Math. Gen. **31** (1998) 4573-4581.

[4] I. Affleck, E.H. Lieb, *A Proof of Part of Haldane's Conjecture on Spin Chains*, Lett. Math. Phys **12** (1986) 57-69.

[5] Y. Ajiro, T. Asano, T. Inami, H. Aruga-Katori, T. Goto, *High-Field Magnetization of One-Dimensional $S = 1/2$ Trimer System 3$CuCl_2$·2dioxane*, J. Phys. Soc. Jpn. **63** (1994) 859-862.

[6] P.W. Anderson, *Theory of Magnetic Exchange Interactions: Exchange in Insulators and Semiconductors*, p. 99 in *Solid State Physics*, Vol. 14, eds. F. Seitz, D. Turnbull, Academic Press (New York, 1963).

[7] M. Arlego, D.C. Cabra, M.D. Grynberg, *Quasiperiodic Spin Chains in a Magnetic Field*, Phys. Rev. **B64** (2001) 134419.

[8] E. Arrigoni, *Spin and Charge Excitations in a Three-Legs Fermionic Ladder: A Renormalization Group Study*, Phys. Lett. **A215** (1996) 91-96.

[9] S.K. Asadov, É.A. Zavadskii, Yu.D. Zavorotnev, B.M. Todris, *Pecularities of Ferrous Fluosilicate Magnetization at Low Temperatures in Randomly Oriented Magnetic Fields*, Sov. J. Low Temp. Phys. **13** (1987) 675-677.

[10] E.G. Batyev, L.S. Braginskiĭ, *Antiferromagnet in a Strong Magnetic Field: Analogy with Bose Gas*, Soviet Physics JETP **60** (1984) 781-786.

[11] J.G. Bednorz, K.A. Müller, *Possible High T_c Superconductivity in the Ba – La – Cu – O System*, Z. Phys. **B64** (1986) 189-193.

[12] K. Bernardet, G.G. Batrouni, J.-L. Meunier, G. Schmid, M. Troyer, A. Dorneich, *Analytical and Numerical Study of Hardcore Bosons in Two Dimensions*, Phys. Rev. **B65** (2002) 104519.

[13] B. Bernu, P. Lecheminant, C. Lhuillier, L. Pierre, *Exact Spectra, Spin Susceptibilities, and Order Parameter of the Quantum Heisenberg Antiferromagnet on the Triangular Lattice*, Phys. Rev. **B50** (1994) 10048-10062.

[14] M.R. Bond, R.D. Willett, R.S. Rubins, P. Zhou, C.E. Zaspel, S.L. Hutton, J.E. Drumheller, *Crystal Structures, Magnetic Studies, and Paramagnetic Resonance of the Copper Trimer Stacks (4-picolinium)$_2Cu_3Cl_8$, (4-picolinium)$_2Cu_3Br_8$, and (1,1,4-trimethylpiperazinium)Cu_3Cl_8*, Phys. Rev. **B42** (1990) 10280-10290.

[15] J.C. Bonner, M.E. Fisher, *Linear Magnetic Chains with Anisotropic Coupling*, Phys. Rev. **135** (1964) A640-A658.

[16] W. Brenig, *Aspects of Electron Correlations in the Cuprate Superconductors*, Phys. Rep. **251** (1995) 153-266.

[17] E. Brück, O. Tegus, X.W. Li, F.R. de Boer, K.H.J. Buschow, *Magnetic Refrigeration– Towards Room-Temperature Applications*, Physica **B327** (2003) 431-437.

[18] D.C. Cabra, A. De Martino, M.D. Grynberg, S. Peysson, P. Pujol, *Random Bond XXZ Chains with Modulated Couplings*, Phys. Rev. Lett. **85** (2000) 4791-4794.

[19] D.C. Cabra, A. De Martino, P. Pujol, P. Simon, *Hubbard Ladders in a Magnetic Field*, Europhys. Lett. **57** (2002) 402-408.

[20] D.C. Cabra, M.D. Grynberg, *Ground State Magnetization of Polymerized Spin Chains*, Phys. Rev. **B59** (1999) 119-122.

[21] D.C. Cabra, M.D. Grynberg, *Massive and Massless Behavior in Dimerized Spin Ladders*, Phys. Rev. Lett. **82** (1999) 1768-1771.

[22] D.C. Cabra, M.D. Grynberg, *Magnetization Plateaus in Dimerized Spin-Ladder Arrays*, Phys. Rev. **B62** (2000) 337-343.

[23] D.C. Cabra, M.D. Grynberg, P.C.W. Holdsworth, P. Pujol, *From Classical to Quantum Kagomé Antiferromagnet in a Magnetic Field*, Phys. Rev. **B65** (2002) 094418.

[24] L. Campos Venuti, E. Ercolessi, G. Morandi, P. Pieri, M. Roncaglia, *Heisenberg Integer Spin Chains in a Uniform Magnetic Field*, Int. Jour. of Mod. Phys. **B16** (2002) 1363-1379.

[25] N. Cavadini, W. Henggeler, A. Furrer, H.-U. Güdel, K. Krämer, H. Mutka, *Magnetic Excitations in the Quantum Spin System $KCuCl_3$*, Eur. Phys. J. **B7** (1999) 519-522.

[26] N. Cavadini, G. Heigold, W. Henggeler, A. Furrer, H.-U. Güdel, K. Krämer, H. Mutka, *Magnetic Excitations in the Quantum Spin System $TlCuCl_3$*, Phys. Rev. **B63** (2001) 172414.

[27] G. Chaboussant, P.A. Crowell, L.P. Lévy, O. Piovesana, A. Madouri, D. Mailly, *Experimental Phase Diagram of $Cu_2(C_5H_{12}N_2)_2Cl_4$: A Quasi-One-Dimensional Antiferromagnetic Spin-$\frac{1}{2}$ Heisenberg Ladder*, Phys. Rev. **B55** (1997) 3046-3049.

[28] G. Chaboussant, M.-H. Julien, Y. Fagot-Revurat, M. Hanson, L.P. Lévy, C. Berthier, M. Horvatić, O. Piovesana, *Zero Temperature Phase Transitions in Spin-Ladders: Phase Diagram and Dynamical Studies of $Cu_2(C_5H_{12}N_2)_2Cl_4$*, Eur. Phys. J. **B6** (1998) 167-181.

[29] M.-C. Chang, M.-F. Yang, *Chern-Simons Theory for Magnetization Plateaus of the Frustrated $J_1 - J_2$ Heisenberg Model*, Phys. Rev. **B66** (2002) 184416.

[30] E. Chattopadhyay, I. Bose, *Magnetization of Coupled Spin Clusters in Ladder Geometry*, Phys. Rev. **B65** (2002) 134425.

[31] W. Chen, K. Hida, H. Nakano, *Magnetization Plateaus in One Dimensional $S = 1/2$ Heisenberg Model with Dimerization and Quadrumerization*, J. Phys. Soc. Jpn. **68** (1999) 625-630.

[32] W. Chen, K. Hida, B.C. Sanctuary, *Magnetization Plateaus and Phase Diagram in Polymerized $S = 1/2$ XXZ Chains*, Phys. Rev. **B63** (2001) 134427.

[33] R. Chitra, T. Giamarchi, *Critical Properties of Gapped Spin-$\frac{1}{2}$ Chains and Ladders in a Magnetic Field*, Phys. Rev. **B55** (1997) 5816-5826.

[34] A.V. Chubukov, D.I. Golosov, *Quantum Theory of an Antiferromagnet on a Triangular Lattice in a Magnetic Field*, J. Phys.: Condensed Matter **3** (1991) 69-82.

[35] R. Citro, E. Orignac, N. Andrei, C. Itoi, S. Qin, *Effective Theory of Magnetization Plateaus in a Three-Leg Ladder with Periodic Boundary Conditions*, J. Phys.: Condensed Matter **12** (2000) 3041-3075.

[36] M.F. Collins, O.A. Petrenko, *Triangular Antiferromagnets*, Can. J. Phys. **75** (1997) 605-655.

[37] B.R. Cooper, *Magnetic Properties of Rare Earth Metals*, p. 393 in *Solid State Physics*, Vol. 21, eds. F. Seitz, D. Turnbull, H. Ehrenreich, Academic Press (New York, 1968).

[38] J.K. Cullum, R.A. Willoughby, *Lanczos Algorithms for Large Symmetric Eigenvalue Computations*, Vol. I & II, Birkhäuser (Boston, 1985).

[39] E. Dagotto, *Experiments on Ladders Reveal a Complex Interplay between a Spin-Gapped Normal State and Superconductivity*, Rep. Prog. Phys. **62** (1999) 1525-1571.

[40] E. Dagotto, T.M. Rice, *Surprises on the Way from One to Two-Dimensional Quantum Magnets: The Ladder Materials*, Science **271** (1996) 618-623.

[41] O. Derzhko, J. Richter, O. Zaburannyi, *Local Magnetic Properties of Periodic Nonuniform Spin-$\frac{1}{2}$ XX Chains*, J. Magnetism and Magnetic Materials **222** (2000) 207-218.

[42] G.I. Dzhaparidze, A.A. Nersesyan, *Magnetic-Field Phase Transition in a One-Dimensional System of Electrons with Attraction*, JETP Lett. **27** (1978) 334-337.

[43] F.H.L. Eßler, H. Frahm, *Density Correlations in the Half-Filled Hubbard Model*, Phys. Rev. **B60** (1999) 8540-8542.

[44] F.H.L. Essler, A. Furusaki, T. Hikihara, *Dynamical Structure Factor in Cu Benzoate and other Spin-1/2 Antiferromagnetic Chains*, preprint cond-mat/0304244.

[45] H.G. Evertz, *The Loop Algorithm*, Adv. Phys. **52** (2003) 1-66.

[46] G. Fáth, *Luttinger Liquid Behavior in Spin Chains with Magnetic Field*, preprint cond-mat/0208580.

[47] G. Fáth, P.B. Littlewood, *Massless Phases of Haldane-Gap Antiferromagnets in Magnetic Field*, Phys. Rev. **B58** (1998) R14709-R14712.

[48] A. Fledderjohann, C. Gerhardt, M. Karbach, K.-H. Mütter, R.M. Wießner, *Soft Modes, Gaps and Magnetization Plateaus in One-Dimensional Spin-$\frac{1}{2}$ Antiferromagnetic Heisenberg Models*, Phys. Rev. **B59** (1999) 991-999.

[49] A. Fledderjohann, K.-H. Mütter, *The Magnetization Process in the 2-Dimensional $J_1 - J_2$ Model*, Eur. Phys. J. **B24** (2001) 211-220.

[50] A. Fledderjohann, K.-H. Mütter, *Magnetic Order in the Shastry-Sutherland Model*, Eur. Phys. J. **B26** (2002) 211-218.

[51] H. Frahm, V.E. Korepin, *Critical Exponents of the One-Dimensional Hubbard Model*, Phys. Rev. **B42** (1990) 10553-10565; *Correlation Functions of the One-Dimensional Hubbard Model in a Magnetic Field*, Phys. Rev. **B43** (1991) 5653-5662.

[52] H. Frahm, C. Rödenbeck, *Properties of the Chiral Spin Liquid State in Generalized Spin Ladders*, J. Phys. A: Math. Gen. **30** (1997) 4467-4479.

[53] H. Frahm, C. Rödenbeck, *A Generalized Spin Ladder in a Magnetic Field*, Eur. Phys. J. **B10** (1999) 409-414.

[54] H. Frahm, C. Sobiella, *Doping Induced Magnetization Plateaus*, Phys. Rev. Lett. **83** (1999) 5579-5582.

[55] M. Fujii, S. Fujimoto, N. Kawakami, *Magnetic and Critical Properties of Alternating Spin Chain with $S = 1/2$, 1 in Magnetic Fields*, J. Phys. Soc. Jpn. **65** (1996) 2381-2384.

[56] M. Fujisawa, J.-I. Yamaura, H. Tanaka, H. Kageyama, Y. Narumi, K. Kindo, *Crystal Structure and Magnetic Properties of the Quasi-One-Dimensional Quantum Spin System $Cu_2Cl_4{\cdot}H_8C_4SO_2$*, J. Phys. Soc. Jpn. **72** (2003) 694-697.

[57] Y. Fukumoto, *Magnetization Plateaus in the Shastry-Sutherland Model for $SrCu_2(BO_3)_2$: Results of Fourth-Order Perturbation Expansion with a Low-Density Approximation*, J. Phys. Soc. Jpn. **70** (2001) 1397-1403.

[58] Y. Fukumoto, A. Oguchi, *Magnetization Process in the Shastry-Sutherland System $SrCu_2(BO_2)_2$: Results of Third-Order Dimer Expansion*, J. Phys. Soc. Jpn. **69** (2000) 1286-1289.

[59] P. Fulde, J. Keller, G. Zwicknagl, *Theory of Heavy Fermions Systems*, Solid State Physics-Advances in Research and Applications **41** (1988) 1-150.

[60] A. Furusaki, S.C. Zhang, *Dynamical Spin Correlations in Heisenberg Ladder under a Magnetic Field and Correlation Functions in the SO(5) Ladder*, Phys. Rev. **B60** (1999) 1175-1187.

[61] M.P. Gelfand, *Linked-Tetrahedra Spin Chain: Exact Ground State and Excitations*, Phys. Rev. **B43** (1991) 8644-8645.

[62] C. Gerhardt, A. Fledderjohann, E. Aysal, K.-H. Mütter, J.F. Audet, H. Kröger, *η-Exponents in the One-Dimensional Antiferromagnetic Heisenberg Model with Next-Nearest Neighbour Coupling*, J. Phys.: Condensed Matter **9** (1997) 3435-3445.

[63] C. Gerhardt, K.-H. Mütter, H. Kröger, *Metamagnetism in the XXZ Model with Next-to-Nearest-Neighbor Coupling*, Phys. Rev. **B57** (1998) 11504-11509.

[64] S. Gluzman, *Two-Dimensional Quantum Antiferromagnet in a Strong Magnetic Field*, Z. Phys. **B90** (1993) 313-318.

[65] A.O. Gogolin, A.A. Nersesyan, A.M. Tsvelik, *Bosonization and Strongly Correlated Systems*, Cambridge University Press (Cambridge, 1998).

[66] O. Golinelli, Th. Jolicoeur, E.S. Sørensen, *Incommensurability in the Magnetic Excitations of the Bilinear-Biquadratic Spin-1 Chain*, Eur. Phys. J. **B11** (1999) 199-206.

[67] D. Green, C. Chamon, *Adsorption on Carbon Nanotubes: Quantum Spin Tubes, Magnetization Plateaus, and Conformal Symmetry*, Phys. Rev. Lett. **85** (2000) 4128-4131; *Geometric Frustration and Magnetization Plateaus in Quantum Spin and Bose-Hubbard Models on Tubes*, Phys. Rev. **B65** (2002) 104431.

[68] R.B. Griffiths, *Magnetization Curve at Zero Temperature for the Antiferromagnetic Heisenberg Linear Chain*, Phys. Rev. **133** (1964) A768-A775.

[69] C. Gros, R. Valentí, J.V. Alvarez, K. Hamacher, W. Wenzel, *Test of the Frustrated Spin-Cluster Model to Describe the Low-Temperature Physics of NaV_2O_5*, Phys. Rev. **B62** (2000) R14617-R14620.

[70] M. Hagiwara, Y. Narumi, K. Minami, K. Tatani, K. Kindo, *Magnetization Process of the $S = 1/2$ and 1 Ferrimagnetic Chain and Dimer*, J. Phys. Soc. Jpn. **68** (1999) 2214-2217.

[71] F.D.M. Haldane, *General Relation of Correlation Exponents and Spectral Properties of One-Dimensional Fermi Systems: Application to the Anisotropic $S = \frac{1}{2}$ Heisenberg Chain*, Phys. Rev. Lett. **45** (1980) 1358-1362.

[72] F.D.M. Haldane, *Nonlinear Field Theory of Large-Spin Heisenberg Antiferromagnets: Semiclassical Quantized Solitons of the One-Dimensional Easy-Axis Néel State*, Phys. Rev. Lett. **50** (1983) 1153-1156; *Continuum Dynamics of the 1-D Heisenberg Antiferromagnet: Identification with the $O(3)$ Nonlinear Sigma Model*, Phys. Lett. **A93** (1983) 464-468.

[73] T. Hamada, J. Kane, S. Nakagawa, Y. Natsume, *Exact Solution of the Ground State for Uniformly Distributed RVB in One-Dimensional Spin-1/2 Heisenberg Systems with Frustration*, J. Phys. Soc. Jpn. **57** (1988) 1891-1894.

[74] K. Hida, *Magnetic Properties of the Spin-1/2 Ferromagnetic-Ferromagnetic-Antiferromagnetic Trimerized Heisenberg Chain*, J. Phys. Soc. Jpn. **63** (1994) 2359-2364.

[75] K. Hida, *Magnetization Process of the $S = 1$ and $1/2$ Uniform and Distorted Kagomé Heisenberg Antiferromagnets*, J. Phys. Soc. Jpn. **70** (2001) 3673-3677.

[76] K. Hida, *Random Magnetism in $S = 1/2$ Heisenberg Chains with Bond Alternation and Randomness on the Strong Bonds*, J. Phys. Soc. Jpn. **72** (2003) 688-693; *Magnetization Plateaux in Random Frustrated $S = 1/2$ Heisenberg Chains*, J. Phys. Soc. Jpn. **72** (2003) 911-915.

[77] Y. Hieida, K. Okunishi, Y. Akutsu, *Magnetization Process of One-Dimensional Quantum Antiferromagnet: The Product Wavefunction Renormalization Group Approach*, Phys. Lett. **A233** (1997) 464-470.

[78] T. Hikihara, A. Furusaki, *Correlation Amplitude for the $S = 1/2$ XXZ Spin Chain in the Critical Region: Numerical Renormalization-Group Study of an Open Chain*, Phys.

Rev. **B58** (1998) R583-R586; *Spin Correlations in the Two-Leg Antiferromagnetic Ladder in a Magnetic Field*, Phys. Rev. **B63** (2001) 134438.

[79] R.P. Hodgson, J.B. Parkinson, *Bethe* Ansatz *for Two-Deviation States in Quantum Spin Chains of Arbitrary S with Anisotropic Heisenberg Exchange*, J. Phys. C: Solid State Phys. **18** (1985) 6385-6395.

[80] T. Inami, Y. Ajiro, T. Goto, *Magnetization Process of the Triangular Lattice Antiferromagnets* $RbFe(MoO_4)_2$ *and* $CsFe(SO_4)_2$, J. Phys. Soc. Jpn. **65** (1996) 2374-2376.

[81] M. Ishii, H. Tanaka, M. Hori, H. Uekusa, Y. Ohashi, K. Tatani, Y. Narumi, K. Kindo, *Gapped Ground State in the Spin-*$\frac{1}{2}$ *Trimer Chain System* $Cu_3Cl_6(H_2O)_2{\cdot}2H_8C_4SO_2$, J. Phys. Soc. Jpn. **69** (2000) 340-343.

[82] N.B. Ivanov, J. Richter, *Competition between Plaquette and Dimer Phases in Heisenberg Chains*, Phys. Lett. **A232** (1997) 308-312.

[83] A.E. Jacobs, T. Nikuni, H. Shiba, *Theory of Magnetic Structure of* $CsCuCl_3$ *in Transverse Magnetic Field*, J. Phys. Soc. Jpn. **62** (1993) 4066-4080.

[84] M.I. Kaganov, A.V. Chubukov, *Interacting Magnons*, Sov. Phys. Usp. **30** (1987) 1015-1040.

[85] H. Kageyama, K. Yoshimura, R. Stern, N.V. Mushnikov, K. Onizuka, M. Kato, K. Kosuge, C.P. Slichter, T. Goto, Y. Ueda, *Exact Dimer Ground State and Quantized Magnetization Plateaus in the Two-Dimensional Spin System* $SrCu_2(BO_3)_2$, Phys. Rev. Lett. **82** (1999) 3168-3171.

[86] N. Katoh, M. Imada, *Spin Gap in Two-Dimensional Heisenberg Model for* CaV_4O_9, J. Phys. Soc. Jpn. **64** (1995) 4105-4108.

[87] V.A. Kashurnikov, N.V. Prokof'ev, B.V. Svistunov, M. Troyer, *Quantum Spin Chains in a Magnetic Field*, Phys. Rev. **B59** (1999) 1162-1167.

[88] A. Kawaguchi, T. Fujii, N. Kawakami, *Magnetic Properties for the One-Dimensional Multicomponent Spin-Gap System*, Phys. Rev. **B63** (2001) 144413.

[89] K. Kawano, M. Takahashi, *Three-Leg Antiferromagnetic Heisenberg Ladder with Frustrated Boundary Condition; Ground State Properties*, J. Phys. Soc. Jpn. **66** (1997) 4001-4008.

[90] H. Kikuchi, *Evidence of the 1/3 Plateau in Magnetization of the Diamond Chain Compound* $Cu_3(CO_3)_2(OH)_2$, talk at '*Second Open Symposium on Field-Induced New Quantum Phenomena in Magnetic Systems*', Kobe, Japan, December 4-6 (2002).

[91] H. Kikuchi, Y. Fujii, M. Chiba, S. Mitsudo, T. Idehara, *Magnetic Properties of the Frustrated Diamond Chain Compound* $Cu_3(CO_3)_2(OH)_2$, to appear in the proceedings of LT23 (2002).

[92] A. Kitazawa, K. Okamoto, *Magnetization-Plateau State of the* $S = 3/2$ *Spin Chain with Single-Ion Anisotropy*, Phys. Rev. **B62** (2000) 940-945.

[93] K. von Klitzing, *The Quantized Hall Effect*, Rev. Mod. Phys. **58** (1986) 519-531.

[94] K. v. Klitzing, G. Dorda, M. Pepper, *New Method for High-Accuracy Determination of the Fine-Structure Constant Based on Quantized Hall Resistance*, Phys. Rev. Lett. **45** (1980) 494-497.

[95] K. Kodama, M. Takigawa, M. Horvatić, C. Berthier, H. Kageyama, Y. Ueda, S. Miyahara, F. Becca, F. Mila, *Magnetic Superstructure in the Two-Dimensional Quantum Antiferromagnet $SrCu_2(BO_3)_2$*, Science **298** (2002) 395-399.

[96] A. Koga, K. Okunishi, N. Kawakami, *First-Order Quantum Phase Transition in the Orthogonal-Dimer Spin Chain*, Phys. Rev. **B62** (2000) 5558-5563.

[97] A.K. Kolezhuk, *Magnetization Plateaus in Weakly Coupled Dimer Spin System*, Phys. Rev. **B59** (1999) 4181-4188.

[98] M. Kohno, M. Takahashi, *Magnetization Process of the Spin-1/2 XXZ Models on Square and Cubic Lattices*, Phys. Rev. **B56** (1997) 3212-3217.

[99] J.M. Kosterlitz, *The Critical Properties of the Two-Dimensional xy Model*, J. Phys. C: Solid State Phys. **7** (1974) 1046-1060.

[100] J.M. Kosterlitz, D.J. Thouless, *Ordering, Metastability and Phase Transitions in Two-Dimensional Systems*, J. Phys. C: Solid State Phys. **6** (1973) 1181-1203.

[101] V.N. Kotov, J. Oitmaa, O.P. Sushkov, Zheng Weihong, *Low-Energy Singlet and Triplet Excitations in the Spin-Liquid Phase of the Two-Dimensional $J_1 - J_2$ Model*, Phys. Rev. **B60** (1999) 14613-14616.

[102] V.N. Kotov, J. Oitmaa, O.P. Sushkov, Zheng Weihong, *Spontaneous Dimer Order, Excitation Spectrum, and Quantum Phase Transitions in the $J_1 - J_2$ Heisenberg Model*, Philosophical Magazine **B80** (2000) 1483-1498.

[103] T. Kuramoto, *Magnetic and Critical Properties of Alternating Spin Heisenberg Chain in a Magnetic Field*, J. Phys. Soc. Jpn. **67** (1998) 1762-1766.

[104] A. Langari, M.A. Martín-Delgado, *Alternating-Spin Ladders in a Magnetic Field: Formation of Magnetization Plateaux*, Phys. Rev. **B62** (2000) 11725-11730.

[105] P. Lemmens, G. Güntherodt, C. Gros, *Magnetic Light Scattering in Low-Dimensional Quantum Spin Systems*, Phys. Rep. **376** (2003) 1-103.

[106] C. Lhuillier, G. Misguich, *Frustrated Quantum Magnets*, p. 161 in *High Magnetic Fields*, eds. C. Berthier, L.P. Lévy, G. Martinez, Lecture notes in physics 595, Springer (Berlin 2001) [`cond-mat/0109146`].

[107] E.H. Lieb, T. Schultz, D. Mattis, *Two Soluble Models of an Antiferromagnetic Chain*, Ann. Phys. **16** (1961) 407-466.

[108] E.H. Lieb, F.Y. Wu, *Absence of Mott Transition in an Exact Solution of the Short-Range, One-Band Model in One Dimension*, Phys. Rev. Lett. **20** (1968) 1445-1448.

[109] Y.E. Lozovik, O.I. Notych, *Magnetization Plateaux of Frustrated Antiferromagnet and Analogy with FQHE*, Solid State Communications **85** (1993) 873-877.

[110] J. Lou, S. Qin, T.-K. Ng, Z.B. Su, I. Affleck, *Finite-Size Spectrum, Magnon Interactions and Magnetization of $S = 1$ Heisenberg Spin Chains*, Phys. Rev. **B62** (2000) 3786-3794.

[111] J. Lou, S. Qin, Z.B. Su, *Magnetization of the $S = 2$ Antiferromagnetic Heisenberg Chain near the Critical Magnetic Field*, Phys. Rev. **B62** (2000) 13832-13835.

[112] S. Lukyanov, *Low Energy Effective Hamiltonian for the XXZ Spin Chain*, Nucl. Phys. **B522** (1998) 533-549.

[113] S. Lukyanov, *Correlation Amplitude for the XXZ Spin Chain in the Disordered Regime*, Phys. Rev. **B59** (1999) 11163-11164.

[114] S. Lukyanov, V. Terras, *Long-Distance Asymptotics of Spin-Spin Correlation Functions for the XXZ Spin Chain*, Nucl. Phys. **B654** (2003) 323-356.

[115] G.D. Mahan, *Many-Particle Physics*, second edition, Plenum Press (New York, 1990).

[116] K. Maisinger, U. Schollwöck, S. Brehmer, H.-J. Mikeska, S. Yamamoto, *Thermodynamics of the (1,1/2) Ferrimagnet in Finite Magnetic Fields*, Phys. Rev. **B58** (1998) R5908-R5911.

[117] E. Manousakis, *The Spin-$\frac{1}{2}$ Heisenberg Antiferromagnet on a Square Lattice and its Applications to the Cuprous Oxides*, Rev. Mod. Phys. **63** (1991) 1-62.

[118] R. Melzi, S. Aldrovandi, F. Tedoldi, P. Carretta, P. Millet, F. Mila, *Magnetic and Thermodynamic Properties of Li_2VOSiO_4: A Two-Dimensional $S = 1/2$ Frustrated Antiferromagnet on a Square Lattice*, Phys. Rev. **B64** (2001) 024409.

[119] R. Melzi, P. Carretta, A. Lascialfari, M. Troyer, P. Millet, F. Mila, *$Li_2VO(Si,Ge)O_4$, a Prototype of a Two-Dimensional Frustrated Quantum Heisenberg Antiferromagnet*, Phys. Rev. Lett. **85** (2000) 1318-1321.

[120] F. Mila, *Ladders in a Magnetic Field: A Strong Coupling Approach*, Eur. Phys. J. **B6** (1998) 201-205.

[121] P. Millet, J.Y. Henry, F. Mila, J. Galy, *Vanadium(IV)-Oxide Nanotubes: Crystal Structure of the Low-Dimensional Quantum Magnet $Na_2V_3O_7$*, J. Solid State Chem. **147** (1999) 676-678.

[122] G. Misguich, B. Bernu, L. Pierre, *Determination of the Exchange Energies in Li_2VOSiO_4 from a High-Temperature Series Analysis of the Square Lattice $J_1 - J_2$ Heisenberg Model*, preprint cond-mat/0302583.

[123] G. Misguich, Th. Jolicoeur, S.M. Girvin, *Magnetization Plateaus of $SrCu_2(BO_3)_2$ from a Chern-Simons Theory*, Phys. Rev. Lett. **87** (2001) 097203.

[124] S. Miyahara, F. Becca, F. Mila, *Theory of Spin Density Profile in the Magnetization Plateaus of $SrCu_2(BO_3)_2$*, preprint cond-mat/0302332.

[125] S. Miyahara, K. Ueda, *Exact Dimer Ground State of the Two Dimensional Heisenberg Model for $SrCu_2(BO_3)_2$*, Phys. Rev. Lett. **82** (1999) 3701-3704.

[126] S. Miyahara, K. Ueda, *Superstructures at Magnetization Plateaus in $SrCu_2(BO_3)_2$*, Phys. Rev. **B61** (2000) 3417-3424.

[127] S. Miyashita, *Magnetic Properties of Ising-Like Heisenberg Antiferromagnets on the Triangular Lattice*, J. Phys. Soc. Jpn. **55** (1986) 3605-3617.

[128] T. Momoi, K. Totsuka, *Magnetization Plateaus as Insulator-Superfluid Transitions in Quantum Spin Systems*, Phys. Rev. **B61** (2000) 3231-3234.

[129] T. Momoi, K. Totsuka, *Magnetization Plateaus of the Shastry-Sutherland Model for $SrCu_2(BO_3)_2$: Spin-Density Wave, Supersolid and Bound States*, Phys. Rev. **B62** (2000) 15067-15078.

[130] E. Müller-Hartmann, R.R.P. Singh, C. Knetter, G.S. Uhrig, *Exact Demonstration of Magnetization Pleateaus and First-Order Dimer-Néel Phase Transitions in a Modified Shastry-Sutherland Model for $SrCu_2(BO_3)_2$*, Phys. Rev. Lett. **84** (2000) 1808-1811.

[131] Y. Narumi, M. Hagiwara, R. Sato, K. Kindo, H. Nakano, M. Takahashi, *High Field Magnetization in an $S = 1$ Antiferromagnetic Chain with Bond Alternation*, Physica **B246-247** (1998) 509-512.

[132] A.A. Nersesyan, A.O. Gogolin, F.H.L. Eßler, *Incommensurate Spin Correlations in Heisenberg Spin-1/2 Frustrated Two-Leg Heisenberg Ladders*, Phys. Rev. Lett. **81** (1998) 910-913.

[133] T. Nikuni, H. Shiba, *Quantum Fluctuations and Magnetic Structures of $CsCuCl_3$ in High Magnetic Field*, J. Phys. Soc. Jpn. **62** (1993) 3268-3276.

[134] H. Nishimori, S. Miyashita, *Magnetization Process in the Spin-*$1/2$ *Antiferromagnetic Ising-Like Heisenberg Model on the Triangular Lattice*, J. Phys. Soc. Jpn. **55** (1986) 4448-4455.

[135] H. Nojiri, Y. Tokunaga, M. Motokawa, *Magnetic Phase Transition of Helical $CsCuCl_3$ in High Magnetic Field*, Journal de Physique **49**, Suppl. C8 (1988) 1459-1460.

[136] K. Okamoto, *Plateau of the Magnetization Curve of the $S = 1/2$ Ferromagnetic-Ferromagnetic-Antiferromagnetic Spin Chain*, Solid State Commun. **98** (1996) 245-248.

[137] K. Okamoto, A. Kitazawa, *Magnetization Plateau and Quantum Phase Transition of the $S = \frac{1}{2}$ Trimerized XXZ Spin Chain*, J. Phys. A: Math. Gen. **32** (1999) 4601-4609.

[138] K. Okamoto, T. Tonegawa, Y. Takahashi, M. Kaburagi, *The Ground State of an $S = 1/2$ Distorted Diamond Chain – A Model of $Cu_3Cl_6(H_2O)_2{\cdot}2H_8C_4SO_2$*, J. Phys.: Condensed Matter **11** (1999) 10485-10498.

[139] N. Okazaki, J. Miyoshi, T. Sakai, *Magnetization Plateau in the Frustrated Spin Ladder*, J. Phys. Soc. Jpn. **69** (2000) 37-40.

[140] K. Okunishi, Y. Hieida, Y. Akutsu, *δ-Function Bose Gas Picture of $S = 1$ Antiferromagnetic Quantum Spin Chains Near Critical Fields*, Phys. Rev. **B59** (1999) 6806-6812.

[141] K. Okunishi, Y. Hieida, Y. Akutsu, *Middle-Field Cusp Singularities in the Magnetization Process of One-Dimensional Quantum Antiferromagnets*, Phys. Rev. **B60** (1999) R6953-R6956.

[142] K. Okunishi, T. Tonegawa, *Magnetic Phase Diagram of the $S = 1/2$ Antiferromagnetic Zigzag Spin Chain in the Strongly Frustrated Region: Cusp and Plateau*, J. Phys. Soc. Jpn. **72** (2003) 479-482.

[143] K. Onizuka, H. Kageyama, Y. Narumi, K. Kindo, Y. Ueda, T. Goto, *1/3 Magnetization Plateau in $SrCu_2(BO_3)_2$ - Stripe Order of Excited Triplets -*, J. Phys. Soc. Jpn. **69** (2000) 1016-1018.

[144] A. Oosawa, T. Ono, K. Kakurai, H. Tanaka, *Magnetic Excitations in the Quantum Spin System NH_4CuCl_3*, preprint cond-mat/0304172.

[145] M. Oshikawa, *Commensurability, Excitation Gap and Topology in Quantum Many-Particle Systems on a Periodic Lattice*, Phys. Rev. Lett. **84** (2000) 1535-1538.

[146] M. Oshikawa, M. Yamanaka, I. Affleck, *Magnetization Plateaus in Spin Chains: "Haldane Gap" for Half-Integer Spins*, Phys. Rev. Lett. **78** (1997) 1984-1987.

[147] J.B. Parkinson, *The $S = 1$ Quantum Spin Chain with Equal Heisenberg and Biquadratic Exchange in a Magnetic Field*, J. Phys.: Condensed Matter **1** (1989) 6709-6715.

[148] J.B. Parkinson, J.C. Bonner, *Spin Chains in a Field: Crossover from Quantum to Classical Behavior*, Phys. Rev. **B32** (1985) 4703-4724.

[149] K. Penc, F. Mila, *Charge Gap in the One-Dimensional Dimerized Hubbard Model at Quarter-Filling*, Phys. Rev. **B50** (1994) 11429-11445.

[150] K. Penc, J. Sólyom, *One-Dimensional Hubbard Model in a Magnetic Field and the Multicomponent Tomonaga-Luttinger Model*, Phys. Rev. **B47** (1993) 6273-6292.

[151] I. Peschel, X. Wang, M. Kaulke, K. Hallberg (eds.), *Density-Matrix Renormalization*, Lecture notes in physics 528, Springer (Berlin 1999).

[152] V.L. Pokrovsky, A.L. Talapov, *Ground State, Spectrum and Phase Diagram of Two-Dimensional Incommensurate Crystals*, Phys. Rev. Lett. **42** (1979) 65-67.

[153] V.N. Popov, *On the Theory of the Superfluidity of Two- and One-Dimensional Bose System*, Theor. Math. Phys. **11** (1972) 565-573.

[154] V.N. Popov, *Functional Integrals in Quantum Field Theory and Statistical Physics*, D. Reidel Publishing (Dordrecht, Holland 1983).

[155] P. Pujol, J. Rech, *Site-Centered Impurities in Quantum Spin Chains*, Phys. Rev. **B66** (2002) 104401.

[156] T.M. Rice, *$t - J$ Ladders and Cuprate Ladder Compounds*, Z. Phys. **B103** (1997) 165-172.

[157] T.M. Rice, *Low Dimensional Magnets*, p. 139 in *High Magnetic Fields*, eds. C. Berthier, L.P. Lévy, G. Martinez, Lecture notes in physics 595, Springer (Berlin 2001).

[158] J. Richter, N.B. Ivanov J. Schulenburg, *The Antiferromagnetic Spin-1/2 Chain with Competing Dimers and Plaquettes: Numerical versus Exact Results*, J. Phys.: Condensed Matter **10** (1998) 3635-3649.

[159] A.G. Rojo, *Absence of Gap for Infinite Half-Integer Spin Ladders with an Odd Number of Legs*, Phys. Rev. **B53** (1996) 9172-9174.

[160] H. Rosner, R.R.P. Singh, W.H. Zheng, J. Oitmaa, S.-L. Drechsler, W.E. Pickett, *Realization of a Large J_2 Quasi-2D Spin-Half Heisenberg System: Li_2VOSiO_4*, Phys. Rev. Lett. **88** (2002) 186405.

[161] H. Rosner, R.R.P. Singh, W.H. Zheng, J. Oitmaa, W.E. Pickett, *High-Temperature Expansions for the $J_1 - J_2$ Heisenberg Models: Applications to ab Initio Calculated Models for Li_2VOSiO_4 and Li_2VOGeO_4*, Phys. Rev. **B67** (2003) 014416.

[162] Ch. Rüegg, *Neutron Scattering Investigations of the $S = 1/2$ Quantum Spin Systems $TlCuCl_3$ and NH_4CuCl_3*, Diplomarbeit ETHZ/PSI, February 2001.

[163] S. Sachdev, T. Senthil, R. Shankar, *Finite-Temperature Properties of Quantum Antiferromagnets in a Uniform Magnetic Field in One and Two Dimensions*, Phys. Rev. **B50** (1994) 258-272.

[164] T. Saha-Dasgupta, R. Valentí, *Comparative Study between Two Quantum Spin Systems $KCuCl_3$ and $TlCuCl_3$*, Europhys. Lett. **60** (2002) 309-315.

[165] T. Sakai, K. Okamoto, *Quantum Magnetization Plateaux of an Anisotropic Ferrimagnetic Spin Chain*, Phys. Rev. **B65** (2002) 214403.

[166] T. Sakai, N. Okazaki, *Magnetic Properties of Frustrated Spin Ladder*, J. Appl. Phys. **87** (2000) 5893-5895.

[167] T. Sakai, M. Takahashi, *$S = 1$ Antiferromagnetic Heisenberg Chain in a Magnetic Field*, Phys. Rev. **B43** (1991) 13383-13393.

[168] T. Sakai, M. Takahashi, *Magnetization Plateau in $S = 3/2$ Antiferromagnetic Heisenberg Chain with Anisotropy*, Phys. Rev. **B57** (1998) R3201-R3204.

[169] T. Sakai, S. Yamamoto, *Critical Behavior of Anisotropic Heisenberg Mixed-Spin Chains in a Field*, Phys. Rev. **B60** (1999) 4053-4056.

[170] T. Sakai, S. Yamamoto, *Coexistent Quantum and Classical Aspects of Magnetization Plateaux in Alternating-Spin Chains*, J. Phys.: Condensed Matter **12** (2000) 9787-9797.

[171] A.W. Sandvik, *Stochastic Series Expansion Method with Operator-Loop Update*, Phys. Rev. **B59** (1999) R14157-R14160.

[172] K. Sano, K. Takano, *Spin Gap of $S = 1/2$ Heisenberg Model on Distorted Diamond Chain*, J. Phys. Soc. Jpn. **69** (2000) 2710-2711.

[173] H.-J. Schmidt, *Linear Energy Bounds for Heisenberg Spin Systems*, J. Phys. A: Math. Gen. **35** (2002) 6545-6555.

[174] M. Schmidt, C. Gerhardt, K.-H. Mütter, M. Karbach, *The Frustrated Antiferromagnetic Heisenberg Model in the Presence of a Uniform Field*, J. Phys.: Condensed Matter **8** (1996) 553-568.

[175] J. Schnack, H.-J. Schmidt, J. Richter, J. Schulenburg, *Independent Magnon States on Magnetic Polytopes*, Eur. Phys. J. **B24** (2001) 475-481.

[176] F. Schönfeld, G. Bouzerar, G.S. Uhrig, E. Müller-Hartmann, *On the Incommensurate Phase in Modulated Heisenberg Chains*, Eur. Phys. J. **B5** (1998) 521-528.

[177] J. Schulenburg, J. Richter, *Infinite Series of Magnetization Plateaus in the Frustrated Dimer-Plaquette Chain*, Phys. Rev. **B65** (2002) 054420.

[178] J. Schulenburg, J. Richter, *Sequence of First-Order Quantum Phase Transitions in a Frustrated Spin Half Dimer-Plaquette Chain*, Phys. Rev. **B66** (2002) 134419.

[179] H.J. Schulz, *Critical Behavior of Commensurate-Incommensurate Phase Transitions in Two Dimensions*, Phys. Rev. **B22** (1980) 5274-5277.

[180] H.J. Schulz, *Correlated Fermions in One Dimension*, Int. Jour. of Mod. Phys. **B5** (1991) 57-74; *Fermi Liquids and Non-Fermi Liquids*, p. 533 in *Proceedings of Les Houches Summer School LXI*, eds. E. Akkermans, G. Montambaux, J. Pichard and J. Zinn-Justin (Elsevier, Amsterdam, 1995) [`cond-mat/9503150`].

[181] H.J. Schulz, *Coupled Luttinger Liquids*, p. 81 in *Correlated Fermions and Transport in Mesoscopic Systems*, eds. T. Martin, G. Montambaux, J. Tran Thanh Van (Editions Frontières, Gif–sur–Yvette, 1996) [`cond-mat/9605075`].

[182] B.S. Shastry, B. Sutherland, *Exact Ground State of a Quantum Mechanical Antiferromagnet*, Physica **108** (1981) 1069-1070.

[183] Y. Shimaoka, T. Goto, K. Kodama, M. Takigawa, H. Tanaka, *NMR Study of the Magnetic Structure in NH_4CuCl_3*, poster at '*Second Open Symposium on Field-Induced New Quantum Phenomena in Magnetic Systems*', Kobe, Japan, December 4-6 (2002).

[184] W. Shiramura, K. Takatsu, B. Kurniawan, H. Tanaka, H. Uekusa, Y. Ohashi, K. Takizawa, H. Mitamura, T. Goto, *Magnetization Plateaus in NH_4CuCl_3*, J. Phys. Soc. Jpn. **67** (1998) 1548-1551.

[185] W. Shiramura, K. Takatsu, H. Tanaka, K. Kamishima, M. Takahashi, H. Mitamura, T. Goto, *High-Field Magnetization Processes of Double Spin Chain Systems $KCuCl_3$ and $TlCuCl_3$*, J. Phys. Soc. Jpn. **66** (1997) 1900-1903.

[186] M.B. Stone, Y. Chen, J. Rittner, H. Yardimci, D.H. Reich, C. Broholm, D.V. Ferraris, T. Lectka, *Frustrated Three-Dimensional Quantum Spin Liquid in CuHpCl*, Phys. Rev. **B65** (2002) 064423.

[187] V. Subrahmanyam, *Effective Chiral-Spin Hamiltonian for Odd-Numbered Coupled Heisenberg Chains*, Phys. Rev. **B50** (1994) 16109-16112.

[188] N. Suzuki, F. Matsubara, *Phase Diagrams of the $S = \frac{1}{2}$ Quantum Antiferromagnetic XY Model on the Triangular Lattice in Magnetic Fields*, Phys. Rev. **B55** (1997) 12331-12337.

[189] D.D. Swank, C.P. Landee, R.D. Willett, *Magnetic Interactions in Copper (II) Trimers*, J. Magnetism and Magnetic Materials **15** (1980) 319-320.

[190] D.D. Swank, R.D. Willett, *The Crystal Structure of $Cu_3Cl_6(H_2O)_2{\cdot}2H_8C_4SO_2$, trans-tetra-$\mu$-[chlorodichlorodiaquocopper(II)]copper(II)bis(tetramethylene sulfone), and the Molecular Structure of the $Cu_3Cl_6(H_2O)_2$ Trimer*, Inorganica Chimica Acta **8** (1974) 143-148.

[191] O.F. Syljuåsen, *Directed Loop Updates for Quantum Lattice Models*, Phys. Rev. **E67** (2003) 046701.

[192] O.F. Syljuåsen, A.W. Sandvik, *Quantum Monte Carlo with Directed Loops*, Phys. Rev. **E66** (2002) 046701.

[193] K. Takano, K. Kubo, H. Sakamoto, *Ground States with Cluster Structures in a Frustrated Heisenberg Chain*, J. Phys.: Condensed Matter **8** (1996) 6405-6411.

[194] H. Tanaka, A. Oosawa, T. Kato, H. Uekusa, Y. Ohashi, K. Kakurai, A. Hoser, *Observation of Field-Induced Transverse Néel Ordering in the Spin Gap System $TlCuCl_3$*, J. Phys. Soc. Jpn. **70** (2001) 939-942.

[195] K. Tandon, S. Lal, S.K. Pati, S. Ramasesha, D. Sen, *Magnetization Properties of Some Quantum Spin Ladders*, Phys. Rev. **B59** (1999) 396-410.

[196] O. Tegus, E. Brück, K.H.J. Buschow, F.R. de Boer, *Transition-Metal-Based Magnetic Refrigerants for Room-Temperature Applications*, nature **415** (2002) 150-151.

[197] T. Tokihiro, *Antiferromagnetic Heisenberg Model on a Quasiperiodic Lattice with Hierarchical Interactions*, Phys. Rev. **B41** (1990) 7334-7337.

[198] T. Tonegawa, I. Harada, *Ground-State Properties of the One-Dimensional Isotropic Spin-1/2 Heisenberg Antiferromagnet with Competing Interactions*, J. Phys. Soc. Jpn. **56** (1987) 2153-2167; *Magnetization Curves in the Ground State of Spin-1/2 Antiferromagnetic XXZ Chains with Competing Interactions*, Physica **B155** (1989) 379-382; *One-Dimensional Isotropic Spin-1/2 Heisenberg Magnet with Ferromagnetic Nearest-Neighbor and Antiferromagnetic Next-Nearest-Neighbor Interactions*, J. Phys. Soc. Jpn. **58** (1989) 2902-2915.

[199] T. Tonegawa, T. Nakao, M. Kaburagi, *Ground-State Phase Diagram and Magnetization Curves of the Spin-1 Antiferromagnetic Heisenberg Chain with Bond Alternation and Uniaxial Single-Ion-Type Anisotropy*, J. Phys. Soc. Jpn. **65** (1996) 3317-3330.

[200] T. Tonegawa, T. Nishida, M. Kaburagi, *Ground-State Magnetization Curve of a Generalized Spin-1/2 Ladder*, Physica **B246-247** (1998) 368-371.

[201] T. Tonegawa, K. Okamoto, T. Hikihara, Y. Takahashi, M. Kaburagi, *Ground State Properties of an $S = 1/2$ Distorted Diamond Chain*, J. Phys. Soc. Jpn. **69** Suppl. A (2000) 332-338; *Ground State of an $S = 1/2$ Distorted Diamond Chain in a Finite Magnetic Field*, J. Phys. Chem. Solids **62** (2001) 125-128.

[202] K. Totsuka, *Magnetization Processes in Bond-Alternating Quantum Spin Chains*, Phys. Lett. **A228** (1997) 103-110

[203] K. Totsuka, *Magnetization Plateau in $S = \frac{1}{2}$ Heisenberg Spin Chain with Next-Nearest-Neighbor- and Alternating Interactions*, Phys. Rev. **B57** (1998) 3454-3465; *Novel Massive Ground States of Spin Chains in a Magnetic Field*, Eur. Phys. J. **B5** (1998) 705-717.

[204] S. Trebst, S. Sengupta, *Spin-Cluster Model for the Low Temperature Phase of $\alpha' - NaV_2O_5$*, Phys. Rev. **B62** (2000) R14613-R14616.

[205] D.C. Tsui, H.L. Stormer, A.C. Gossard, *Two-Dimensional Magnetotransport in the Extreme Quantum Limit*, Phys. Rev. Lett. **48** (1982) 1559-1562.

[206] H. Tsunetsugu, M. Sigrist, K. Ueda, *The Ground-State Phase Diagram of the One-Dimensional Kondo Lattice Model*, Rev. Mod. Phys. **69** (1997) 809-863.

[207] M. Usami, S. Suga, *Critical Properties of Frustrated $S = 1/2$ Spin Chain with Bond Alternation in Magnetic Fields*, Phys. Lett. **A240** (1998) 85-90.

[208] A. Voigt, *Quantum Disorder due to Singlet Formation: The Plaquette Lattice*, Computer Physics Communications **146** (2002) 125-128.

[209] J. Voit, *One-Dimensional Fermi Liquids*, Rep. Prog. Phys. **58** (1995) 977-1116.

[210] Ch. Waldtmann, H.-U. Everts, private communication.

[211] S. Watanabe, *Magnetization Process in Heavy Electron Systems*, J. Phys. Soc. Jpn. **69** (2000) 2947-2952.

[212] B.C. Watson, V.N. Kotov, M.W. Meisel, D.W. Hall, G.E. Granroth, W.T. Montfrooij, S.E. Nagler, D.A. Jensen, R. Backov, M.A. Petruska, G.E. Fanucci, D.R. Talham, *The Magnetic Spin Ladder $(C_5H_{12}N)_2CuBr_4$: High Field Magnetization and Scaling Near Quantum Criticality*, Phys. Rev. Lett. **86** (2001) 5168-5171.

[213] S. Wessel, S. Haas, *Magnetic Field Induced Ordering in Quasi-One-Dimensional Quantum Magnets*, Eur. Phys. J. **B16** (2000) 393-396; *Three-Dimensional Ordering in Weakly Coupled Antiferromagnetic Ladders and Chains*, Phys. Rev. **B62** (2000) 316-323.

[214] S. Wessel, M. Olshanii, S. Haas, *Field-Induced Magnetic Order in Quantum Spin Liquids*, Phys. Rev. Lett. **87** (2001) 206407.

[215] S.R. White, *Density Matrix Formulation for Quantum Renormalization Group*, Phys. Rev. Lett. **69** (1992) 2863-2866; *Density-Matrix Algorithms for Quantum Renormalization Groups*, Phys. Rev. **B48** (1993) 10345-10356.

[216] S.R. White, I. Affleck, *Dimerization and Incommensurate Spiral Spin Correlations in the Zigzag Spin Chain: Analogies to the Kondo Lattice*, Phys. Rev. **B54** (1996) 9862-9869.

[217] R. Wießner, A. Fledderjohann, K.-H. Mütter, M. Karbach, *Spontaneous Magnetization in Spin-Ladder Systems with Competing Interactions*, Phys. Rev. **B60** (1999) 6545-6551.

[218] R.M. Wießner, A. Fledderjohann, K.-H. Mütter, M. Karbach, *A Numerical Study of the Formation of Magnetisation Plateaus in Quasi One-Dimensional Spin-1/2 Heisenberg Models*, Eur. Phys. J. **B15** (2000) 475-481.

[219] R.D. Willett, C. Dwiggins Jr., R.F. Kruh, R.E. Rundle, *Crystal Structures of $KCuCl_3$ and NH_4CuCl_3*, J. Chem. Phys. **38** (1963) 2429-2436.

[220] F. Woynarovich, H.-P. Eckle, T.T. Truong, *Non-Analytic Finite-Size Corrections in the One-Dimensional Bose Gas and Heisenberg Chain*, J. Phys. A: Math. Gen. **22** (1989) 4027-4043.

[221] T. Yamamoto, R. Manago, Y. Mori, *Magnetization Cusp Singularities of Frustrated Kondo Necklace Model*, preprint cond-mat/0204588.

[222] S. Yamamoto, T. Sakai, *Multiplateau Magnetization Curves of One-Dimensional Heisenberg Ferrimagnets*, Phys. Rev. **B62** (2000) 3795-3800.

[223] M.S. Yang, K.-H. Mütter, *The Two Dimensional Antiferromagnetic Heisenberg Model in the Presence of an External Field*, Z. Phys. **B104** (1997) 117-123.

[224] É.A. Zavadskii, B.M. Todris, Yu.D. Zavorotnev, S.K. Asadov, *Enery Spectrum of the Fe^{2+} Ion in Fluorosilicate*, Sov. J. Low Temp. Phys. **11** (1985) 44-45.

[225] M.E. Zhitomirsky, *Field-Induced Transitions in Kagomé Antiferromagnet*, Phys. Rev. Lett. **88** (2002) 057204.

[226] M.E. Zhitomirsky, *Enhanced Magnetocaloric Effect in Frustrated Magnets*, Phys. Rev. **B67** (2003) 104421.

[227] M.E. Zhitomirsky, T. Nikuni, *Magnetization Curve of a Square-Lattice Heisenberg Antiferromagnet*, Phys. Rev. **B57** (1998) 5013-5016.

[228] M.E. Zhitomirsky, I.A. Zaliznyak, *Static Properties of a Quasi-One-Dimensional Antiferromagnet in a Magnetic Field*, Phys. Rev. **B53** (1996) 3428-3435.